Title
Cell Autonomous and Non-Cell Autonomous Mechanisms of Smoothened Inhibition by Patched1 and Patched2

Author
Roberts, Brock William

Publication Date
2015

Peer reviewed|Thesis/dissertation

Cell Autonomous and Non-Cell Autonomous Mechanisms of Smoothened Inhibition by Patched1 and Patched2

By

Brock William Roberts

A dissertation submitted in partial satisfaction of the

requirements for the degree of

Doctor of Philosophy

in

Molecular and Cell Biology

in the

Graduate Division

of the

University of California, Berkeley

Committee in charge:

Professor Henk Roelink, Chair
Professor Gian Garriga
Professor Craig Miller
Professor Danica Chen

Summer 2015

Abstract

Cell Autonomous and Non-Cell Autonomous Mechanisms of Smoothened Inhibition by Patched1 and Patched2

by

Brock William Roberts

Doctor of Philosophy in Molecular and Cell Biology

University of California, Berkeley

Professor Henk Roelink, Chair

The Hedgehog (Hh) signaling pathway in vertebrates is regulated by the interaction of three key components: Sonic Hedgehog (Shh) ligand, its receptors Patched1 (Ptch1) and Patched2 (Ptch2), and the pathway activator Smoothened (Smo). Shh binding to Ptch1, the key Shh receptor, results in the release of Ptch1-mediated inhibition of Smo, leading to Smo activation and subsequent cell autonomous activation of the Shh response, with a similar but less important role for the Ptch1 paralog Ptch 2. Using genome editing I disrupted the core hedgehog pathway genes *Ptch1*, *Ptch2*, *Smo*, *Shh* in most combinations in mouse embryonic stem cells (mESCs). I differentiated these unique cell lines into neural tissue in which I interrogated mechanisms of Smo regulation by Ptch1 and Ptch2. I present an important role for Ptch2 as a cell-autonomous Smo regulator in the absence of Ptch1. I also demonstrate a role for Ptch1 and Ptch2 as non-cell autonomous Smo regulators, which I attribute to their efflux of a Smo inhibitory molecule into the extracellular space.

Chapter 1

The hedgehog signaling pathway and the Ptch-Smo regulatory mechanism

The Hedgehog signaling pathway in the biosphere and in scholarship

To know the path from molecules to morphology stands as the ultimate quest for developmental biologists. Three decades of research have confirmed that the hedgehog (Hh) signaling pathway lies central to this quest in animals. Like other prominent families of developmental signaling molecules—Wnt, TGF-Beta, growth factor signaling, Notch—what the research community has come to know about hedgehog signaling comprises a very large part of the foundation of the field of modern developmental biology. The history of this pathway's elucidation over the past approximately thirty years has gone hand in hand with a larger understanding of developmental mechanisms at work during embryogenesis in animals. Conserved roles in embryonic development make Hh signaling fundamental to metazoan life (Briscoe & Thérond 2013; Hooper & Scott 2005; Ingham & McMahon 2001; Zhu & Scott 2004; Gerhart 1999). It is no exaggeration to state that the majority of animal organs are likely under the influence of Hh signaling either during embryonic development or as a factor in their adult homeostasis, or both

Hh ligands, and the downstream cellular events by which they transduce their signal, are well conserved in animals as distantly related as fruit flies and vertebrates. The evolutionary legacies of Hh ligands extend deeply to the pre-metazoan choanoflagellates, and their receptors evolved from protein families ubiquitous throughout the kingdoms of life (Nichols et al. 2012; Adamska et al. 2007; Nikaido & Takatsuka 2009). It is reasonably to suggest that metazoans evolved such complex forms in large part because of the ancient coalescence of the Hh pathway (Hausmann et al. 2009).

Beyond its prominent role in embryology, development, and evolution, Hh signaling also stands with other exceptional families of developmental signaling molecules for its remarkable importance to disease and human health. A number of cancer etiologies are intimately linked to defects in Hh signaling (Wang & Scott 1999; Johnson et al. 1996). While Hh signaling contributes exquisitely to myriad events during development of the embryo, a process as robust as it is complex, cases where Hh mediated events go awry lead to severe birth defects (Nieuwenhuis & Hui 2004; Roessler et al. 1996). More upliftingly, Hh signaling has been found to play a large role in stem cell biology. The maintenance of stem cell populations in adult tissues involves many Hh signals (Petrova & Joyner 2014). *In vitro* organ development applications employ Hh signaling, where events natural to the embryo can be employed in the dish for research and ultimately, the hope goes, therapies (Meinhardt et al. 2014). This approach forms the foundation of the present thesis.

While undeniably vital to the developmental biology of metazoans, several molecular mechanisms at the core of the Hh pathway have proven elusive in efforts to characterize them. The mysterious mechanism responsible for the repressive effect of Patched on Smoothened—two of the most well interrogated and vital molecules in the Hh pathway and the subject of must discussion in this thesis—stands as the most towering example.

The history of discovery in the Hh signaling field is built in large part around the discipline of genetics. The first Hh signaling events, and the genes and gene products responsible for them, were discovered in the early 1980s in now-legendary *Drosophila* forward genetic screens, culminating in a Nobel prize (Nüsslein-Volhard & Wieshaus 1980). Genetic experiments in *Drosophila* have led to the discovery of most of the molecules as the core of the Hh pathway, in fact. As Hh signaling in most contexts involves secreted signals acting at a distance, experimental systems where the ability to assess the effects of mutations in both cells

harboring that mutation and cells in its signaling environment are critical. This classic concept of cell autonomy and non-autonomy in the genetic analysis of signaling pathways, with respect mutations affecting signaling pathway components, has made the establishment of genetically mosaic platforms important. *Drosophila* genetics allows for genetic mosaicism with tremendous elegance (Hartl & Scott 2014).

Genetic experiments in mouse, principally involving targeted disruptions in the vertebrate orthologs of Hh pathway genes discovered in *Drosophila*, have additionally been instrumental in this field (Goodrich et al. 1997; Kawakami et al. 2002; Chiang et al. 1996; X. M. Zhang et al. 2001; Ma et al. 2002; Nieuwenhuis et al. 2006). The same can be said for chicken embryology, which features the ability to mosaically manipulate specific Hh pathway components in tissues under its influence during development, such as the neural tube and limb bud. Research on the Hh pathway in vertebrates has largely supported the view that this signaling system is highly conserved with *Drosophila*, but with a twist: a specialized organelle known as the primary cilium is integral to Hh signaling in vertebrates (Sasai & Briscoe 2012).

The work presented in this thesis coincided with the advent of a new era in genetics: genome editing (Doudna et al. ; Cox et al. 2015). It was our goal in pursuing this work to explore novel molecular mechanisms of Hh signaling in vertebrates by taking advantage of the expanding horizons of genetic research afforded by genome editing advances. In particular, we sought to generate a system where genetic mosaicism can be rigorously explored in tissue with complex genotypes, much like in the *Drosophila* system, but in a vertebrate model. It has been traditionally difficult to generate complex genotypes—for example, cells genetically null for more than one or two genes—in vertebrate genetic model systems. It has been a pleasure to witness over the course of this thesis the realization of this goal, and harvest its rewards in the form of novel insights into this pathway, to be discussed at length herein.

It would not be an overstatement to label the mechanistic mysteries of how Patched regulates Smoothened as something of a scientific "holy grail." How living beings acquire their physical form stands as an existential question for the ages. Aristotle was interested (Aristotle & Peck, ~BC 330, trans. 1942). As long as we remain organic beings, however sophisticated we become, we will retain an interest in the acquisition of biological form, if for no other reason than to re-stock our organ farms. Hh signaling has some large role in that process in all animals and ourselves. Our investment in human health makes the quest to know the Hh pathway's inner workings all the more important, an urgent and practical consideration for the clinic as much as a classic curiosity case of academics. To have done work with even the possibility of illuminating a shadowy corner of our understanding of this molecular phenomenon has been a true honor.

A cursory introduction to the Hedgehog signaling pathway

The Hh signal transduction pathway involves a series of molecular events orchestrated principally by the Hh ligands, their receptor, Patched (Ptch) and a second receptor, Smoothened (Smo). Dispatched (Disp), a molecule related to Ptch, is necessary for appropriate Hh ligand secretion and is therefore also a core regulator. According to the most canonical model for Hh signaling, Ptch negatively regulates Smo activity. Hh ligands processed and secreted by Disp reverse this inhibition through binding to Ptch, activating Smo (Hooper & Scott 2005; Ingham & McMahon 2001). Downstream of the regulatory interplay between these molecules, a transcriptional response mediated by the Gli family of transcription factors becomes elicited upon Smoothened activation. When Smoothened is inactive under steady state conditions, a

downstream signaling cascade of kinases and proteases leads to the post-translational processing of the Gli/Ci family of transcription factors, which then function as transcriptional repressors. Smo activation inhibits proteolytic processing. Consequently, Gli/Ci transcription factors instead function as activators (Cohen et al. 2015; Stamataki et al. 2005; Briscoe & Thérond 2013).

The canonical model for Hh signaling suffers from many mechanistic knowledge gaps and very likely requires expansion and perhaps revision. However, it serves as a framework for the field. In this thesis I will explore at length the mechanism responsible for Smo repression by Ptch, as well as the general mechanism of Disp/Ptch function, given their shared evolutionary history. For the purposes of this thesis, focus will be maintained on the upstream molecules in the response.

Hh pathway nomenclature

Hh signaling is investigated in a number of model organisms and is widely conserved throughout animal evolution. Most research discussed in this thesis involves *Drosophila* or the amniotes, chick, mouse or human. Most genes and their protein products are named after mutant phenotypes in *Drosophila* and in most cases these names are used as well in amniotes. As is common for many gene/protein families, Hh ligands, Ptch, and Disp, but not Smo, are expanded in amniotes to include several paralogs. A numbering system (e.g. Ptch1/2) distinguishes Ptch/Disp paralogs in amniotes, whereas Hh ligands have been separately named. I use "Hh signaling" generically to refer to conserved mechanisms shared between species, invoking the original namesake molecule of the pathway, the *Drosophila* ligand Hh. In referencing general mechanisms involving Ptch/Disp, I refer to these molecules by their un-enumerated names. In referencing specific experiments, I will use the recognized gene/protein name (e.g. Ptch, Hh for *Drosophila*, Shh, Ptch1 or Ptch2 for amniotes). Inconsistency has unfortunately arisen in the naming of the gene encoding the Patched protein, in both *Drosophila* and vertebrates. I refer here to the gene and protein as Ptch but acknowledge that the *Drosophila* gene was originally named *ptc* and that this nomenclature is sometimes used in vertebrates as well.

The Hh pathway and neural patterning in vertebrates

Hh-mediated induction of neural cell fates in vertebrates represents a classic signaling system that forms the basis of the experimental work in this thesis. This process can be manipulated in vertebrate embryos through the introduction of exogenous genetic elements, studied in mutant animals by way of genetic tools in mice, and modeled in the dish using stem cell differentiation protocols. An overview of this process follows.

During vertebrate gastrulation, cell movements in and around designated cellular signaling centers, often termed "organizers," give rise to the three germ layers by way of inductive signaling (Spemann & Mangold 1924). Ongoing cell movements in the ectoderm partition cells fated to contribute to the nervous system from the skin and tissue lining lineage. This process involves a rather mechanical inward pinching of cells from what begins as a sheet of cells to form a tubular neuroepithelium along the embryonic axis. Meanwhile, mesodermal cells beneath the ectoderm organize into rod-like structures also situated axially, including the notochord, the defining structure of the phylum chordata. It was classically postulated by early embryologists that signals emanated throughout the embryo along the dorso-ventral, as well as

rostral-caudal axis, thereby specifying cell fates in three dimensional space (Jessell & Melton 1992).

Caudal portions of the neural tube gives rise to the spinal cord, in which numerous distinct, stereotyped neural fates can be easily appreciated later in development (Alaynick et al. 2011). Classical embryology experiments where the underlying notochord was removed demonstrated a requirement for signals between the notochord and overlying neural tube in order for the full complement of cell fates to emerge (Placzek et al. 1990). This motivated intense interest in the identity of this signal, given its apparent ability to control fates in a morphogenetic field in a manner similar to that proposed for classic morphogens (Wolpert 1971).

In one of the first reported functions of Hh signaling in vertebrates, Shh was identified as the notochord-derived signal specifying ventral fates in the neural tube (Roelink et al. 1994; Roelink et al. 1995). Shh originating from the notochord specifies a second organizing center that also expresses Shh, the floor plate, at the neural tube's ventral midline. Shh secreted from both the floor plate and notochord emanates dorsally. A gradient of downstream Hh pathway activity, in the form of a nuanced transcriptional output, results. A number of transcription factors under direct control of the Hh pathway, by way of Gli activator binding, are expressed at distinct positions along the dorso-ventral axis of the neural tube, and these serve as markers for neural tube cell fates (Briscoe et al. 2000). In many cases these factors regulate each other, establishing a transcriptional code for cell fates in the neural tube (Jessell 2000). Based on their transcription factor expression profile, approximately 12 distinct neural progenitor pools can be identified at relatively caudal positions along the embryonic axis, relatively soon after induction. Shh is found to directly control the five most ventral pools, among them progenitors of the very familiar motor neurons. Several classes of GABA-ergic and glutamatergic interneurons essential for regulating motor neuron function within the spinal cord also emerge from Shh-specified progenitor pools (Alaynick et al. 2011).

The Hh pathway recapitulates neural patterning in stem cell culture

Numerous etiologies arise from defects in specific neural cell types. Stem cell biologists have thus taken a vested interest in the patterning molecules at work in establishing neural cell type diversity within the neural tube. The hope was, and still is, that endogenous regulatory molecules might be harnessed *in vitro* to instruct developmentally naïve cells to adopt defined fates for their ultimate therapeutic use. Motor neurons were among the first neural cell types whose differentiation from pluripotent stem cells was demonstrated *in vitro* (Wichterle et al. 2002). This work took advantage of the known ability of mouse embryonic stem cells (mESCs) to both proliferate as undifferentiated cells in culture, and acquire diverse embryonic lineages after aggregation into "embryoid bodies" in the appropriate culture conditions (Martin 1981). While it had been known that embryoid bodies gave rise to neurons, it was reported that retinoic acid, a molecule endogenously involved in embryonic patterning, could much more efficiently direct embryoid bodies into a pro-neural fate (Bain et al. 1995). This protocol can be used to quite efficiently generate tissue derived from mESC lines that mimics the neural tube and expresses molecular markers of dorsal neural fates. Ventral fates can be efficiently induced by exposure to Shh and these cells thus recapitulate the *in vivo* Hh response (Wichterle et al. 2002; Alfaro et al. 2014; Meinhardt et al. 2014).

Hh ligands are morphogens that undergo their own molecular metamorphosis

Hh ligands are secreted lipoproteins first discovered in Nobel Prize winning genetic screens for developmental genes in *Drosophila* (Nüsslein-Volhard & Wieshaus 1980). The *Drosophila* genome encodes a single such molecule, known simply as hedgehog (Hh) (Lee et al. 1992). Its absence of function during embryogenesis, like many other now famous developmental genes, results in a mispatterned larvae lacking "segment polarity." This is manifest by mispatterned denticle belts, structures normally arrayed in a precise, segmented pattern in the larval cuticle.

The Hh gene product was found after cloning in these early studies to act as a secreted paracrine signaling molecule in patterning cell fates in the larval cuticle. Hh expression was soon reported in other *Drosophila* tissues later in development such as the developing wings and legs. In the wing imaginal disc, a previously and since-appreciated model system for developmental signaling, Hh expression is confined to the posterior compartment from which the secreted protein spreads, patterning more anterior cells (Tabata et al. 1992). The *Drosophila* wing disc remains a classic experimental context for investigations into the Hh signaling mechanism (Hooper & Scott 2005; Ingham & McMahon 2001).

In vertebrates this family of ligands has expanded during evolution to include three paralogous ligands. Sonic Hedgehog (Shh) was the first Hh homolog characterized at a molecular level in vertebrates, which followed soon after the molecular description of Hh in *Drosophila* (Roelink et al. 1994; Ingham & McMahon 2001; Briscoe & Thérond 2013; Echelard et al. 1993; Chang et al. 1994; Krauss et al. 1993). It is by far the most well investigated ligand in the family. Leading investigators detected its expressing in several embryonic cell populations known to function as "organizers," signaling centers capable of influencing the cell fates of surrounding cells. These tissues include most famously the aforementioned notochord and floor plate cells situated ventral to the developing neural tube, as well as the zone of polarizing activity (ZPA) in the embryonic limb bud. Prior to Shh's elucidation, these tissues were known as sources of secreted inductive signals (Placzek 1995; Tabin 1991). We now know that Shh is key to patterning neural fates in the embryonic neural tube, a process that is very much the focus of this thesis. Its role as a regulator of limb identity has also become well accepted.

As for the other two Hh homologs in vertebrates, Indian Hedgehog (Ihh) is expressed in fewer embryonic tissues but plays an important overlapping role with Shh in the developing node, and also has well characterized roles in bone development (Long et al. 2004; Zhang et al. 2001). Desert Hedgehog (Dhh) is most intimately known to be associated with gonadal development in mammals, as well as nerve sheath maintenance (Yao et al. 2002; Bitgood et al. 1996; Briscoe & Thérond 2013).

All Hh ligands consist of an N-terminal domain secreted as the signaling peptide after autocatalytic post-translational processing by a C-terminal domain (Porter et al. 1996; Porter et al. 1995). As part of this process, cholesterol acts as a nucleophile, displacing the pro-peptide's C-terminus in an autocatalytic reaction within the endoplasmic reticulum. The original C-terminal domain is displaced in the reaction and has no known function (Porter et al. 1996). Before its maturation as a signaling molecule is complete, Hh ligands undergo another post-translational lipidation at a conserved N-terminal residue, the addition of a palmitate group in a reaction catalyzed by the endoplasmic reticulum localized enzyme Skinny Hedgehog (Ski/Skn) (Chamoun et al. 2001). All of these post-translational events are well conserved throughout animals and are believed to be central to their functional mechanism (Guerrero & Kornberg 2014).

It is noteworthy that Hh ligands retain their signaling ability in the absence of the C-terminal cholesterol adduct when the N-terminal signaling domain is expressed alone. The resulting protein is soluble and of great utility in experiments requiring quantifiable ligand concentrations. It is nevertheless an artificial stand-in for the physiological ligand (Ingham & McMahon 2001; Hooper & Scott 2005).

The high degree of lipidation common to Hh ligands causes them to be highly insoluble and highly associated with cell membranes (Peters et al. 2004; Guerrero & Kornberg 2014). Given these properties, how ligands are transported from their sites of synthesis to recipient cells stands tall as a fundamental mystery. Various models have been advanced to reconcile the insoluble properties of Hh ligands with the fact that they act in many contexts at considerable distances from their sites of synthesis (Zhu & Scott 2004; Guerrero & Kornberg 2014). These models include their possible localization to long, dynamic signaling filopodia called cytonemes, exosomes secreted by multi-vesicular bodies, secreted lipoprotein particles, or shedding from cell membranes after lipid adducts are enzymatically removed (Roy et al. 2014; Palm et al. 2013; Ohlig et al. 2012; Gradilla et al. 2014).

Patched: the oddball transporter/receptor for Hh ligands

Relatively soon after characterizing Hh as a putative signaling molecule, investigators focused on understanding its mechanism of reception and transduction. Another segmental identity gene, Patched (Ptch), emerged as a negative regulator of the Hh signal in the *Drosophila* embryo, and was also a response gene. In its absence other known response genes became inappropriately activated such that denticle patterning was again disrupted (Ingham 1991). Ptch was proposed as a receptor for Hh whose function was restrictive in the absence of signaling. This model found traction in epistatic experiments showing that the Ptch mutant phenotype predominated over the Hh mutant phenotype in double mutants (Bejsovec & Wieschaus 1993).

As appreciation grew for the role of Hh in inducing multiple genes at distinct thresholds of presumed signaling activity within the *Drosophila* imaginal disc, it became obvious that Hh induced Ptch at relatively high levels of Hh signaling in a stripe of several cell diameters from the posterior compartment where Hh is produced (Basler & Struhl 1994). It followed that Ptch has a dual role in endocytosing Hh and allowing its signal to activate target gene transcription in the wing imaginal disc. These studies confirmed its steady state role as a negative regulator (Chen & Struhl 1996).

Vertebrate studies soon showed that a Ptch homolog (now known as Ptch1) is expressed as a conserved response to signaling by Shh in the neural tube and limb bud organizing centers (Marigo & Tabin 1996; Goodrich et al. 1996). Biochemical studies followed demonstrating binding between the non-cholesteroylated N-terminal fragment of Shh and the second extracellular inter-membrane loop domain of Ptch1 (Stone et al. 1996). Genetic loss of function experiments were performed on Ptch1 and appeared to confirm its status as a negative regulator of the downstream Hh pathway in its non-signaling state. $Ptch1^{-/-}$ mouse embryos were reported and display neural tube phenotypes consistent with constitutive over-activation of the pathway, although this phenotype is challenging to interpret for reasons to be discussed further in this thesis (Goodrich et al. 1997). Support for what has become an accepted model has emerged from experiments in both vertebrates and *Drosophila* where alleles of Ptch with mutations in the second extracellular loop act as strong inhibitors of the pathway where expressed, even if close to a ligand source (Briscoe et al. 2001). According to this model, which is still largely observed,

Ptch acts as a constitutive repressor of the pathway whose activity is reversed upon binding to Hh ligands at the cell surface. This allows the pathway to become active. The mechanism at the heart of these events, now known to intimately involve Smoothened (Smo), will be further discussed but is believed to involve the identity of Ptch as a transporter.

Ptch1 seems to play a larger role in vertebrate development than another paralogous protein, which can nevertheless mediate signaling in the absence of Ptch1, and negatively regulate the pathway (Nieuwenhuis et al. 2006; Goodrich et al. 1997; Holtz et al. 2013; Alfaro et al. 2014; Zhulyn et al. 2015). Genetic disruption of Ptch2 in mice has little effect on embryonic development, leading to its being frequently overlooked as a Smo regulator (Carpenter et al. 1998). Ptch2 does however have a recognized role as a tumor suppressor (Smyth et al. 1999; Lee et al. 2006). However, until very recently the developmental role of Ptch2 in tissues where Ptch1 activity is perturbed had been mostly ignored. An outstanding question had been the extent to which Ptch2 mediated signaling by upregulated Shh in $Ptch1^{-/-}$ mice (Goodrich et al. 1997). There now seems to be emerging consensus that in the absence of Ptch1, Ptch2 mediates a number of ligand dependent induction events, in both the neural tube and the vertebrate limb bud (Holtz et al. 2013; Zhulyn et al. 2015). This dilemma applies also to cell lines genetically devoid of Ptch1, where Ptch2 may assume some of its functions. In this thesis will be discussed a number of experiments in which tissue genetically null for both Ptch1 and Ptch2 is assessed in comparison with tissue null for Ptch1 only, supporting this view.

That Ptch2 mediates ligand-dependent, Ptch1-independent signaling is also supported by experiments in which Ptch1 null tissue is directly compared to tissue genetically null for both Ptch1 and Shh, where less signaling is observed, suggesting a role for ligand mediated effects in the absence of Ptch1 only (Alfaro et al. 2014). Interestingly, conserved differences in the C-terminal intracellular domain of Ptch1 and Ptch2 suggest fundamental differences in their stability, and therefore the signaling events they mediate may have differing kinetics and/or dynamics (Kawamura et al. 2008).

Beyond binding and endocytosing Hh ligands during the signaling response, Ptch is noteworthy for belonging to a large family of ubiquitous transporter molecules known as the RND permeases. Proteins in this superfamily act as trimeric transmembrane proton antiporters. As with other RND transporters, conserved acidic amino acid residues required for proton translocation are also required for Ptch function and their mutation can perturb endogenous Ptch function in dominant negative fashion (Alfaro et al. 2014; Taipale et al. 2002; Strutt et al. 2001).

This leads to the inevitable but oft-perplexing conclusion that in mediating the Hh response, Ptch transports a molecule with downstream regulatory effects on the Hh pathway, and that binding to Hh ligands affect this transport process in a manner that stimulates the pathway. A great deal of genetic evidence has emerged to suggest that a third protein, Smoothened (Smo) functions as the target of these effects. The biology of Smo, its interaction with Ptch, and the RND superfamily are discussed below in greater depth.

Smoothened, a GPCR liganded by an unknown Ptch substrate, among other molecules

Smoothened (Smo) initially emerged as a candidate receptor for Hh ligands at roughly the same time as Ptch. It was described in *Drosophila* as phenocopying $hh^{-/-}$ larva, but epistatisis experiments placed it downstream of Hh action. Its cloning revealed Smo to be a G-coupled protein receptor (GPCR) and thus an outstanding candidate as the principle Hh receptor (Alcedo et al. 1996; Van Den Heuvel & Ingham 1996). It was immediately recognized in this pioneering

work that Smo is most conserved with Frizzled, the Wnt receptor and defining member of a GPCR family (Class F). Smo was contemporaneously found to be necessary for Hh pathway transduction in the fly wing, where its mutant phenotype is epistatic to mutations inactivating Ptch, placing it downstream in the pathway (Chen & Struhl 1996). Work later followed supporting this view in vertebrates (Zhang et al. 2001). These initial findings seemed to point toward a receptor complex involving Ptch and Smo.

However, Smo and Ptch were not found to colocalize to a great extent, as predicted by the co-receptor model (Denef et al. 2000). Nor did any convincing evidence emerge of a binding interaction between Smo and Ptch, or Smo and a Hh ligand, from biochemical studies. This led investigators to a new model whereby Smo was subject to negative regulation by Ptch via a mechanism lacking any physical interaction between the two proteins, but rather involving a molecular substrate of Ptch transport. Several important studies reinforced this view by providing evidence that Ptch seemed to inhibit Smo sub-stoichiometrically, in catalytic fashion (Taipale et al. 2002). That Smo regulation by Ptch involves a transport mechanism remains the prevailing model in the field today. Whether Ptch regulates Smo access to a positive regulatory molecule or ensconces Smo in a negative regulator, with either scenario being ligand-reversible, has been debated without clear resolution.

We now know Smo to be the central positive regulator of the Hh signaling response. It is required for and Hh response in practically all contexts in which its genetic loss of function has been investigated (Sharpe et al. 2015; Briscoe & Thérond 2013; Ingham & McMahon 2001; Hooper & Scott 2005). Smo is also a potent oncogene. In addition to becoming activated in tumors via loss of Ptch function, mutations in Smo can render it insensitive to Ptch mediated inhibition and a constitutively active molecule (Xie et al. 1998; Barakat et al. 2010). It has thus attracted a tremendous amount of attention from the field of tumor biology.

Regulation of Smo localization by Ptch

In vertebrates, Smo accumulates in the primary cilium when activated, while in As mentioned previously, this dynamic localization behavior of Smo likely reflects its regulatory relationship with Ptch.

Among the most impactful observations that followed the recognition of Ptch and Smo as key Hh pathway regulators was these proteins extraordinary subcellular localization dynamics. Patched is observed to influence Smo subcellular localization, leading to the segregation of these molecules into different endosomal compartments following exposure to Hh ligands (Incardona et al. 2002; Denef et al. 2000; Zhu et al. 2003). Signaling by Hh in *Drosophila* increases Smo stability at the plasma membrane and recruitment from intracellular vesicles (Denef et al. 2000; Milenkovic et al. 2009; Rohatgi et al. 2007). Studies performed in both mammalian cell culture and also *in vivo* in *Drosophila* largely reinforce this view each other.

A major sea change in the field involved the discovery of intraflagellar transport proteins as important regulators of Hh signaling (Huangfu et al. 2003; Liu et al. 2005). It emerged that these proteins' link to the pathway involved the primary cilium, a signaling organelle found on most vertebrate cells, and subject to a great deal of regulation by intraflagellar transport proteins in very large multi-subunit complexes (Singla & Reiter 2006). Primary cilia became appreciated around this time for not only constituting the anatomical structure underlying sensory signaling by photoreceptors, olfactory receptors and mechanoreceptors, among other cell types, but for also playing host to factors involve in intercellular communication.

Several descriptions of Smo and Gli localization to the primary cilium fueled this uptick in appreciation of this organelle's role in signaling (Corbit et al. 2005). It followed that Ptch also localized to the primary cilium in the absence of Shh, but that upon ligand addition Smo replaced Ptch there (Rohatgi et al. 2007; Milenkovic et al. 2009). It has now become accepted that Hh signaling and primary cilia are meaningfully intertwined, and Smo ciliary localization has become an assay for pathway activation in vertebrates.

Curiously, the extent to which proper Hh signaling requires the primary cilium can be questioned by the observation that embryos null for essential cilia biogenesis genes confer mild phenotypes (Sasai & Briscoe 2012). Embryos null for the ciliary motor proteins Kif3A and Ift88 lack detectable cilia but furnish Hh patterning phenotypes much more mild than those arising from loss of pathway components themselves (Liu et al. 2005; Corbit et al. 2008).

Drosophila lack primary cilia. Smo and Ptch would therefore seem to regulate Hh signaling in a manner independent of the ciliary localization dynamics observed in vertebrates. *Drosophila* Smo associates with proteins homologous to those of the ciliary trafficking complex in vertebrates, such as Costal2, homologue of the kinesin Kif7 (Robbins et al. 1997; Sisson et al. 1997). Hh signal transduction in *Drosophila* may involve similar changes in Smo localization that are obscured by the anatomical absence of a primary cilium.

Smoothened Structure and Function

Recent investigations into Smo have focused on elements of its structure as they pertain to its function. Smoothened possesses the diagnostic architecture of the widespread G-protein couple receptor class of signaling receptors (GPCR). Smo can be more specifically assigned to the Frizzed class (Class F) of GPCRs (MacDonald & He 2012). Interestingly, Frizzleds are well conserved canonical receptors in Wnt signaling, linking Hh signaling to this other prominent developmental signaling pathway at some ancient level (Clevers & Nusse 2012; Hausmann et al. 2009).

Several protein domains are common to both Frizzled and Smoothened. As GPCRs, both possess seven transmembrane helices that cluster into a bundle (Wang et al. 2013). Their N-terminal extracellular domains are comprised of both a linker element, and a cysteine rich domain (CRD) (Myers et al. 2013). The CRD is especially well-conserved, suggesting that Smo binds an endogenous ligand similar to the palmitate moiety of Wnt, which binds Frizzled (Janda et al. 2012).

The c-terminus constitutes an intracellular domain, which packs closely to the membrane in crystals (Wang et al. 2014). Smoothened and Frizzled are defined as Class F GPCRs because of their distinct extracellular CRDs and atypically long, looping, transmembrane domains, which are relatively poorly conserved with other GPCRs (Kristiansen 2004). These long extracellular loops in the transmembrane region also feature disulfide bridges to the linker domain which are conserved between Frizzled and Smo (Wang et al. 2013). Some question has endured whether Smo functions as a legitimate GPCR based on its paucity of associated signaling molecules thought to largely define GPCR-driven signaling cascades. Studies showing that Smoothened can interact with G proteins lay this concern to rest (Riobo et al. 2006; Polizio et al. 2011; Ayers & Thérond 2010).

Evidence has emerged suggesting that Smo is conformationally dynamic, and its activity may be regulated in connection with this property (Zhao et al. 2007). The Smo intracellular domain also exhibits dynamic dimerization as a function of its phosphorylation state (Zhao et al.

2007). Evidence has emerged indicating substantial divergence in the biology of Smo between vertebrates and *Drosophila*. *Drosophila* Smo expressed heterologously in mammalian cells has no function, but becomes constitutively active when the intracellular c-terminus is replaced with the mammalian c-terminus (Myers et al. 2013). This may suggest that Smo has evolved differing sensitivities to endogenous regulators of its activities, or may be under the control of different endogenous regulators altogether.

Synthetic and naturally occurring molecules have been identified that bind Smo and regulate its activity, both as antagonists and agonists (Sharpe et al. 2015). Structural studies of Smo have been performed in conjunction with many of these molecules, with some insights having been gained with regard to Smo function. Molecules found to regulate Smo activity can be broadly categorized into two groups, those binding the CRD and those found to bind the heptahelical bundle. I will review molecules in both classes.

Smoothened regulation by small molecules at the transmembrane heptahelical domain

The first molecule discovered to inhibit Smo activity was cyclopamine. A steroid-like molecule, its discovery stemmed from investigations into birth defects, including cyclopia, in range animals who consumed the wild plant *Veratrum californicum* (Keeler & Binns 1968). It was pointed out that phenotypes associated with cyclopamine exposure during gestation were similar to those that arise from perturbations in Shh function, including most notably unmistakable loss of midline patterning in the central nervous, resulting in cyclopia (Chiang et al. 1996; Roessler et al. 1996). This led to its introduction as an anti-cancer drug, used to control medulloblastomas with some success (J K Chen et al. 2002). It was then established that cyclopamine likely functioned at the level of Smo modulation, based on the observations that it inhibited Smo in the absence of Ptch and that it had reduced effect on oncogenic Smo mutations (Taipale et al. 2000).

Biochemical studies followed demonstrating that cyclopamine perturbs Smo function through direct binding, and this binding event was lost in Smo alleles with deletions in the heptahelical domain (J K Chen et al. 2002). Ptch1 was found to promote the association of Smo with cyclopamine in a Shh reversible manner, suggesting that it may be directly involved in its transport. Cyclopamine binding to the heptahelical domain is a property shared by other Smo antagonists, such as SANT-1 and vismodegib and cannabinoids (Khaliullina et al. 2015).

Heptahelical binding is not a property exclusive to Smo antagonists, however, as shown by the heptahelical binding of the known Smo activator SAG (Frank-Kamenetsky et al. 2002; Wang et al. 2014). The Smo agonist purmorphamine also binds to the heptahelical bundle (Sinha & Chen 2006). It is interesting to note that a given molecule's effect on Smo activity cannot be predicted based alone on its binding to the heptahelical domain (James K Chen et al. 2002).

Structural studies have been performed on Smo complexed with several of these small molecules, and these suggest that they bind to distinct to sites within the heptahelical bundle (Wang et al. 2014; Wang et al. 2013; Weierstall et al. 2014). Cyclopamine binds Smo relatively superficially within the hydrophobic pit defined by the heptahelical domain's extracellular loops (Weierstall et al. 2014; Sharpe et al. 2015). SANT-1 binds much deeper within the hydrophobic pit (Sharpe et al. 2015). In these studies SAG was found to bind at a very similar location as cyclopamine, relatively superficially within the hydrophobic heptahelical pit, but to contact different residues (Wang et al. 2014). In these studies, many of the residues identified as contacts in crystals are affected by oncogenic mutations in Smo (Sharpe et al. 2015; Xie et al. 1998).

It has also emerged that SANT-1 inhibits Smo at equivalent concentrations in the presence or absence of SAG or Shh, solidifying that Ptch-mediated Smo inhibition, and SAG activation, act at steps distinct from ciliary localization. In agreement with this two-step mechanism, SANT-1 can inhibit the SmoM2 oncogenic allele, which is refractory to regulation by Ptch, while this study also demonstrated that Smo ciliary localization is insufficient for Smo activation (Rohatgi et al. 2009).

It had previously been shown that SAG is sensitive to the degree of Ptch mediated Smo repression, suggesting that SAG acts further downstream in the kinetic pathway to Smo activation (James K Chen et al. 2002). The same can be said of SAG with regard to cyclopamine, as in this same study SAG was found to fully rescue the effect of cyclopamine on Smo activity. Finally, this impactful study demonstrated that cyclopamine can overcome the effect of oncogenic Smo alleles becoming refractory to Ptch-mediated suppression, leading to declining Smo activity, but that this effect is in turn overcome by SAG.

A common assay in inferring commonality between Smo binding sites at the heptahelical domain has been competition for a fluorescently labeled cyclopamine analog (James K Chen et al. 2002). Notably, despite binding different sites within the hydrophobic pit defined by the heptahelical domain, SANT-1 and cyclopamine compete in this assay, illustrating its limitations. The antifungal molecule itraconazole, a Smo inhibitor approved like vismodegib for clinical use, does not compete for cyclopamine in this assay, interestingly (J. Kim et al. 2010).

Different Smo antagonists, despite binding in the same hydrophobic binding pocket, have different effects on the subcellular localization of Smo. Interestingly, cyclopamine is observed to promote Smo accumulation in the primary cilium. By contrast, SANT-1and vismodegib prevent its ciliary localization (Rohatgi et al. 2009). This has led to the view that Smo adopts multiple conformational states, with at least one promoting ciliary localization and another promoting its activation, with the two states not being obligately linked kinetically as part of the response (Wilson et al. 2009; Zhao et al. 2007).

Smoothened regulation by small molecules at the CRD

Frizzled receptors bind lipidated Wnt ligands via structural complementarity between the ligand's palmitoyl adduct and the Frizzled CRD (Janda et al. 2012). While it is tempting speculate that a similar interaction might exist between Smo Hh ligands, which are also palmitoylated, none has been reported. It was first reported that a Smo allele lacking the CRD (named SmoΔCRD) retained normal Ptch regulation, suggesting that the CRD does not mediate this effect (Taipale et al. 2002). This study did not in fact unmask any functional consequences for deletion of the CRD and demonstrated a similar level of baseline activity as the wild-type allele, an observation that begs for reconciliation with the fact that the Smo CRD is highly conserved between *Drosophila* and vertebrates and the finding that mutations in the CRD affect signaling (Ayers & Thérond 2010; Myers et al. 2013).

An answer to this puzzle emerged from studies that reported Smo activating properties of molecules in the oxysterol family. It had been generally accepted that normal sterol biogenesis was required for a fully functional Hh response and that pathway antagonists acted independently of this requirement (Cooper et al. 2003; Incardona et al. 2000). It had also been observed that defects in sterol biogenesis did not affect the activity of constitutively active Smo allele found in basal cell carcinoma (Lewis et al. 2001; Xie et al. 1998). Medulloblastomas, a cancer associated with Hh pathway overactivation, were found to develop in mice lacking full

Ptch1 function, and this in turn was found to require normal sterol biogenesis. Known analogs of intermediates in sterol synthesis were then added back singly in an attempt to rescue this effect and establish necessity and sufficiency for activating the Hh pathway (Corcoran & Scott 2006). 25-O-Hydroxycholesterol and 22-O-Hydroxycholesterol were found to directly stimulate Smo in this manner.

The original conclusion was that these intermediates in the sterol synthesis pathway are necessary for signal transduction. Oxysterols were proposed as the Ptch cargo, in a model where Ptch sequestered them from Smo, preventing its activation. However, it was not easy to reconcile the Smo-activating properties of oxysterols with the observations that other intermediates in the sterol biogenesis pathway, when accumulated by pharmacological or genetic disruption of the pathway, silenced the pathway (Cooper et al. 1998; Cooper et al. 2003). For example, the genetic disorders Smith-Lemli-Opitz (SLO) and desmosterolosis are implicated in holoprosencephaly, itself linked to impaired Hh signaling in development (Wassif et al. 1998; Waterham et al. 1998). Drugs that result in 7-dehydroxycholesterol accumulation also silence the pathway in chick neural tube explant assays (Incardona et al. 1998). This repressive function was attributed to the 7-DHC derivative Vitamin D, which interestingly was proposed to function non-cell autonomously via a secretion mechanism, in another report (M F Bijlsma et al. 2006). This finding is supported by a more recent finding that calcitriol, in a Vitamin D product, can also regulate Smo negatively (Linder et al. 2015). It thus seemed at this time that sterol synthesis pathways were necessary for the cellular accumulation of molecules with opposing effects on Smo (Bijlsma 2006). Around the same time, this model was confused by a report that 7-DHC reductase acted as a negative regulator of Hh signaling, despite its most obvious function in depleting 7-DHC , itself a Smo inhibitor (Koide et al. 2006).

Oxysterols were next implicated in Hh signaling as modulators of osteogenesis, an example of the many biological processes regulated by Hh signaling that nevertheless escape a great deal of attention from non-specialists (Dwyer et al. 2007). 20(S) and 22(S) hydroxycholesterol were known to stimulate osteogenesis in a stem cell model and this report demonstrated that this was via Smo activation. Cyclopamine blocked this response but neither molecule was found to compete with labeled cyclopamine for binding to Smo, suggesting that these classes of molecule acted at different Smo binding sites.

More recent reports tested whether endogenous oxysterols found to activate an unrelated GPCR with a ligand binding pocket similar to Smo, also activate Smo. These oxysterols, 7keto-25-hydroxycholesterol and 7keto-27-hydroxycholesterol were found to activate Smo in a CRD-dependent manner, along with several other oxysterols (Myers et al. 2013). These molecules were displaced by a synthetic inhibitor, 22-azacholesterol, that was also found to bind the Smo CRD, but which had no effect on the binding of Smo modulators shown to bind at the hepthelical domain (Nedelcu et al. 2013). It was thus shown that the Smo CRD is a site vulnerable to negative regulation, in addition to the site of stimulations by agonists.

Interestingly, this inhibitor perturbed signaling by Shh, which would otherwise be assumed to function entirely independently of the CRD, given that its only known receptor is Ptch, and Ptch can fully regulate SmoΔCRD (Myers et al. 2013). Kinetic studies suggested however that this was a non-competitive interaction with Shh, suggesting that Shh does not actually bind the CRD but secondarily affects the activity of a molecule there. Hydroxycholesterols binding at the CRD of Smo were found to promote ciliary localization at levels equivalent to SAG (Nedelcu et al. 2013).

Endogenous hydroxycholesterols were also shown to activate Smo alleles lacking residues necessary for cyclopamine inhibition, lending further support that cyclopamine and oxysterols act allosterically. This was in agreement with other studies showing a lack of competition between oxysterols and cyclopamine for Smo binding, as well as the finding that oxysterols could stimulate Smo co-localization with Ptch1 in the primary cilium, suggesting that its agonism was distinct from Ptch-mediated inhibition (Dwyer et al. 2007; Nachtergaele et al. 2012; Rohatgi et al. 2007). Sterol depletion was found to inhibit SmoCRD, as well as SAG mediated Smo activation. In addition to being unresponsive to oxysterols, SmoCRD had elevated baseline activity and also diminished response to ShhN (Myers et al. 2013).

Importantly, SmoCRD is susceptible to Ptch-mediated inhibition. Biochemical binding assays were used in multiple studies to confirm that the Smo CRD mediates binding to 20(S) and 22(S) hydroxycholesterol (Myers et al. 2013; Nachtergaele et al. 2012; Nedelcu et al. 2013). Residues of the Frizzled CRD found to be necessary for lipidated Wnt binding were perturbed in the Smo CRD in order to the test the hypothesis that the physical interaction with oxysterols is homologous to that of the Wnt-Frizzled complex, and this hypothesis was confirmed (Janda et al. 2012; Myers et al. 2013).

These studies thus point toward a general consensus that Smo is susceptible to the action of a number of regulatory molecules. Sterol synthesis seems to be required, regardless of whether the CRD is intact, although oxysterols are demonstrated to act there. Sterol synthesis is also required for activation of Smo alleles defunct for cyclopamine binding, suggesting yet another allosteric binding site. It is important to note that SmoΔCRD seems to have normal cilia localization, suggesting that there are parallel pathways leading to Smo ciliary localization, both CRD-dependent and CRD-independent. Agonists acting at the CRD can promote ciliary localization, as can agonists acting at the heptahelical domain, but the CRD is not required for ciliary localization (Nedelcu et al. 2013; Myers et al. 2013; Dwyer et al. 2007; Rohatgi et al. 2007).

Altogether these studies illustrate rather clearly that oxysterols can activate Smo at the CRD domain. This mode of regulation seems, but is not entirely proven, to be distinct from Ptch, which by all accounts represses Smo via regulating the activity of molecules acting at the heptahelical domain. Oxysterols do not seem to bind the SSD domain, an argument favoring Ptch-independency of oxysterol action (Radhakrishnan et al. 2004). These studies also do not prove a role for oxysterols, despite the fact that they are endogenous molecules. Relatively high concentrations are required, and may result in off target effects or artifacts (Sharpe et al. 2015). Oxysterols may simply mimic a true endogenous Smo regulator. This view is possibly reinforced by observations that other, less related molecules also act as Smo CRD agonists, such as glucocorticoids (Rana et al. 2013).

Each structure-function study published to date reinforces that binding elements required for oxysterol binding resemble those required for palmitate binding in the Wnt-Frizzled interaction. It remains possible, particularly in light of the observation that the Smo CRD is required for high level activation by Shh, that Shh binds and activates Smo through binding to the CRD. Recent structural studies of the CRD of Zebrafish Smo highlight its similarity to the palmitate binding groove of Frizzled (Nachtergaele et al. 2013). It is also noteworthy that mutations inspired by the CRD structure and predicted contacts with oxysterols, perturb signaling but in degrees inconsistent with the predicted magnitudes of their effects (Myers et al. 2013; Nedelcu et al. 2013; Nachtergaele et al. 2012). Oxyterols may simply be functioning as proxies of the truly relevant Smo CRD regulator, and that regulator may be palmitoylated Shh.

This radical thought necessitates a signaling system devoid of Ptch if it is to be rigorously evaluated.

Dispatched: a Patched-like RND required for Hh ligand secretion

The final upstream Hh pathway component necessitating discussion for the purposes of this thesis is Dispatched (Disp), a relative of Ptch and fellow member of the RND superfamily. Disp is required for the release of Hh ligands from cells in which they are expressed, and for their activity at a distance, as paracrine signaling molecules (Etheridge et al. 2010; Ma et al. 2002; Kawakami et al. 2002; Burke et al. 1999; Tian et al. 2005). Members of the Dispatched family are curiously understudied relative to other protein families important for Hh signaling, which is striking given that in their absence, Hh signaling is abrogated nearly to the same extent as loss of ligand, or loss of Smo. As an RND, Disp functions as an obligate trimeric proton-driven co-transporter (Nikaido & Takatsuka 2009; Etheridge et al. 2010). Like Ptch, its substrate is unknown. Like other eukaryotic RNDs, little is known about its mechanism of action.

Disp was discovered in a genetic screen in *Drosophila*, where it was shown to prevent Hh signaling at multiple distances within fly wing discs (Burke et al. 1999). Notably, Hh was observed to signal normally in a juxtracrine fashion and some support exists for this observation in the *Disp1*$^{-/-}$ mouse, where signaling mediated by Shh is entirely defunct except for the notochord, the original Shh source during embryonic neural tube patterning. The notochord is observed to develop normally, on contrast to *Smo*$^{-/-}$ mice, where Hh signaling is entirely absent. One interpretation of this observation is that autocrine and juxtacrine signaling is normal in *Disp1*$^{-/-}$ embryos (Ma et al. 2002; Kawakami et al. 2002). It has been established that Disp1 is necessary for Ihh secretion, as well as Shh (Tian et al. 2005).

Dispatched2 (Disp2), the paralog of Disp1 in vertebrates, is uninvestigated beyond the observation that unlike Disp1 it does not facilitate the release of Shh in heterologous tissue culture experiments (Ma et al. 2002). As with Ptch, mutations in conserved acidic residues required for proton co-transport impair Disp in dominant negative fashion, establishing a requirement for its catalytic transporter activity in mediating ligand secretion (Etheridge et al. 2010; Ma et al. 2002). Intriguingly Disp2 lacks these acidic residues, and this oddity is conserved in vertebrates.

It has been reported that while Disp is required for secretion of fully mature, dual-lipidated Hh ligands, uncholesteroylated Shh can be secreted from cells lacking Disp function (Etheridge et al. 2010). Disp also has a conserved sterol sensing domain (SSD, discussion to follow) linking it to sterol transport. Early models held that the cholesterol moiety and Disp secretion were intimately linked. This connection may not be as direct as once envisioned. However, this is a difficult question to directly address based on the paucity of mechanistic evidence available. I will now investigate the RND superfamily in greater depth in an effort to reconcile mechanistic questions about Ptch and Disp.

The RND permease protein family

Efforts to mechanistically dissect the Hh pathway are invariable forced to reconcile known roles of Ptch and Disp with the fact that these molecules are transporters belong to the RND permease family. RND (resistance-nodulation-division) transporters are famously one of five transporter superfamilies involved in antibiotic resistance in pathogens (Delmar et al. 2014).

It is in this context that they are most studied, given the gravity of antibiotic resistance as a medical challenge. However, they are also vital to the homeostasis and normal biology of all prokaryotes investigated, functioning to dispose of metabolic wastes, regulate biofilm formation, and buffer against high concentrations of myriad molecules in diverse natural environments (Anes et al. 2015). RNDs are ubiquitous throughout all life forms and have been divided into seven classes based on their phylogenetic distribution and substrate specificity. Three families are specific to gram-negative bacteria and are the best understood mechanistically, while another designates RNDs in eukaryotes. Because many of the RNDs investigated in eukaryotes possess a domain known as the sterol sensing domain (SSD), this class of RNDs is frequently referred to as the RND-SSD family (Incardona 2005).The remaining RND families in far flung, diverse organisms are largely unexplored (Saier & Paulsen 2001). While this thesis is principally concerned with the RND-SSD family, RNDs are best understood from a mechanistic point of view in gram negative bacteria, necessitating their review.

Mechanistic insights into RND permease function in gram-negative bacteria

RNDs are extensively studied in gram negative bacteria, where they contribute to a larger order efflux complex that directly bridges both the inner and outer bacterial membranes. These complexes are remarkable for their ability to actively transport myriad molecular cargos out of bacterial cells. They utilize the ubiquitous electrochemical pH gradient arising from proton accumulation in the periplasm, or intermembrane space, of all prokaryotic cells, to energetically drive transport. To illustrate RND versatility in transport, consider that only within elucidated RNDs in E. coli, of which seven have been described, cargoes as diverse as Beta-lactam antibiotics, steroid hormones, benzene, fatty acids, SDS, ethidium bromide and heavy metals find their way out of bacterial cells through RND transporters (Anes et al. 2015). Between the seven described RNDs in E. coli, only broad level cargo specificity exists, with one class transporting hydrophobic and amphipathic substrates and a second class principally found to transport metal ions (Nikaido & Pagès 2012; Anes et al. 2015).

RND transporters are understood to form obligate trimeric complexes in the inner bacterial membrane where their function is absolutely dependent on proton accumulation in the periplasm for energetic coupling (Nikaido 2011). Structure-function studies have been performed on several E. coli RNDs by expressing the entire RND as a giant homotrimer, bypassing its endogenous assembly process (Anes et al. 2015). One RND, AcrB, was co-crystalized with a number of cargos, all of which bound to the transmembrane region (Seeger et al. 2006; Murakami et al. 2006; Murakami et al. 2002). These crystals revealed different conformations for each monomer within the trimer, suggesting that they operate together as a “peristaltic” pump. These structures also suggest that cargo molecules can move through trimeric complexes several different ways, and much debate has arisen regarding their transport route through the trimer. It was originally assumed that substrate molecules entered through the central transmembrane pore defined by the three monomers and were transported from the cytoplasm to the periplasm. The first structural studies made clear that substrates can also enter the complex from the periplasm through a second entry point toward the side of the complex. In both cases, a proton is obligately transported in the opposite direction from the periplasm to the cytoplasm by contacting acidic residues in a relay mechanism that is less controversial (Murakami et al. 2006; Seeger et al. 2006).

The remarkable flexibility in possible routes taken by RND substrates may explain how RNDs can actively transport such a variety of molecules. Most cargoes have a lipophilic domain but how capture from a cell membrane occurs is not well understood in any case (Anes et al. 2015). There is growing traction for the model whereby all RND efflux cargoes in bacteria are captured from the inner membrane or periplasm, and that the transmembrane pore in the inner membrane defined by the RND trimer is only used for proton translocation (Nikaido & Takatsuka 2009; Nikaido & Pagès 2012). This view is predominantly based on findings that point change mutagenesis and intermolecular domain swapping affects substrate specificity only when performed on periplasmic domains. Still, abundant evidence exists to support multiple transport mechanisms for different cargoes, such as different classes of inhibitors that compete with some but not other substrates, suggesting distinct binding sites. Crystal structures of AcrB complexed with several different substrates support this view (Seeger et al. 2006; Murakami et al. 2006).

A highly homologous E. coli RND, AcrD, has also been extensively examined both with regard to structure and function. Mechanistically it is thought to share its primary features with AcrB but has differing substrate specificity (Aires & Nikaido 2005). Exchanging the external (periplasmic) domains of these two RNDs in chimeric molecules caused cargo specificity to change to match the identity of the RND whose periplasmic domains were present, suggesting that the periplasmic domain is responsible for defining what cargoes are transported.

Still other E. coli RNDs are interesting with regard to the fact that unlike AcrB/D, they function as heterotrimers. MdtBC is an obligately heterotrimeric complex comprised of two MdtB monomeric subunits and one MdtC monomer, whose sequence homology is 49% (H.-S. Kim et al. 2010). While no structural data exists for this complex, there is some evidence that these subunits are functionally distinct, with MdtC principally involved in binding and extruding cargoes while MdtB is principally responsible for proton binding and the ensuing conformational change (H.-S. Kim et al. 2010).

Several lines of evidence beyond the crystal structure mechanism build a strong case for proton flux being indispensable for the RND transport mechanism. While RNDs are difficult to target specifically using pharmacological approaches, compounds that disrupt the proton motive force in bacteria also inhibit RND function (Ikonomidis et al. 2008). RNDs also require a pH gradient for transport when reconstituted on proteoliposomes (Zgurskaya & Nikaido 1999). Genetic studies have solidified in a number of bacterial RNDs that conserved acidic residues in the fourth transmembrane domain are necessary for proton transport. When substituted for non-charged residues, RND pump action in several assays is lost, despite no changes in the stability of the trimeric complex (Guan & Nakae 2001; Goldberg et al. 1999). This has also been observed for Disp1, Ptch1 and Ptch2, as will be discussed further (Etheridge et al. 2010; Alfaro et al. 2014).

A speculative but intriguing mechanistic possibility for RND function in the Hh signaling emerges from what is known about RND function in prokaryotes. Because most RND substrates are at least partially lipophilic, and presumably partially membrane associated, and because they can be captured from the periplasmic space, it remains possible that these molecules can energetically couple lipid extraction from the membrane to proton transport. How lipophilic substrates are captured by RNDs is unclear in prokaryotes, much less animals, but can presumably occur from either leaflet in the inner membrane. In animals, where there is only one cell membrane, Ptch and/or Disp may function as lipid flippases. There is some tangential support for this hypothesis in the fact that NPC1 transports lipids into lysosomes and *C. elegans*

RNDs are involved in membrane curvature. This hypothesis had been previously entertained for the capture of RND substrates in E. coli as well (Nikaido 1996; Nikaido & Takatsuka 2009).

Cholesterol transport by the RND-SSD NPC1

NPC1 takes its name from Nieman-Pick disease, a fatal autosomal recessive disorder typified by impaired cholesterol and sphingomyelin transport from late endosomes and lysomes, a cellular defect with devastating consequences on the nervous system in patients (Karten et al. 2009). A colony of mice with similar phenotypes was also identified, and used to pinpoint the genetic cause of the defect to an RND transmembrane protein that took the name NPC1 (Loftus et al. 1997). It was later confirmed that the same protein was perturbed via a number of mutations in 95% of human Nieman-Pick disease pedigrees, as well as in one case a family of cats (Carstea et al. 1997; Karten et al. 2009). NPC1 appears to be well conserved, as homologs are recognizable and have been investigated in *Drosophila* and yeast. In both cases, lipid metabolism is perturbed in a manner consistent with an ancient role for these proteins in lipid transport (Huang et al. 2005; Malathi et al. 2004). It is now thought that NPC1 represents a family of molecules with ubiquitous roles in eukaryotes in regulating the transport of cholesterol from endosomes, after it is taken up from the extracellular environment, to the cytoplasm. NPC1 seems to be expressed in all cells and likely has a ubiquitous role in this process (Karten et al. 2009). This process involves a soluble protein, NPC2, that likely serves to shuttle cholesterol after NPC1-mediated transport (Infante et al. 2008). A related molecule, NPC1-like1, has also been characterized in mammals. It seems to be necessary for cholesterol uptake from the extracellular environment (Yu 2008).

NPC1 is atypical in that it possesses one additional transmembrane domain at its c-terminus in addition to the normal 12 transmembrane domains that characterize RND proteins. It also contrasts with other well-studied RNDs, both in eukaryotes and bacteria, in that its largest non-integral domains face in the opposite topological direction, relative to the N-terminus (Carstea et al. 1997). NPC1 has been found to localize to the intraluminal vesicles and limiting membrane of multivesicular endosomes (Patel et al. 1999; M. Zhang et al. 2001).

NPC1 comes into clearer view as a eukaryotic RND and relative of Ptch and Disp when one takes into account its possession of a recognizable sterol sensing domain (SSD) (Karten et al. 2009; Nohturfft et al. 1999; Nohturfft et al. 1998). This domain spans five transmembrane helices and is shared by transmembrane-spanning regulatory proteins in the famous cholesterol synthesis pathway. This domain has been demonstrated to directly bind cholesterol and cholesterol derivatives and mutations in this domain perturb cholesterol binding (Nohturfft et al. 1998). Mutations that affect the SSD in NPC1 are common in disease families (Karten et al. 2009). It is thus reasonable to conclude that NPC1 directly binds cholesterol as part of the transport process that goes so horribly awry in the disease state, and this has more recently been shown in biochemical assays with NPC1 (Ohgami et al. 2004).

Frustratingly, for the purposes of inferring functions for Ptch/Disp based on NPC1, the mechanism whereby NPC1 regulates export from intraluminal vesicles to the cytoplasm is unclear. Nevertheless, it seems reasonable to postulate, based on its loss of function phenotype, identity as an RND and possession of a SSD, that NPC1 captures cholesterol and cholesterol-like molecules from intraluminal vesicle membranes with high lipid concentrations, after their uptake. This process is presumably proton driven and thus likely reserved to the step in which cholesterol is extracted from intraluminal membranes, where a proton gradient is established and

could be harnessed for this process. According to this view, localization to the outer membrane of multi-vesicular endosomes is incidental to cholesterol transport and may represent an intermediate state in inner vesicle formation. A view that has received attention, like with bacterial RNDs, is the possibility that NPC1 functions as a lipid flippase, facilitating the exchange of cholesterol between inner membrane leaflets, promoting budding of smaller membrane bound compartments and facilitating their transport within the multivesicular endosome. A non-mutually exclusive possibility is that the same mechanism is used to facilitate lipid exchange between the outer limiting membrane and other membrane bound compartments in the cell, such as the ER (Ko et al. 2001).

Patched and Dispatched-like RND-SSDs as abundant regulators of morphogenesis in *C. elegans*

Soon after the recognition of Ptch as the Hh signaling receptor, and Disp as another key regulator, RND protein homologs were described in *C. elegans*. This came as a surprise due to the absence of Hh ligands or Smo in the *C. elegans* genome, and thus the apparent lack of a Hh signaling pathway. Stunningly, thirty genes were described from genome searches encoding predicted proteins with RND membrane topology and SSD domains, placing them in the Ptch/Disp/NPC1 RND class (Kuwabara et al. 2000; Kuwabara & Labouesse 2002). To date, four have been investigated using genetic tools available in the *C. elegans* system.

The nearest Ptch1 homolog in *C. elegans*, ce-Ptc1, was the first such RND to be investigated in a genetic loss of function experiment. RNAi Kkockdown and mutant animals displayed defects in their gonads, where membrane furrows in syncytial germ cells are necessary for proper gametogenesis (Kuwabara et al. 2000). Not long after, another RND protein, Che-14, found to more resemble Disp, was targeted. Che-14$^{-/-}$ animals displayed defects in the formation of tubular sensory structures called amphids, due to inappropriate membrane morphogenesis (Michaux et al. 2000). These structures are defined by curved membranes from surrounding cells that envelop a luminal space, and are well studied as an animal model for the morphogenesis of luminal structures. In the absence of Che-14 this channel is lost amid myriad disorganized vesicles (Michaux et al. 2000). Other tubular luminal structures, for example the gut, are similarly disorganized. Daf-6, another gene encoding a Ptch-like protein, resulted in similar defects in amphid structures when perturbed (Perens & Shaham 2005). More dramatic effects were observed in a variety of enveloped luminal structures in che-14/daf-6 double mutants, suggesting overlapping functions for these genes' products (Perens & Shaham 2005). Another *C. elegans* gene similar to Ptch, ce-Ptc3, was found to be essential, required intact acidic channel residues for function, but not an intact SSD, and likely regulates excretion as mutant phenotypes primarily affected physiology but not structure of the excretory system (Soloviev et al. 2011).

In fusion protein experiments, both daf-6 and che-14 localized to apical membranes in cells surrounding tubular lumen membranes and also to a lesser extent in vesicles near the apical membrane surfaces defining the lumen. Daf-6 is unusual because it lacks the conserved acidic residues in the SSD found in other RNDs, although it is possible that it trimerizes with Che-14 or another *C. elegans* RND that can supply acid residues in a functional heterotrimer. The model for Daf-6 action in the amphid was later expanded to suggest that it has a role in limiting the amount of membrane expansion that can occur during amphid lumen formation, assigning it a fundamentally negative role (Oikonomou et al. 2011). Because the extracellular loops of Daf-6 were found to be important for its function, as with Ptch, these experiments raised the interesting

question whether a molecule derived from neural cells within the amphid channel might signal to Daf-6, blocking its function and allowing the luminal membrane to expand.

The sterol sensing domain

The sterol sensing domain (SSD) that is seemingly vital to Ptch/Disp/NPC1 function, and presumably each member of the RND-SSD family in eukaryotes, was first described in several proteins vital to mammalian cholesterol homeostasis. These include the endoplasmic reticulum localized integral proteins HMG CoA Reductase (HMGR) and SREBP cleavage activating protein (Scap) (Goldstein et al. 2006). Both of these proteins promote cholesterol biogenesis via different mechanisms. In brief, these molecules' activities are sensitive to the presence of cellular cytoplasmic cholesterol. When cellular cholesterol concentations are high, they are negatively regulated via a mechanism thought to involve direct binding to the SSD.

Cholesterol homeostasis represents a fascinating and important process involving both environmental uptake as well as biogenesis. Interestingly, some animals do not have an intact cholesterol biogenesis pathway, and this includes *Drosophila*. A great many molecules are derived from cholesterol via many biochemical pathways (Chang et al. 2006). Cholesterol biogenesis is notably absent in *Drosophila* despite the importance of many cholesterol-derived molecules, such as steroid hormones, for insect development and homeostasis. Rather few protein families possess a sterol sensing domain, and rather little is known about its biophysical mechanism of function.

Key residues that are important for cholesterol binding to SCAP, the best studied cholesterol binding protein with an SSD, are conserved in Ptch. However, mutations in the SSD in Ptch1 do not seem to abrogate Smo inhibition (Taipale et al. 2002). They do seem to disrupt Ptch function in Flies, according to Strutt 2001 look this up.

Key residues that are important for cholesterol binding to SCAP, the best studied cholesterol binding protein with an SSD, are conserved in Ptch. However, mutations in the SSD in Ptch1 do not seem to abrogate Smo inhibition (Taipale et al. 2002). They do seem to disrupt Ptch function in Flies, according to Strutt 2001 look this up.

Interrogating the SSD-sterol binding relationship at a mechanistic level represents an immense challenge. An *in vitro* assay for sterol binding to the SSD of Scap exists (Goldstein et al. 2006; Radhakrishnan et al. 2004) and it shows cholesterol binding but not hydroxysterol binding. Ptch therefore may not transport hydroxysterols.

Arguments that RND-SSDs likely function in acidified compartments

The RND proton translocation mechanism suggested by crystal structures of bacterial transporters suggests that RND transport cargoes in a manner obligately linked to proton flux (Nikaido & Takatsuka 2009). It follows that these trimeric transporters are found in membranes separating compartments differing with respect to pH. This is no surprise in bacteria, where the periplasm is acidic. It is a potentially large clue as to how eukaryotic RND-SSDs function.

Several observations confirm the necessity of proton translocation for the RND-SSDs Disp and Ptch. When conserved acidic residues necessary for proton transport are lost, Ptch no longer represses Smo in *Drosophila* (Strutt et al. 2001). The same can be said for Disp1 in vertebrates, where expression of a construct lacking acidic channel residues has dominant negative inhibitory activity (Etheridge et al. 2010). The same can be said for Ptch1 and Ptch2,

although it is more challenging to interpret their consequences of misexpression. A Ptch1 allele lacking ligand binding acts as a dominant repressor of Smo (Briscoe et al. 2001). This allele nevertheless has no effect when acidic channel residues are substituted (Alfaro et al. 2014). Overexpressing Ptch2 alleles lacking acidic channel residues activates the pathway, consistent with dominant negative effects. However, penetrance is low and may require precise timing of construct delivery (Alfaro et al. 2014). One model that may explain these inconsistencies is a scenario where Ptch1 mutant alleles cannot heterotrimerize and perturb Ptch2 function, allowing Ptch2 to compensate for dominantly inhibited Ptch1 trimers. According to the view the reverse must not be true, and Ptch2 mutant alleles must dominantly inhibit both Ptch1 and Ptch2 trimers, but in a timing specific manner.

Regardless, it can be inferred from this data that Ptch and Disp function in an acidic compartment, such as in the endosomal/lysosomal trafficking pathway. This is consistent with localization studies with overexpressed Ptch, although overexpressed constructs localizing to these compartments is inconclusive (Incardona et al. 2002). More intriguingly in this study, presumptive de-acidification of endosomes with chloroquine blocks the Hh response. So too does anti-LBPA, which targets a specific lipid with possible roles in membrane folding.

Given the established localization of NPC1 to multi-vesicular endosomes, it may be reasonable to suggest that all three eukaryotic RND-SSD families function in compartments within a similar endosomal compartment (Neufeld et al. 1999; M. Zhang et al. 2001). The elucidation of endosomal trafficking pathways leading to exosome production raises the question of whether the Ptch/Disp substrate might be secreted (Record et al. 2014). This would perhaps agree with the role of Disp in mediating Hh ligand secretion.

Arguments for the non-autonomy of Ptch-mediated Smo repression

Patched inhibits Smo cell-autonomously likely by influencing the subcellular localization of a small molecule regulator of its function in a manner reversible upon ligand binding (Sharpe et al. 2015; James K Chen et al. 2002; Taipale et al. 2002). It is widely assumed that such a molecule is a substrate of the proton driven transporter activity it shares with all members of the RND family. Might such a molecule reach the extracellular space and inhibit Smo on other cells in the environment if Ptch functions in an endosome that could enter the exosomal pathway? Several reports lend additional intrigue to this possibility.

One report demonstrated that fibroblasts overexpressing Ptch1 repressed the response in co-cultured cells harboring reporter constructs. Conversely, Ptch1 knockdown activated co-cultured reporter cells (Bijlsma et al. 2006). This effect was also transferable via conditioned medium and analyzing the medium identified vitamin D3 as the Smo inhibitory molecule. Another more recent report identified endocannabinoids in lipoprotein particles in *Drosophila* hemolymph and showed that they inhibit Smo both in flies and vertebrates (Khaliullina et al. 2015). These molecules inhibited Smo activity downstream of ciliary localization, making them candidates for the Ptch substrate.

Hh pathway in cancer

While not central to this thesis, no discussion of Hh signaling is complete without acknowledging this pathway's relevance to tumor biology. Cancers are linked to Hh pathway activation via the inactivation of Ptch as a central negative regulator, mutations in Smo that make it refractory to Ptch-mediated inhibition, and Shh upregulation (Barakat et al. 2010). Ptch1 was first identified as a candidate gene with mutations in Gorlin syndrome, which is typified by increased incidence of basal cell carcinoma (BCC), medulloblastoma (MB) and rhabdomyosarcoma (RMS) (Hahn et al. 1996; Johnson et al. 1996). Mouse models for each of these cancers suggest that Hh pathway activation is sufficient to initiate tumor formation (Barakat et al. 2010).

Gorlin syndrome patients are frequently heterozygous for loss of function alleles in Ptch1, and frequently present tumors with no functional Ptch1 activity (Barakat et al. 2010). Oncogenic mutations in Smo from BCC were identified soon afterwards (Xie et al. 1998). In follow up studies, these Smo alleles (named SmoM2) were found to be refractory to Ptch inhibition. They are thus frequently employed in experiments investigating the signaling mechanism. Smo is thus a classic oncogene, and a great deal of interest has developed in Smo inhibitors as anti-cancer therapies.

Shh is also expressed in many tumor environments in a manner that reinforces tumor growth via a non-autonomous mechanism (Yauch et al. 2008). In several different cancers, including colon and pancreatic cancer, primary tumors express Shh, which signals to stromal cells. This signaling event results in increased signaling, via factors that are ill-understood, that re-inforce tumor growth. For this reason therapies that target the Shh ligand, such as antibodies, have promise. Because cancers often recapitulate normal developmental process, and because so many organs receive Shh signals during development, it should be no surprise that Shh signaling in a paracrine fashion stimulates cancers (Barakat et al. 2010).

While not the focus of this thesis, as many as one third of human cancers are thought to be influenced by inappropriate hedgehog signaling, and these include the most common cancer, BCC, the most common juvenile cancer, MB, the fourth most common, and often very lethal, pancreatic cancer, and myriad others (Barakat et al. 2010). The stakes are thus very high in understanding Hh signaling mechanisms, such that defense mechanisms against their tumorous over-activation can be conceived.

REFERENCES

Adamska, M. et al., 2007. The evolutionary origin of hedgehog proteins. *Curr Biol*, 17(19), pp.R836–7.

Aires, J.R. & Nikaido, H., 2005. Aminoglycosides are captured from both periplasm and cytoplasm by the AcrD multidrug efflux transporter of Escherichia coli. *Journal of Bacteriology*, 187(6), pp.1923–1929.

Alaynick, W. a., Jessell, T.M. & Pfaff, S.L., 2011. SnapShot: Spinal cord development. *Cell*, 146(1), pp.178–178.e1.

Alcedo, J. et al., 1996. The Drosophila smoothened gene encodes a seven-pass membrane protein, a putative receptor for the hedgehog signal. *Cell*, 86(2), pp.221–232.

Alfaro, A.C. et al., 2014. Ptch2 mediates the Shh response in Ptch1-/- cells. *Development*, 141(17), pp.3331–3339.

Anes, J. et al., 2015. The ins and outs of RND efflux pumps in Escherichia coli. *Frontiers in Microbiology*, 6(June), pp.1–14.

Aristotle & Peck, A.L., 1942. *Generation of Animals*, Harvard University Press.

Ayers, K.L. & Thérond, P.P., 2010. Evaluating Smoothened as a G-protein-coupled receptor for Hedgehog signalling. *Trends in Cell Biology*, 20(5), pp.287–298.

Barakat, M.T., Humke, E.W. & Scott, M.P., 2010. Learning from Jekyll to control Hyde: Hedgehog signaling in development and cancer. *Trends in Molecular Medicine*, 16(8), pp.337–348.

Basler, K. & Struhl, G., 1994. Hedgehog, a product of posterior compartment cells in Drosophila, organizes anterior compartment pattern. *NATURE*, 368, pp.208–214.

Bejsovec, A. & Wieschaus, E., 1993. Segment polarity gene interactions modulate epidermal patterning in Drosophila embryos. *Development*, 119(2), pp.501–517.

Bijlsma, M.F., 2006. A dual role for 7-dehydrocholesterol reductase in regulating Hedgehog signalling? *Development*, 133(20), pp.3951–3951.

Bijlsma, M.F. et al., 2006. Repression of smoothened by patched-dependent (pro-)vitamin D3 secretion. *PLoS Biol*, 4(8), p.e232.

Bijlsma, M.F. et al., 2006. Repression of smoothened by patched-dependent (pro-)vitamin D3 secretion. *PLoS biology*, 4(8), p.e232.

Bitgood, M.J., Shen, L. & McMahon, a P., 1996. Sertoli cell signaling by Desert hedgehog regulates the male germline. *Current biology : CB*, 6(3), pp.298–304.

Briscoe, J. et al., 2001. A hedgehog-insensitive form of patched provides evidence for direct long-range morphogen activity of sonic hedgehog in the neural tube. *Molecular cell*, 7(6), pp.1279–91.

Briscoe, J. et al., 2000. A homeodomain protein code specifies progenitor cell identity and neuronal fate in the ventral neural tube. *Cell*, 101(4), pp.435–445.

Briscoe, J. & Thérond, P.P., 2013. The mechanisms of Hedgehog signalling and its roles in development and disease. *Nature reviews. Molecular cell biology*, 14(7), pp.416–29.

Burke, R. et al., 1999. Dispatched, a novel sterol-sensing domain protein dedicated to the release of cholesterol-modified hedgehog from signaling cells. *Cell*, 99(cc), pp.803–815.

Carpenter, D. et al., 1998. Characterization of two patched receptors for the vertebrate hedgehog protein family. *Proc. Natl. Acad. Sci. U. S. A.*, 95(23), pp.13630–13634.

Carstea, E.D. et al., 1997. Niemann-Pick C1 disease gene: homology to mediators of cholesterol homeostasis. *Science*, 277(5323), pp.228–231.

Chamoun, Z. et al., 2001. Skinny hedgehog, an acyltransferase required for palmitoylation and activity of the hedgehog signal. *Science*, 293(5537), pp.2080–2084.
Chang, D.T. et al., 1994. Products, genetic linkage and limb patterning activity of a murine hedgehog gene. *Development*, 120, pp.3339–3353.
Chang, T.-Y. et al., 2006. Cholesterol sensing, trafficking, and esterification. *Annual review of cell and developmental biology*, 22, pp.129–157.
Chen, J.K. et al., 2002. Inhibition of Hedgehog signaling by direct binding of cyclopamine to Smoothened. *Genes and Development*, 16(21), pp.2743–2748.
Chen, J.K. et al., 2002. Small molecule modulation of Smoothened activity. *Proceedings of the National Academy of Sciences of the United States of America*, 99(22), pp.14071–14076.
Chen, Y. & Struhl, G., 1996. Dual roles for patched in sequestering and transducing Hedgehog. *Cell*, 87(3), pp.553–63.
Chiang, C. et al., 1996. Cyclopia and defective axial patterning in mice lacking Sonic hedgehog gene function. *NATURE*, 383(6599), pp.407–413.
Clevers, H. & Nusse, R., 2012. Wnt/β-Catenin Signaling and Disease. *Cell*, 149(6), pp.1192–1205.
Cohen, M. et al., 2015. Ptch1 and Gli regulate Shh signalling dynamics via multiple mechanisms. *Nature Communications*, 6, pp.1–12.
Cooper, M.K. et al., 2003. A defective response to Hedgehog signaling in disorders of cholesterol biosynthesis. *Nat Genet*, 33(4), pp.508–513.
Cooper, M.K. et al., 1998. Teratogen-mediated inhibition of target tissue response to Shh signaling. *Science*, 280(5369), pp.1603–1607.
Corbit, K.C. et al., 2008. Kif3a constrains beta-catenin-dependent Wnt signalling through dual ciliary and non-ciliary mechanisms. *Nat Cell Biol*, 10(1), pp.70–76.
Corbit, K.C. et al., 2005. Vertebrate Smoothened functions at the primary cilium. *NATURE*, 437(7061), pp.1018–1021.
Corcoran, R.B. & Scott, M.P., 2006. Oxysterols stimulate Sonic hedgehog signal transduction and proliferation of medulloblastoma cells. *Proc. Natl. Acad. Sci. U. S. A.*, 103(22), pp.8408–8413.
Cox, D.B.T., Platt, R.J. & Zhang, F., 2015. Therapeutic genome editing: prospects and challenges. *Nature Medicine*, 21(2), pp.121–131.
Delmar, J. a, Su, C.-C. & Yu, E.W., 2014. Bacterial Multidrug Efflux Transporters. *Annual review of biophysics*, (March), pp.1–25.
Denef, N., Perez, L. & Cohen, S.M., 2000. Hedgehog induces opposite changes in turnover and subcellular localization of Patched and Smoothened. *Cell*, in press.
Doudna, J.A., Charpentier & Emmanuelle, The new frontier of genome engineering with CRISPR-Cas9. *Science*.
Dwyer, J.R. et al., 2007. Oxysterols are novel activators of the hedgehog signaling pathway in pluripotent mesenchymal cells. *Journal of Biological Chemistry*, 282(12), pp.8959–8968.
Echelard, Y. et al., 1993. Sonic hedgehog, a member of a family of putative signaling molecules, is implicated in the regulation of CNS polarity. *Cell*, 75(7), pp.1417–1430.
Etheridge, L.A. et al., 2010. Evidence for a role of vertebrate Disp1 in long-range Shh signaling. *Development (Cambridge, England)*, 137(1), pp.133–40.
Frank-Kamenetsky, M. et al., 2002. Small-molecule modulators of Hedgehog signaling: identification and characterization of Smoothened agonists and antagonists. *J Biol*, 1(2), p.10.

G. Bain, D. Kitchens, M. Yao, J.E. Huettner, D.I.G., 1995. Embryonic stem cells express neuronal properties in vitro. *Developmental biology*, 168, pp.342–357.
Gerhart, J., 1999. 1998 Warkany Lecture: Signaling pathways in development. *Teratology*, 60(4), pp.226–239.
Goldberg, M. et al., 1999. Energetics and topology of CzcA, a cation/proton antiporter of the resistance-nodulation-cell division protein family. *J. Biol. Chem.*, 274(37), pp.26065–26070.
Goldstein, J.L., DeBose-Boyd, R. a. & Brown, M.S., 2006. Protein sensors for membrane sterols. *Cell*, 124(1), pp.35–36.
Goodrich, L. V et al., 1996. Conservation of the hedgehog/patched signaling pathway from flies to mice: induction of a mouse patched gene by Hedgehog. *Genes Dev*, 10(3), pp.301–312.
Goodrich, L. V., 1997. Altered Neural Cell Fates and Medulloblastoma in Mouse patched Mutants. *Science*, 277(5329), pp.1109–1113.
Gradilla, A.-C. et al., 2014. Exosomes as Hedgehog carriers in cytoneme-mediated transport and secretion. *Nature communications*, 5, p.5649.
Guan, L. & Nakae, T., 2001. Identification of essential charged residues in transmembrane segments of the multidrug transporter MexB of Pseudomonas aeruginosa. *J Bacteriol*, 183(5), pp.1734–1739.
Guerrero, I. & Kornberg, T.B., 2014. Hedgehog and its circuitous journey from producing to target cells. *Seminars in cell & developmental biology*, pp.1–11.
Hahn, H. et al., 1996. Mutations of the human homolog of Drosophila patched in the nevoid basal cell carcinoma syndrome. *Cell*, 85(6), pp.841–851.
Hartl, T. a. & Scott, M.P., 2014. Wing tips: The wing disc as a platform for studying Hedgehog signaling. *Methods*, 68(1), pp.199–206.
Hausmann, G., Von Mering, C. & Basler, K., 2009. The Hedgehog signaling pathway: Where did it come from? *PLoS Biology*, 7(6).
Van den Heuvel, M. & Ingham, P.W., 1996. Smoothened encodes a receptor-like serpentine protein required for hedgehog signalling. *NATURE*, 382(6591), pp.547–551.
Holtz, A.M. et al., 2013. Essential role for ligand-dependent feedback antagonism of vertebrate hedgehog signaling by PTCH1, PTCH2 and HHIP1 during neural patterning. *Development*, 140(16), pp.3423–3434.
Hooper, J.E. & Scott, M.P., 2005. Communicating with Hedgehogs. *Nature reviews. Molecular cell biology*, 6(4), pp.306–317.
Huang, X. et al., 2005. A Drosophila model of the Niemann-Pick type C lysosome storage disease: dnpc1a is required for molting and sterol homeostasis. *Development (Cambridge, England)*, 132(22), pp.5115–5124.
Huangfu, D. et al., 2003. Hedgehog signalling in the mouse requires intraflagellar transport proteins. *NATURE*, 426(6962), pp.83–87.
Ikonomidis, a. et al., 2008. Effect of the proton motive force inhibitor carbonyl cyanide- m -chlorophenylhydrazone (CCCP) on Pseudomonas aeruginosa biofilm development. *Letters in Applied Microbiology*, 47(4), pp.298–302.
Incardona, J.P. et al., 2000. Cyclopamine inhibition of Sonic hedgehog signal transduction is not mediated through effects on cholesterol transport. *Dev. Biol.*, 224(2), pp.440–452.
Incardona, J.P., 2005. From sensing cellular sterols to assembling sensory structures. *Developmental Cell*, 8(6), pp.798–799.

Incardona, J.P. et al., 1998. The teratogenic Veratrum alkaloid cyclopamine inhibits sonic hedgehog signal transduction. *Development*, 125(18), pp.3553–3562.
Incardona, J.P., Gruenberg, J. & Roelink, H., 2002. Sonic hedgehog induces the segregation of patched and smoothened in endosomes. *Curr Biol*, 12(12), pp.983–995.
Infante, R.E. et al., 2008. NPC2 facilitates bidirectional transfer of cholesterol between NPC1 and lipid bilayers, a step in cholesterol egress from lysosomes. *Proceedings of the National Academy of Sciences of the United States of America*, 105(40), pp.15287–15292.
Ingham, P.W., 1991. Segment polarity genes and cell patterning within the Drosophila body segment [published erratum appears in Curr Opin Genet Dev 1991 Oct;1(3):417]. [Review]. *Current Opinion In Genetics {&} Development*, 1(2), pp.261–267.
Ingham, P.W. & McMahon, A.P., 2001. Hedgehog signaling in animal development: paradigms and principles. *Genes and Development*, 15(23), pp.3059–3087.
Janda, C.Y. et al., 2012. Structural basis of Wnt recognition by Frizzled. *Science*, 337(6090), pp.59–64.
Jessell, T.M., 2000. Neuronal specification in the spinal cord: inductive signals and transcriptional codes. *Nat Rev Genet*, 1(1), pp.20–29.
Jessell, T.M. & Melton, D.A., 1992. Diffusible factors in vertebrate embryonic induction. *Cell*, 68(2), pp.257–270.
Johnson, R.L. et al., 1996. Human homolog of patched, a candidate gene for the basal cell nevus syndrome. *Science*, 272(5268), pp.1668–1671.
Karten, B., Peake, K.B. & Vance, J.E., 2009. Mechanisms and consequences of impaired lipid trafficking in Niemann–Pick type C1-deficient mammalian cells. *Biochimica et Biophysica Acta (BBA) - Molecular and Cell Biology of Lipids*, 1791(7), pp.659–670.
Kawakami, T. et al., 2002. Mouse dispatched mutants fail to distribute hedgehog proteins and are defective in hedgehog signaling. *Development*, 129(24), pp.5753–5765.
Kawamura, S. et al., 2008. Two patched protein subtypes and a conserved domain of group I proteins that regulates turnover. *J. Biol. Chem.*, 283(45), pp.30964–30969.
Keeler, R.F. & Binns, W., 1968. Teratogenic compounds of Veratrum californicum (Durand). V. Comparison of cyclopian effects of steroidal alkaloids from the plant and structurally related compounds from other sources. *Teratology*, 1(1), pp.5–10.
Khaliullina, H. et al., 2015. Endocannabinoids are conserved inhibitors of the Hedgehog pathway. *Proceedings of the National Academy of Sciences*, 112(11), pp.3415–3420.
Kim, H.-S., Nagore, D. & Nikaido, H., 2010. Multidrug Efflux Pump MdtBC of Escherichia coli Is Active Only as a B2C Heterotrimer. *Journal of Bacteriology*, 192(5), pp.1377–1386.
Kim, J. et al., 2010. Itraconazole, a Commonly Used Antifungal that Inhibits Hedgehog Pathway Activity and Cancer Growth. *Cancer Cell*, 17(4), pp.388–399.
Ko, D.C. et al., 2001. Dynamic movements of organelles containing niemann-pick c1 protein: npc1 involvement in late endocytic events. *Mol. Biol. Cell*, 12(3), pp.601–614.
Koide, T., Hayata, T. & Cho, K.W.Y., 2006. Negative regulation of Hedgehog signaling by the cholesterogenic enzyme7-dehydrocholesterol reductase. *Development*, 133(12), pp.2395–2405.
Krauss, S., Concordet, J.P. & Ingham, P.W., 1993. A functionally conserved homolog of the Drosophila segment polarity gene hh is expressed in tissues with polarizing activity in zebrafish embryos. *Cell*, 75(7), pp.1431–1444.

Kristiansen, K., 2004. Molecular mechanisms of ligand binding, signaling, and regulation within the superfamily of G-protein-coupled receptors: molecular modeling and mutagenesis approaches to receptor structure and function. *Pharmacol Ther*, 103(1), pp.21–80.
Kuwabara, P.E. et al., 2000. A C. elegans patched gene, ptc-1, functions in germ-line cytokinesis. *Genes and Development*, 14(15), pp.1933–1944.
Kuwabara, P.E. & Labouesse, M., 2002. The sterol-sensing domain: multiple families, a unique role? *Trends In Genetics*, 18(4), pp.193–201.
Lee, J.J. et al., 1992. Secretion and localized transcription suggest a role in positional signaling for products of the segmentation gene hedgehog. *Cell*, 71(1), pp.33–50.
Lee, Y. et al., 2006. Patched2 modulates tumorigenesis in patched1 heterozygous mice. *Cancer research*, 66(14), pp.6964–71.
Lewis, P.M. et al., 2001. Cholesterol modification of sonic hedgehog is required for long-range signaling activity and effective modulation of signaling by Ptc1. *Cell*, 105(5), pp.599–612.
Linder, B. et al., 2015. A functional and putative physiological role of calcitriol in Patched1/Smoothened interaction. *Journal of Biological Chemistry*, p.jbc.M115.646141.
Liu, A., Wang, B. & Niswander, L.A., 2005. Mouse intraflagellar transport proteins regulate both the activator and repressor functions of Gli transcription factors. *Development*, 132(13), pp.3103–3111.
Loftus, S.K. et al., 1997. Murine model of Niemann-Pick C disease: mutation in a cholesterol homeostasis gene. *Science*, 277(5323), pp.232–235.
Long, F. et al., 2004. Ihh signaling is directly required for the osteoblast lineage in the endochondral skeleton. *Development (Cambridge, England)*, 131(6), pp.1309–1318.
Ma, Y. et al., 2002. Hedgehog-mediated patterning of the mammalian embryo requires transporter-like function of dispatched. *Cell*, 111(1), pp.63–75.
MacDonald, B.T. & He, X., 2012. Frizzled and LRP5/6 Receptors for Wnt/β-Catenin Signaling. *Cold Spring Harbor Perspectives in Biology*, 4(12), pp.a007880–a007880.
Malathi, K. et al., 2004. Mutagenesis of the putative sterol-sensing domain of yeast Niemann Pick C-related protein reveals a primordial role in subcellular sphingolipid distribution. *Journal of Cell Biology*, 164(4), pp.547–556.
Marigo, V. & Tabin, C.J., 1996. Regulation of patched by sonic hedgehog in the developing neural tube. *Proceedings Of The National Academy Of Sciences Of The United States Of America*, 93(18), pp.9346–9351.
Martin, G.R., 1981. Isolation of a pluripotent cell line from early mouse embryos cultured in medium conditioned by teratocarcinoma stem cells. *Proceedings of the National Academy of Sciences of the United States of America*, 78(12), pp.7634–7638.
Meinhardt, A. et al., 2014. 3D Reconstitution of the Patterned Neural Tube from Embryonic Stem Cells. *Stem Cell Reports*, 3, pp.987–999.
Michaux, G. et al., 2000. CHE-14, a protein with a sterol-sensing domain, is required for apical sorting in C. elegans ectodermal epithelial cells. *Curr Biol*, 10(18), pp.1098–1107.
Milenkovic, L., Scott, M.P. & Rohatgi, R., 2009. Lateral transport of Smoothened from the plasma membrane to the membrane of the cilium. *J Cell Biol*, 187(3), pp.365–374.
Murakami, S. et al., 2002. Crystal structure of bacterial multidrug efflux transporter AcrB. *Nature*, 419(6907), pp.587–593.
Murakami, S. et al., 2006. Crystal structures of a multidrug transporter reveal a functionally rotating mechanism. *Nature*, 443(7108), pp.173–179.

Myers, B.R. et al., 2013. Hedgehog pathway modulation by multiple lipid binding sites on the smoothened effector of signal response. *Dev Cell*, 26(4), pp.346–357.
Nachtergaele, S. et al., 2012. Oxysterols are allosteric activators of the oncoprotein Smoothened. *Nat Chem Biol*, 8(2), pp.211–220.
Nachtergaele, S. et al., 2013. Structure and function of the Smoothened extracellular domain in vertebrate Hedgehog signaling. *eLife*, 2, p.e01340.
Nedelcu, D. et al., 2013. Oxysterol binding to the extracellular domain of Smoothened in Hedgehog signaling. *Nat Chem Biol*.
Neufeld, E.B. et al., 1999. The Niemann-Pick C1 protein resides in a vesicular compartment linked to retrograde transport of multiple lysosomal cargo. *J. Biol. Chem.*, 274(14), pp.9627–9635.
Nichols, S. a. et al., 2012. Origin of metazoan cadherin diversity and the antiquity of the classical cadherin/ -catenin complex. *Proceedings of the National Academy of Sciences*, 109(32), pp.13046–13051.
Nieuwenhuis, E. et al., 2006. Mice with a targeted mutation of patched2 are viable but develop alopecia and epidermal hyperplasia. *Molecular {&} Cellular Biology*, 26(17), pp.6609–6622.
Nieuwenhuis, E. & Hui, C., 2004. Hedgehog signaling and congenital malformations. *Clinical Genetics*, 67(3), pp.193–208.
Nikaido, H., 1996. Multidrug efflux pumps of gram-negative bacteria. *Journal of Bacteriology*, 178(20), pp.5853–5859.
Nikaido, H., 2011. Structure and mechanism of RND-type multidrug efflux pumps. *Advances in enzymology and related areas of molecular biology*, 77(11), pp.1–60.
Nikaido, H. & Pagès, J.-M., 2012. Broad-specificity efflux pumps and their role in multidrug resistance of Gram-negative bacteria. *FEMS Microbiology Reviews*, 36(2), pp.340–363.
Nikaido, H. & Takatsuka, Y., 2009. Mechanisms of RND multidrug efflux pumps. *Biochimica et Biophysica Acta*, 1794(5), pp.769–781.
Nohturfft, A. et al., 1999. Sterols regulate cycling of SREBP cleavage-activating protein (SCAP) between endoplasmic reticulum and Golgi. *Proc. Natl. Acad. Sci. U. S. A.*, 96, pp.11235–11240.
Nohturfft, A., Brown, M.S. & Goldstein, J.L., 1998. Topology of SREBP cleavage-activating protein, a polytopic membrane protein with a sterol-sensing domain. *J. Biol. Chem.*, 273(27), pp.17243–17250.
Nüsslein-Volhard, C. & Wieshaus, E., 1980. Mutations affecting segment number and polarity in Drosophila. *NATURE*, 287, pp.795–801.
Ohgami, N. et al., 2004. Binding between the Niemann-Pick C1 protein and a photoactivatable cholesterol analog requires a functional sterol-sensing domain. *Proceedings of the National Academy of Sciences of the United States of America*, 101(34), pp.12473–12478.
Ohlig, S. et al., 2012. An emerging role of Sonic hedgehog shedding as a modulator of heparan sulfate interactions. *J. Biol. Chem.*, 287(52), pp.43708–43719.
Oikonomou, G. et al., 2011. Opposing activities of LIT-1/NLK and DAF-6/patched-related direct sensory compartment morphogenesis in C. elegans. *PLoS Biology*, 9(8).
Palm, W. et al., 2013. Secretion and signaling activities of lipoprotein-associated hedgehog and non-sterol-modified hedgehog in flies and mammals. *PLoS biology*, 11(3), p.e1001505.

Patel, S.C. et al., 1999. Localization of Niemann-Pick C1 protein in astrocytes: implications for neuronal degeneration in Niemann- Pick type C disease. *Proc. Natl. Acad. Sci. U. S. A.*, 96(4), pp.1657–1662.

Perens, E. a. & Shaham, S., 2005. C. elegans daf-6 encodes a patched-related protein required for lumen formation. *Developmental Cell*, 8(6), pp.893–906.

Peters, C. et al., 2004. The cholesterol membrane anchor of the Hedgehog protein confers stable membrane association to lipid-modified proteins. *Proc. Natl. Acad. Sci. U. S. A.*, 101(23), pp.8531–8536.

Petrova, R. & Joyner, a. L., 2014. Roles for Hedgehog signaling in adult organ homeostasis and repair. *Development*, 141(18), pp.3445–3457.

Placzek, M. et al., 1990. Mesodermal control of neural cell identity: floor plate induction by the notochord. *Science*, 250(4983), pp.985–988.

Placzek, M., 1995. The role of the notochord and floor plate in inductive interactions. *Curr. Opin. in Genet. Dev.*, 5, pp.499–506.

Polizio, A.H. et al., 2011. Heterotrimeric Gi Proteins link Hedgehog signaling to activation of Rho small GTPases to promote fibroblast migration. *J. Biol. Chem.*

Porter, J.A., Ekker, S.C., et al., 1996. Hedgehog patterning activity: role of a lipophilic modification mediated by the carboxy-terminal autoprocessing domain. *Cell*, 86(1), pp.21–34.

Porter, J.A. et al., 1995. The product of hedgehog autoproteolytic cleavage active in local and long-range signalling. *NATURE*, 374(6520), pp.363–366.

Porter, J.A., Young, K.E. & Beachy, P.A., 1996. Cholesterol modification of hedgehog signaling proteins in animal development. *Science*, 274(5285), pp.255–259.

Radhakrishnan, A. et al., 2004. Direct binding of cholesterol to the purified membrane region of SCAP: Mechanism for a sterol-sensing domain. *Molecular Cell*, 15(2), pp.259–268.

Rana, R. et al., 2013. Structural insights into the role of the Smoothened cysteine-rich domain in Hedgehog signalling. *Nat Commun*, 4, p.2965.

Record, M. et al., 2014. Exosomes as new vesicular lipid transporters involved in cell-cell communication and various pathophysiologies. *Biochim. Biophys. Acta*, 1841(1), pp.108–120.

Riobo, N.A. et al., 2006. Activation of heterotrimeric G proteins by Smoothened. *Proc. Natl. Acad. Sci. U. S. A.*, 103(33), pp.12607–12612.

Robbins, D.J. et al., 1997. Hedgehog elicits signal transduction by means of a large complex containing the kinesin-related protein costal2. *Cell*, 90(2), pp.225–234.

Roelink, H. et al., 1995. Floor plate and motor neuron induction by different concentrations of the amino-terminal cleavage product of sonic hedgehog autoproteolysis. *Cell*, 81(3), pp.445–455.

Roelink, H. et al., 1994. Floor plate and motor neuron induction by vhh-1, a vertebrate homolog of hedgehog expressed by the notochord. *Cell*, 76(4), pp.761–775.

Roessler, E. et al., 1996. Mutations in the human Sonic Hedgehog gene cause holoprosencephaly. *Nat Genet*, 14(3), pp.357–360.

Rohatgi, R. et al., 2009. Hedgehog signal transduction by Smoothened: pharmacologic evidence for a 2-step activation process. *Proc. Natl. Acad. Sci. U. S. A.*, 106(9), pp.3196–3201.

Rohatgi, R., Milenkovic, L. & Scott, M.P., 2007. Patched1 regulates hedgehog signaling at the primary cilium. *Science*, 317(5836), pp.372–376.

Roy, S. et al., 2014. Cytoneme-Mediated Contact-Dependent Transport of the Drosophila Decapentaplegic Signaling Protein. *Science (New York, N.Y.)*, (January), pp.1–13.
Saier, M.H. & Paulsen, I.T., 2001. Phylogeny of multidrug transporters. *Seminars in cell & developmental biology*, 12(3), pp.205–213.
Sasai, N. & Briscoe, J., 2012. Primary cilia and graded Sonic Hedgehog signaling. *Wiley Interdisciplinary Reviews: Developmental Biology*, 1(5), pp.753–772.
Seeger, M.A. et al., 2006. Structural asymmetry of AcrB trimer suggests a peristaltic pump mechanism. *Science*, 313(5791), pp.1295–1298.
Sharpe, H.J. et al., 2015. Regulation of the oncoprotein Smoothened by small molecules. *Nature Chemical Biology*, 11(4), pp.246–255.
Singla, V. & Reiter, J.F., 2006. The primary cilium as the cell's antenna: signaling at a sensory organelle. *Science (New York, N.Y.)*, 313(5787), pp.629–633.
Sinha, S. & Chen, J.K., 2006. Purmorphamine activates the Hedgehog pathway by targeting Smoothened. *Nat Chem Biol*, 2(1), pp.29–30.
Sisson, J.C. et al., 1997. Costal2, a novel kinesin-related protein in the Hedgehog signaling pathway. *Cell*, 90(2), pp.235–245.
Smyth, I. et al., 1999. Isolation and characterization of human patched 2 (PTCH2), a putative tumour suppressor gene inbasal cell carcinoma and medulloblastoma on chromosome 1p32. *Hum Mol Genet*, 8(2), pp.291–297.
Soloviev, A. et al., 2011. C. elegans patched-3 is an essential gene implicated in osmoregulation and requiring an intact permease transporter domain. *Developmental Biology*, 351(2), pp.242–253.
Spemann, H. & Mangold, H., 1924. Induction of embryonic primordia by implantation of organizers from a different species. *International Journal of Developmental Biology*, 45(1 SPEC. ISS. 1), pp.13–38.
Stamataki, D. et al., 2005. A gradient of Gli activity mediates graded Sonic Hedgehog signaling in the neural tube. *Genes and Development*, 19(5), pp.626–641.
Stone, D.M. et al., 1996. The tumour-suppressor gene patched encodes a candidate receptor for Sonic hedgehog. *NATURE*, 384(6605), pp.129–134.
Strutt, H. et al., 2001. Mutations in the sterol-sensing domain of Patched suggest a role for vesicular trafficking in Smoothened regulation. *Curr Biol*, 11(8), pp.608–13.
Tabata, T., Eaton, S. & Kornberg, T.B., 1992. The drosophila hedeghog gene is expressed specifically in posterior compartment cells and is a target of engrailed regulation. *Genes Dev*, 6, pp.2635–2645.
Tabin, C.J., 1991. Retinoids, homeoboxes, and growth factors: toward molecular models for limb development. *Cell*, 66(2), pp.199–217.
Taipale, J. et al., 2000. Effects of oncogenic mutations in Smoothened and Patched can be reversed by cyclopamine. *NATURE*, 406(6799), pp.1005–9.
Taipale, J. et al., 2002. Patched acts catalytically to suppress the activity of Smoothened. *NATURE*, 418(6900), pp.892–897.
Tian, H. et al., 2005. Mouse Disp1 is required in sonic hedgehog-expressing cells for paracrine activity of the cholesterol-modified ligand. *Development*, 132(1), pp.133–142.
Wang, C. et al., 2014. Structural basis for Smoothened receptor modulation and chemoresistance to anticancer drugs. *Nature communications*, 5, p.4355.
Wang, C. et al., 2013. Structure of the human smoothened receptor bound to an antitumour agent. *Nature*, 497(7449), pp.338–43.

Wang, G. & Scott, S.A., 1999. Independent development of sensory and motor innervation patterns in embryonic chick hindlimbs. *Dev. Biol.*, 208(2), pp.324–336.
Wassif, C.A. et al., 1998. Mutations in the human sterol delta7-reductase gene at 11q12-13 cause Smith-Lemli-Opitz syndrome. *Am J Hum Genet*, 63(1), pp.55–62.
Waterham, H.R. et al., 1998. Smith-Lemli-Opitz syndrome is caused by mutations in the 7-dehydrocholesterol reductase gene. *Am J Hum Genet*, 63(2), pp.329–338.
Weierstall, U. et al., 2014. Lipidic cubic phase injector facilitates membrane protein serial femtosecond crystallography. *Nature Communications*, 5, p.3309.
Wichterle, H. et al., 2002. Directed differentiation of embryonic stem cells into motor neurons. *Cell*, 110(3), pp.385–397.
Wilson, C.W., Chen, M.H. & Chuang, P.T., 2009. Smoothened adopts multiple active and inactive conformations capable of trafficking to the primary cilium. *PLoS One*, 4(4), p.e5182.
Wolpert, L., 1971. Positional information and pattern formation. *Curr Top Dev Biol*, 6(6), pp.183–224.
Xie, J. et al., 1998. Activating Smoothened mutations in sporadic basal-cell carcinoma. *NATURE*, 391(6662), pp.90–92.
Yao, H.H.C., Whoriskey, W. & Capel, B., 2002. Desert Hedgehog/Patched 1 signaling specifies fetal Leydig cell fate in testis organogenesis. *Genes and Development*, 16(11), pp.1433–1440.
Yauch, R.L. et al., 2008. A paracrine requirement for hedgehog signalling in cancer. *Nature*, 455(7211), pp.406–10.
Yu, L., 2008. The structure and function of Niemann-Pick C1-like 1 protein. *Current opinion in lipidology*, 19(3), pp.263–269.
Zgurskaya, H.I. & Nikaido, H., 1999. Bypassing the periplasm: reconstitution of the AcrAB multidrug efflux pump of Escherichia coli. *Proc. Natl. Acad. Sci. U. S. A.*, 96(13), pp.7190–7195.
Zhang, M. et al., 2001. Sterol-modulated glycolipid sorting occurs in niemann-pick C1 late endosomes. *J. Biol. Chem.*, 276(5), pp.3417–3425.
Zhang, X.M., Ramalho-Santos, M. & McMahon, A.P., 2001. Smoothened mutants reveal redundant roles for Shh and Ihh signaling including regulation of L/R asymmetry by the mouse node. *Cell*, 105(6), pp.781–792.
Zhao, Y., Tong, C. & Jiang, J., 2007. Hedgehog regulates smoothened activity by inducing a conformational switch. *NATURE*, 450(7167), pp.252–258.
Zhu, A.J. et al., 2003. Altered localization of Drosophila Smoothened protein activates Hedgehog signal transduction. *Genes Dev*, 17(10), pp.1240–1252.
Zhu, A.J. & Scott, M.P., 2004. Incredible journey: how do developmental signals travel through tissue? *Genes & development*, 18(24), pp.2985–97.
Zhulyn, O. et al., 2015. Ptch2 shares overlapping functions with Ptch1 in Smo regulation and limb development. *Dev. Biol.*, 397(2), pp.191–202.

Chapter 2

Ptch2 mediates the Shh response in *Ptch1*-/- cells

Astrid C. Alfaro*, Brock Roberts*, Lina Kwong, Maarten F. Bijlsma, and Henk Roelink

Department of Molecular and Cell Biology, 16 Barker Hall, 3204, University of California, Berkeley CA 94720, USA

* AA and BR contributed equally to the manuscript

Mouse embryonic stem cells

Summary

The Hedgehog (Hh) signaling response is regulated by the interaction of three key components that include the Sonic Hedgehog (Shh) ligand, its receptor Patched1 (Ptch1), and the pathway activator Smoothened (Smo). Under the prevailing model of Shh pathway activation, Shh binding to Ptch1, the key Shh receptor, results in the release of Ptch1-mediated inhibition of Smo, leading to Smo activation and subsequent cell autonomous activation of the Shh response. Consistent with this model, *Ptch1*-/- cells show a strong upregulation of the Shh response. Our finding that this response can be inhibited by the Shh blocking antibody 5E1 indicates that the Shh response in *Ptch1*-/- cells remains ligand-dependent. Furthermore, we find that Shh induces a strong response in *Ptch1*-/-;*Shh*-/- cells, and that *Ptch1*-/- fibroblasts retain their ability to migrate towards Shh, demonstrating that *Ptch1*-/- cells remain sensitive to Shh. Expression of a dominant-negative Ptch1 mutant in the developing chick neural tube had no effect on Shh-mediated patterning, but expression of a dominant-negative form of Patched 2 (Ptch2) caused an activation of the Shh response. This indicates that at early developmental stages Ptch2 functions to suppress Shh signaling. We found that *Ptch1*-/-;*Ptch2*-/- cells cannot further activate the Shh response, demonstrating that Ptch2 mediates the response to Shh in the absence of Ptch1.

Introduction

Shh signaling is regulated by the interaction between Ptch1 (Marigo et al. 1996; Stone et al. 1996) and Smo (Marigo et al. 1996; Murone et al. 1999). Shh binding to Ptch1 releases the Ptch1-mediated inhibition of Smo (Taipale et al. 2002). Smo then localizes to the cell surface (Incardona et al. 2002) and subsequently to the primary cilium (Milenkovic et al. 2009) where it mediates the activation of the Shh response (Corbit et al. 2005; Huangfu & Anderson 2005; Rohatgi et al. 2007). This model explains the widespread activation of the Shh response observed in the absence of Ptch1 (Goodrich et al. 1997).

Drosophila genetics strongly supports the canonical model of Hh signaling by demonstrating that the loss of Ptch is epistatic to the loss of Hh (Bejsovec & Wieschaus 1993). In amniotes there are two *Ptch* homologs, *Ptch1* and *Ptch2*, and of these two genes *Ptch1* appears to be the most important. The loss of *Ptch1* results in an embryonic lethal phenotype characterized by the widespread upregulation of the Shh response, including extensive induction of Shh expression and ventral identity in the developing neural tube (Goodrich et al., 1997). In contrast, *Ptch2*-/- mice are fertile and viable, but develop skin abnormalities characterized by basal cell hyperplasia (Nieuwenhuis et al. 2006). Since these data suggested that the functions of Ptch1 and Ptch2 are largely non-overlapping, *Ptch1*-/- cell lines have been used extensively for their high level of cell-autonomous activation of the Shh response. For example, neuralized cells derived from *Ptch1*-/- mouse embryonic stem cells (mESCs) acquire a phenotype typically associated with the induction of the Shh response without the inclusion of Shh in the medium (Crawford & Roelink 2007). This is consistent with a ligand-independent induction of the Shh response in cells devoid of Ptch1. Similarly, *Ptch1*-/- fibroblasts have been widely studied for having a constitutively upregulated Shh response (Taipale et al. 2000).

We now demonstrate that *Ptch1*-/- fibroblasts display Shh chemotaxis indistinguishable from wild type cells, indicating that *Ptch1*-/- is not required to mediate this Shh response. Furthermore, we show that upregulation of the Shh response in neuralized embryoid bodies (NEBs) derived from *Ptch1*-/- mESCs is dependent on endogenously expressed Shh by mutating the *Shh* locus in *Ptch1*-/- mESCs, and by treating these cells with a Shh-blocking antibody. The role of Ptch2 in mediating the Shh response in the absence of Ptch1 was further supported by the observation that *Ptch1*-/-;*Ptch2*-/- cells cannot respond to activators of the Shh response, and that expression of a dominant negative Ptch2 mutant results in an activation of the Shh response. Together these results demonstrate that the Shh responses observed in *Ptch1*-/- cells can be mediated by Ptch2.

Results

The proton-driven antiporter activity of Ptch1 can mediate the inhibition of Smo

Ptch1 is a putative member of the Resistance, Nodulation and Division (RND) family of proton-driven antiporters (Taipale et al. 2002). This transporter family shares a conserved aspartic acid residue in the fourth trans-membrane region (Van Bambeke et al. 2000). Mutating this residue in other members of the RND family, including Disp1 (Etheridge et al. 2010), results in dominant-negative molecules that are able to inhibit the antiporter function of normal endogenous proteins. Expressing a Ptch1 allele lacking antiporter activity (Ptch1D499A) (Taipale et al. 2002) in the chick neural tube does not recapitulate the loss of Ptch1 function in mouse embryos (Goodrich et al. 1997), since we did not observe an increase in Shh activation as assessed by changes in Shh-mediated dorsoventral patterning (Fig. 1A,B). On occasion we did find some cells expressing Pax7 ectopically, indicating a minor loss of Shh signaling (Fig. S1). We attribute this to the ability of Ptch1D499A to sequester Shh away from endogenous Ptch1, leading to both an autonomous and non-autonomous inhibition of Shh signaling.

For members of the RND family to act as dominant negatives, they must retain the ability to form trimers (Nikaido & Takatsuka 2009). It remains a possibility that the electroporated mouse Ptch1 cannot form trimers with endogenous chicken Ptch1. We therefore tested if chicken Ptch1 lacking antiporter activity was able to induce the Shh response, after misexpression in the developing neural tube. Again we observed little effect on neural tube patterning (Fig. S1), indicating that suppressing the proton-driven antiporter activity of Ptch1 has little effect on the Shh response. The inability of Ptch1D499A to apparently act a dominant-negative inhibitor of endogenous Ptch1 raises the question if the proton-driven antiporter activity is important to regulate the Shh response at these stages of development.

Ptch1Δloop2, a deletion mutant of Ptch1 that is unable to bind Shh is a potent inhibitor of the Shh response. Consistent with an earlier observation (Briscoe et al. 2001), we found that expression of Ptch1Δloop2, had a strong cell-autonomous inhibitory effect on the Shh response (Fig. 1C,D). To assess if this effect is mediated by its antiporter activity we expressed a Ptch1 allele that was unable to bind Shh but also lacks antiporter activity, Ptch1Δloop2/D499A. Ptch1Δloop2/D499A had no effect on Shh activity based on the lack of ectopic cell autonomous Pax7 induction, and only mildly inhibited motor neuron induction, as determined by Isl1/2 expression (Fig. 1E,F). The dramatic difference between the strong inhibition of the Shh response by Ptch1Δloop2 and the mild effects of Ptch1Δloop2/D499A demonstrates that the proton-driven antiporter activity is critical for Smo inhibition by Ptch1Δloop2. Importantly, the loss of repressive activity of Ptch1 did not automatically result in the cell-autonomous activation of the Shh response, indicating that Ptch1Δloop2/D499A is not a strong inhibitor of endogenous Ptch1 function.

To assess the activities of the Ptch1 mutants in the absence of endogenous Ptch1 activity, we expressed them in *Ptch1*-/- immortalized mouse embryonic fibroblasts (MEFs). *Ptch1*-/- MEFs have an autonomously upregulated Shh response (Taipale et al. 2000) that can be measured due to the integration of the *LacZ* gene into the *Ptch1* locus (Goodrich et al. 1997). We found that SAG, a Smo agonist, further induce Shh pathway activity in the *Ptch1*-/- MEFs, while cyclopamine reduced Shh pathway activity (Taipale et al. 2000; Chen et al. 2002) (Fig. 2A). This indicates that despite the absence of Ptch1, Smo can be activated or inhibited in these cells. The

addition of ShhN (a truncated and soluble form of Shh) also increased the Shh response, indicating that there is a Ptch1-independent response to Shh.

In line with their abilities to inhibit Smo, we found that expression of Ptch1 and Ptch1Δloop2 decreased the autonomous Shh response, relative to control transfection with Disp1, which was normalized to 100 (Fig. 2B). In these experiments we measured the Shh response by co-transfecting a construct in which luciferase is driven by a Shh-inducible promoter (Taipale et al. 2002). Furthermore, whereas *Ptch1*-/- cells expressing Ptch1 were responsive to ShhN, cells expressing Ptch1Δloop2 were unresponsive (Fig. 2B), consistent with the inability of Ptch1Δloop2 to bind Shh, mirroring our observations in vivo (Fig. 1C,D). For comparison, Ptch1+/+ MEFs were assayed (control 100%±18 *vs* ShhN 239%±52). In line with their abilities to inhibit Smo, we found that expression of Ptch1 and Ptch1Δloop2 decreased the autonomous Shh response (Fig. 2C). To test if the downregulation of the Shh response pathway required the antiporter activity of Ptch1, we expressed the antiporter mutant and found an increase of the autonomous activation of the Shh response as compared to wild type Ptch1 (Fig. 2B,C). Nevertheless, these Ptch1 mutants repressed Smo to a much greater degree than the negative control, Disp1. Moreover, cells expressing Ptch1 antiporter mutants retained their sensitivity to ShhN (Fig. 2B). This demonstrates that Smo inhibition can be regulated independently of Ptch1 antiporter activity.

Combining mutations that antagonize both the proton-driven antiporter activity of Ptch1 as well as Shh binding in the same molecule resulted in forms of Ptch1 that blocked the response to ShhN in *Ptch1*-/- cells (Fig. 2B). We expanded this experiment using different mutations in the putative proton pore, replacing the critical aspartic acid with a lysine or tyrosine residue (Ptch1D499K and Ptch1D499Y), and combined these mutations with the Shh binding deletion (Ptch1Δloop2/D499K and Ptch1Δloop2/D499Y). To address the ligand dependency we treated these cells with ShhN or 5E1, a Shh specific monoclonal antibody. Similar to Ptch1D499A, we found that cells expressing Ptch1D499K or Ptch1D499Y retained their ability to respond to ShhN, but mutants combining the antiporter activity mutations with the loop2 deletion resulted in forms of Ptch1 that were unable to mediate the Shh response in *Ptch1*-/- cells, but nevertheless inhibited Smo as compared to our control, Disp1 (Fig. 2C).

These results raise the question of how forms of Ptch1 that are unable to bind Shh and repress Smo can nevertheless still inhibit the Shh response. Since these experiments were performed in *Ptch1*-/- cells, Ptch1Δloop2/D499X mutant alleles must inhibit the Shh response independent of endogenous Ptch1. They also support the notion that Shh can induce Smo activity via a mechanism that does not involve Ptch1 antiporter activity.

Neuralized Ptch1-/- embryonic stem cells remain Shh-dependent for the induction of ventral cell types

Mouse embryonic stem cells (mESCs), aggregated in defined medium containing retinoic acid, form neuralized embryoid bodies (NEBs) that closely resemble the early caudal neural tube (Wichterle et al. 2002). Consistent with the inhibitory role of Ptch1 on Smo, we have shown that in the absence of exogenous Shh, *Ptch1*-/- NEBs have higher expression levels of Shh-induced differentiation markers than wild type NEBs. Smo is required for the Shh response and in concordance with this observation we found that *Smo*-/- NEBs cannot respond to Shh (Crawford & Roelink 2007). To determine if endogenously produced Shh is responsible for the induction of Shh-mediated differentiation in the absence of *Ptch1*, *Ptch1*-/- NEBs were cultured in the

presence of the Shh-blocking antibody 5E1 (Ericson et al. 1996) or an α-Myc antibody (9E10) (Chan et al. 1987) as a control. After 5 days in culture, NEBs were analyzed for expression of Isl1/2 and Nkx2.2, transcription factors that are induced by activation of the Shh response (Briscoe et al. 1999) and Pax7, which is inhibited by Shh signaling (Ericson et al. 1996). In *Ptch1*-/- NEBs cultured with 5E1, Isl1/2 and Nkx2.2 expression was reduced compared to the 9E10 treated *Ptch1*-/- NEBs (Fig. 3A, B, G, H). This loss of ventral cell types was concomitant with an increase of Pax7 expression, further demonstrating that the upregulation of the Shh response in *Ptch1*-/- cells is not due to an autonomous loss of Smo inhibition, but is at least in part dependent on the presence of Shh in the NEBs (Fig. 3I). Both RT-PCR and immunofluorescence showed abundant Shh expression in *Ptch1*-/- NEBs (Fig. 3E, F). Moreover, in the absence of Ptch1 function, the number of cells expressing Isl1/2 and Nkx2.2 was increased by the Smo agonist SAG (Chen et al. 2002), and the number of cells expressing Pax7 was suppressed, regardless of the presence of 5E1 (Fig. 3C, D, G, H), indicating that even in absence of Ptch1, Smo was not fully activated.

To demonstrate that *Ptch1*-/- cells can respond to Shh delivered *in trans*, we generated mixed NEBs composed of varying ratios of *Ptch1*-/- and *Smo*-/- mESCs (Fig 3J-O). Neuralized *Smo*-/- mESCs are unable to respond to Shh itself but this particular clone expresses Shh (Fig 3M). Shh derived from these *Smo*-/- cells induced Nkx2.2 and Isl1/2 expression in *Ptch1*-/- cells. This induction could be blocked by the inclusion of 5E1 demonstrating that this induction is mediated by Shh (Fig. 3P). Wild type mESCs did not display an induction of their Shh response when co-aggregated with *Smo*-/- mESCs (Fig. 3Q). It appears that the concentration of Shh provided by the *Smo*-/- cells within the NEB is not sufficient to activate the response in wild type cells. These results demonstrate that *Ptch1*-/- mESCs are more sensitive to Shh than wild type mESCs, but nevertheless remain dependent on the ligand for full induction of the Shh response. Based on our results using blocking antibodies, we wanted to further address the requirement of Shh in cells by creating genetic nulls.

Ptch1-/-;Shh-/- cells respond to exogenous Shh

To determine if endogenous Shh mediates the Shh response in *Ptch1*-/- cells, we made mutations in the *Shh* locus of *Ptch1*+/- and *Ptch1*-/- mESCs using transcription activator-like effector nucleases (TALENs) (Cermak et al. 2011) directed against an amino-terminal coding sequence of *Shh*. The *Shh*-/- clones were detected by sequencing of PCR products surrounding the area targeted by the TALENs. The clones used for subsequent experiments had small deletions in both *Shh* alleles that caused premature stop codons, resulting in protein products truncated soon after the signal sequence. NEBs derived from these cells were grown in the absence or presence of 5nM ShhN and the induction of Nkx2.2 positive cells was assessed. In NEBs derived from both the *Ptch1*+/-;*Shh*-/- and *Ptch1*-/-;*Shh*-/- cells we observed a significant induction of Nkx2.2 positive cells by ShhN (Fig. 4A,B). In addition, we found that the *Ptch1* promoter, as measured by the induction of LacZ was induced in the *Ptch1*-/-;*Shh*-/- cells in response to ShhN (Fig. 4C). These results show that cells without Ptch1 are sensitive to Shh, and that the upregulation of the Shh response in *Ptch1*-/- cells is at least in part mediated by endogenous Shh..

To further assess the mechanism of Ptch1-independent signaling, we tested the ability of *Ptch1*-/- cells to migrate towards a localized source of Shh. This Shh chemotaxis response is fast,

and independent of transcription and the primary cilium (Bijlsma et al. 2012). Since this response does require Smo, it assesses more directly upstream events in the Shh response.

Shh chemotaxis is unaffected in the absence of Ptch1, but remains dependent on Cdon and Boc

We tested the migratory response of *Ptch1*-/- and *Ptch1*+/+ immortalized MEFs in a modified Boyden chamber assay (Fig. S2). Shh chemotaxis of *Ptch1*+/+ cells does not require transcription (Bijlsma et al. 2008), but is dependent on Smo. The migratory response to ShhN and purmorphamine of *Ptch1*-/- cells was very similar to that of *Ptch1*+/+ cells (Fig. 5A, B), and this assay thus provides us with a robust Ptch1-independent response to Shh. The migration was specific towards ShhN, since it was inhibited by the inclusion of 5E1 in the upper and lower compartments of the Boyden chamber. Migration to both ShhN and purmorphamine could be ablated by expressing Ptch1Δloop2 or performing the assay in a Smo deficient background (Fig. 5A, B). These results indicate that Ptch1 is not required for migration of MEFs towards sources of Shh, further supporting the notion that Ptch1 is not required for cell to respond to Shh.

We next examined what receptors could potentially perceive Shh in *Ptch1*-/- cells. Several Shh binding proteins such as Gas1, Cdon, and Boc have been proposed to function as co-receptors acting in conjunction with Ptch1 (Allen et al. 2011; Izzi et al. 2011; Tenzen et al. 2006). We tested if these molecules mediated the Shh response in the absence of Ptch1. Stable *Gas1* knockdown in *Ptch1*-/- MEFs did not affect Shh chemotaxis, but stable knockdown of *Cdon* and *Boc* diminished this response (Fig. 5C). This effect was confirmed using a transient silencing strategy (Fig. S3). *Ptch1*-/- MEFs stably expressing Cdon or Boc showed an increased chemotactic response to ShhN (Fig. 5D). These experiments indicate that the related Shh (co-)receptors Cdon and Boc mediate Shh chemotaxis even in the absence of Ptch1. Since Boc and Cdon are thought to form complexes with Ptch1 and Shh (Izzi et al. 2011), it is a distinct possibility that that they can also form such complexes with Ptch2.

Ptch1-/-;Ptch2-/- NEBs have a higher level of Shh pathway activation than Ptch1-/- NEBs

To assess if Ptch2 is required for the Ptch1-independent response, we mutated the *Ptch2* locus in *Ptch1*-/- mESCs and found that in NEBs derived from *Ptch1*-/-;*Ptch2*-/- cells, the Shh response was higher than in the *Ptch1*-/- and *Ptch1*+/- NEBs (Fig. 6A-C). This indicates that the Shh response in *Ptch1*-/- cells is inhibited by Ptch2. The *Ptch1*-/-;*Ptch2*-/- NEBs had more Nkx2.2+ cells and fewer Isl1/2+ cells than the *Ptch1*-/- NEBs. We conclude that cells in *Ptch1*-/-;*Ptch2*-/- NEBs acquire an even more ventral phenotype resulting in a loss of the number of motorneurons induced. We indeed found that in *Ptch1*-/-;*Ptch2*-/- NEBs the Shh-inducible *Ptch1* promoter was considerably more active than in *Ptch1*-/- and *Ptch1*+/- NEBs (Fig. 6D). We were unable to further alter the Shh pathway activation level by inclusion of the Smo agonist SAG (Fig. 6D). This indicates that in the absence of both Ptch1 and Ptch2, Smo activation via its heptahelical domain is saturated (Chen et al. 2002). It is thought that Ptch1, via its proton driven antiporter activity re-localizes a sterol that inhibits Smo at this heptahelical site, and our results thus indicate that Ptch2 could also fulfill this role.

Expression of Ptch2 antiporter mutants induces the Shh response in vivo

We assessed whether the proton-driven antiporter activity of the Ptch1 paralog Ptch2 is involved in regulating the Shh response in vivo. Ptch2 has been shown to modulate the Shh response in mouse embryos (Holtz et al. 2013). Whereas Ptch1Δloop2 misexpression in chick embryos causes a significant cell autonomous inhibition of the Shh response (Fig. 1), we have been unable to find any autonomous inhibitory effects of Ptch2 (not shown), suggesting that the inhibitory action of Ptch2 in the developing neural tube is less important than that of Ptch1, consistent with the normal development of *Ptch2*-/- embryos. To create a dominant negative allele of Ptch2, we mutated the aspartic acid analogous to the one in Ptch1 to alanine, Ptch2D469A. Like Ptch1D499A, expression of Ptch2D469A, did not cause cell autonomous changes in Shh induced patterning (Fig. 7A). Co-expression of Ptch2D469A and Ptch1D499A also failed to affect neural tube patterning cell-autonomously (not shown). However, in 4 out of twenty 20 embryos electroporated with *Ptch2D469A* we found widespread upregulation of Shh expression (Fig. 7B) and of the Shh response (Fig. 7C,D). These embryos were characterized by a bilateral, additional Nkx2.2 domain, localized dorsal to the normal domain (Fig. 7C), or by the widespread expression of Isl1/2 and Nkx2.2 (Fig. 7D). The induction of the Shh response was largely non-cell autonomous, and it is likely that the ectopic induction of Nkx2.2 and Isl1/2 is a consequence of the expanded domain of Shh expressing cells. This phenotype bears striking resemblance to the phenotype observed in *Ptch1*-/- mouse embryos, which might indicate that Ptch2D469A can inhibit Ptch1 function *in trans*.

Discussion

Our results demonstrate that the loss of Ptch1 function is not always sufficient to cell-autonomously initiate maximal Smo-dependent Shh responses, and that Ptch2 mediates the residual responsiveness retained in *Ptch1-/-* cells. In flies, based on the embryonic cuticular phenotype, Ptch is epistatic to Hh, and Smo is epistatic to Ptch, consistent with a cell autonomous activation of Smo in the absence of Ptch. The phenotype of *Ptch1*-/- mouse embryos is also consistent with a cell autonomous activation of Smo, although this issue is clouded by the widespread induction of Shh (Goodrich et al. 1997).

The induction of Shh is in part responsible for the upregulation of the Shh response in the absence of Ptch1. This is evident by 5E1-mediated blockade of endogenous Shh ligand in *Ptch1*-/-neuralized embryonic bodies (NEBs), which results in the loss of ventral cell types, presumably by preventing Shh binding to its receptors. This notion is further supported by NEBs derived from *Ptch1-/-;Shh*-/- mESCs, which can respond to exogenous ShhN. The ability of *Ptch1*-/- NEBs to respond to endogenous ligand highlights the importance of Shh receptors distinct from Ptch1 within these cells. These results indicate that the interpretation of the phenotype of *Ptch1*-/- embryos is incomplete. Our results predict that the phenotype of *Ptch1-/-;Shh*-/- embryos will be different from *Ptch1*-/- embryos, and that this difference can be attributed to Ptch2-mediated Shh signaling.

Ptch1-/- MEFs also retain the ability to respond to Shh, both transcriptionally and via cell migration. While Shh chemotaxis is very similar in *Ptch1*-/- and wildtype MEFs, the Shh-induced transcriptional response of *Ptch1*-/- MEFs is weaker than that of *Ptch1*+/+ MEFs. It is possible that Ptch1-independent signaling is more efficient in mediating the migratory than the transcriptional response. Boc and Cdon are Shh co-receptors required both for the transcriptional response (Allen et al. 2011) as well as neural path finding to Shh (Izzi et al. 2011). It is conceivable that like the transcriptional response, Ptch2 can mediate Shh chemotaxis. Boc and Cdon have been proposed to make a tripartite complex with Ptch1 and Shh (Izzi et al. 2011). The Boc and Cdon requirement for Shh chemotaxis in *Ptch1*-/- MEFS suggests that they may also form complexes with Shh and Ptch2.

As a member of the RND family of proton-driven antiporters, Ptch1, like Drosophila Ptc (Lu et al. 2006), is expected to function as a trimer, mediating its transporter activity via a rotatory mechanism (Nikaido & Takatsuka 2009; Nikaido & Zgurskaya 2001). In the absence of endogenous Ptch1 as a trimerization partner, the Ptch1 paralog Ptch2 could fulfill this role. Like Ptch1, Ptch2 expression is upregulated in response to Shh resulting in a significant overlap in their expression domains (Resende et al. 2010; Holtz et al. 2013). This leaves open the possibility that Ptch1 and Ptch2 can form heterotrimers (Rahnama et al. 2003), and that Ptch1/2 heterotrimers in which Ptch1 subunits lack the Shh binding loop cannot mediate the Shh response. RND heterotrimerization is not without precedent. MdtB and MdtC, two bacterial RND proteins that are encoded within a single operon, must be co-expressed in order for drug efflux (a measure of activity) to occur. MdtB and MdtC share 45% sequence identity, which is much less than the 56% sequence identity shared between Ptch1 and Ptch2, further supporting the possibility that Ptch1 and Ptch2 could also form heterotrimers. The Mdt complex is an $MdtB_2C_1$ heterotrimer. Importantly, mutating the proton translocation pathway of MdtB blocked transporter activity, while the analogous mutation in MdtC did not affect the activity of the trimer (Kim et al. 2010). This result indicates that subunits of RND heterotrimers can contribute

different activities to the trimer, and that the proton driven antiporter activity is not required to be active in all three subunits.

The observation that Ptch1Δloop2D499A both inhibits Smo activity in *Ptch1*-/- cells and is insensitive to regulation by Shh would support the notion that in Ptch1/2 heterotrimers, Smo inhibition is mediated by Ptch2 subunits. This is further supported by the observation that Ptch2D469A expression can activate the Shh response when expressed in vivo. An interpretation of this result is that the high levels of expression reached in electroporation drive the formation of Ptch1/2 heterotrimers in which the Ptch2 subunits fail to mediate proton driven antiporter activity and thus prevent the heterotrimers from inhibiting Smo. Together these observations support the model in which the Ptch1 and Ptch2 subunits of a Ptch1/2 heterotrimer mediate distinct activities. Ptch1, via its Shh binging loop2 imparts Shh sensitivity upon the heterotrimers, independent of its proton-driven antiporter activity. Ptch2 on the other hand is not particularly sensitive to Shh, but mediates the antiporter activity.

The non-cell autonomous activation of the Shh response resulting from Ptch2D496A expression in the developing chick neural tube is consistent with the predicted role of Ptch2 on Smo activity. Very strong activation of the Shh response can result in the induction of Shh expression (Ericson et al. 1996), and consistent with this, we find that expression of Ptch2D496A results in an ectopic or expanded population of Shh expressing cells. It is likely that Shh released from these Shh expressing cells mediates the subsequent ectopic induction of Nkx2.2 and Isl1/2 on both sides of the neural tube. The induction of Shh expression could explain the apparent cell non-autonomous effects of Ptch2D496A expression.

The origin of these ectopic Shh-expressing cells remains unclear but their presence indicates incorrect patterning of the neural tube. Shh-mediated induction of Shh expression occurs in the node (Charrier et al. 1999; Charrier et al. 2002), and soon after when the nascent notochord induces the floor plate (Placzek et al. 1993). The high levels of Ptch1 and Ptch2 expression around the node (Resende et al. 2010) might render this structure particularly sensitive to the consequences of Ptch2D496A overexpression, and explain the nature of the phenotype observed. It is striking that Ptch2D469A overexpression causes a phenotype reminiscent of the loss of Ptch1 in mouse embryos (Goodrich et al. 1997).

In summary, our results reveal that the upregulation of the Shh response in *Ptch1*-/- cells is in part mediated by Shh and we propose that Ptch2 acts as a Shh receptor. The function of Ptch2 becomes more apparent in the absence of Ptch1. Since *Ptch2*-/- mice are viable and fertile, it is obvious that the role of Ptch1 in the regulation of Smo activity is greater than that of Ptch2. Ptch1 can compensate for the loss of Ptch2, but not *vice versa* (Rahnama et al. 2003). Nevertheless, the increased tumor incidence in *Ptch1*+/- mice lacking one or two *Ptch2* alleles (Lee et al. 2006; Smyth et al. 1999) is most easily explained by the ability of Ptch2 to regulate Smo activity in the absence of Ptch1. The modulation of Ptch2 activity by Shh provides a simple explanation for why tumors in *Ptch1*+/- mice often occur at known locations of Shh signaling, such as the skin and the cerebellum (Goodrich et al. 1997; Stone et al. 1996), since we predict that loss of function of the normal *Ptch1* allele does not render these cells completely ligand independent.

Further indications that the functions of Ptch1 and Ptch2 are not entirely overlapping comes from the observation that in *ptc1*-/-;*ptc2*-/- zebrafish embryos a more extensive upregulation of the Hh response is observed than in *ptc1*-/- embryos (Koudijs et al. 2008). In mouse embryos without Ptch2, and with Ptch1 expressed off a constitutively active and Shh-insensitive promoter, a mild upregulation of the response is observed. Subsequent loss of the Shh

antagonist Hhip results in a strong upregulation of the Shh response (Holtz et al. 2013), indicating that Ptch2 provides ligand-dependent feedback on the Shh response. However, neither the mouse mutants described by Holtz et al. (due to the presence of constitutively expressed Ptch1), nor the *ptc1*-/-;*ptc2*-/- zebrafish (due to the partial genome duplication) address the consequence for the Hh response in the complete absence of Ptch activity.

The question remains to what degree the observed activation of the Shh response in cells without Ptch1 is ligand dependent *in vivo*. The phenotype of *Shh*-/-;*Ptch1*-/- embryos is not yet known, but any slight modification of the *Ptch1*-/- phenotype due to the loss of Shh could be attributable to Shh signaling via Ptch2 (Lee et al. 2006). Similarly, comparing early phenotypes of *Ptch1*-/- and *Ptch1*-/-;*Ptch2*-/- embryos could demonstrate further roles of Ptch2 when Ptch1 is absent.

Materials and methods

Materials
Cyclopamine was from Biomol (Plymouth Meeting, PA). Purmorphamine and SAG were from EMD Biochemicals (Darmstadt, Germany). Cell Tracker Green was from Invitrogen (Carlsbad, CA). Recombinant ShhN was from R&D Systems (Minneapolis, MN).

Immunohistochemistry
Antibodies for mouse Pax7, HB9, Nkx2.2 (745-A5), Shh (5E1) and Myc (9E10) were obtained from the Developmental Studies Hybridoma Bank. Rabbit α-GFP was from Invitrogen (Carlsbad, CA) and guinea pig α-Isl1/2 was a gift from Dr. Thomas Jessell (Columbia University). In all experiments, Alexa488- or Alexa568- or Alexa647- conjugated secondary antibodies were from Invitrogen.

Electroporations
Hamburger-Hamilton (HH) Stage 10 *Gallus gallus* embryos were electroporated caudally in the developing neural tube using standard procedures (Meyer & Roelink 2003). Embryos were incubated for another 48 hours following electroporation, fixed in 4% PFA, mounted in Tissue-Tek® O.C.T.™ Compound
(Sakura) and sectioned.

EB differentiation, antibody and ShhN treatment
mESCs were neuralized using established procedures (Wichterle et al. 2002). NEBs were cultured in the presence of α-Shh (5E1) or α-Myc (9E10) conditioned in DFNB medium at 1:5 for the duration of the experiment. NEBs were harvested after 5 days in culture, fixed and stained for Isl1/2 and Nkx2.2, or Pax7 (Kawakami et al. 1997). NEBs were mounted in Fluormount and quantified for number of positive nuclei.

Reporter Gene Assays for β-Galactosidase
mESCs were neuralized using established procedures (Wichterle et al. 2002). NEBs were cultured in 5nM of Shh-N conditioned HEK293T supernatant or an equivalent volume of control, empty vector, conditioned HEK293T supernatant. NEBs were collected after 5 days in culture and lysed into a standard lysis buffer (100 mM Potassium Phosphate, pH 7.8, 0.2 % Triton X-100). *Ptch1-/-* MEFs were allowed to grow to confluence before switching to a low serum medium (0.5% FCS) and ShhN, SAG, or cyclopamine was added for another 24 hours when cells were lysed. Lysates were analyzed using the Galacto-Light^{TM} chemiluminescence kit (Applied Biosciences) for level of LacZ expression.

RT-PCR
RNA isolation was performed using Trizol (Invitrogen) according to the manufacturer's recommendations. For cDNA synthesis, SuperScript III (Invitrogen) was used on 1 µg RNA. PCR was performed using ReddyMix (Thermo Scientific).

Expression vectors

pcDNA3.1 vector was obtained from Invitrogen. *Ptch1Δloop2* was a gift from Dr. Thomas Jessell (Columbia University). The Gli-luciferase reporter and the Renilla control were a gift from Dr. H. Sasaki (Sasaki et al. 1997). *Boc* and *Cdon* constructs were a gift from Dr. Krauss (Mount Sinai School of Medicine). *Ptch1* was a gift of Dr. Scott (Stanford University). *Ptch2* was obtained from Thermo Scientific. *Ptch1* and *Ptch2* channel mutants were created by Quikchange mutagenesis (Stratagene). In the *Ptch2* mutant the aspartic acids residues at positions 469 and 470 were changed to alanines.

Cell culture

Smo-/- fibroblasts (gift of Dr. Taipale), *Ptch1-/-* and wild type MEFs (gift of Dr. Scott) were cultured in Dulbecco's modified Eagle's medium (DMEM, Invitrogen) supplemented with 10% fetal calf serum (FCS, Invitrogen). mESCs were maintained under standard conditions without feeder cells.

Lentiviral transductions

HEK293T cells were transfected with *psPAX2* and *pMD2.G* helper plasmids and *pLKO.1* clones from the Sigma TRC1.0 shRNA library using FuGene HD (Roche, Basel, Switzerland). Following virus production, supernatant was filtered, and *Ptch1-/-* MEFs were transduced using 1:1 supernatant with 5 µg/mL polybrene (Sigma), transduced cells were selected with 1 µg/mL puromycin. Knockdown was verified by RT-PCR.

Transfections

Transient DNA transfections were performed using Effectene (Qiagen, Hilden, Germany). DNA was used at a 1:15 ratio of DNA/Effectene. Cells were incubated with transfection complexes for 16h. For RNA transfections, 100 nm siRNA was transfected using 5 µL DharmaFect 3 (Dharmacon, Lafayette, CO) in OptiMem (Invitrogen).

Luciferase Assay

Ptch1-/- MEFS were transfected with *Ptch1* mutant constructs, *Gli-luciferase* and *CMV-Renilla*. Cells were allowed to grow for two days after transfection before switching to a low serum medium (0.5% FCS), ShhN conditioned medium, or 5E1 conditioned medium for an additional two days. Cells were subsequently lysed and luciferase activity was determined by using the Dual-Luciferase Reporter Assay System (Promega).

Western blotting

Cells were lysed using LDS sample buffer (Invitrogen) and subjected to SDS-PAGE. Proteins were transferred to PVDF membranes, blocked with 5% milk/Tris-buffered saline with 0.1% Tween-20 (TBS-T), and incubated in 9B11 a-Myc 9B11 (Cell Signaling Technology, Danvers, MA) at 1:5,000, or a-FLAG M2 (Sigma) at 1:2,000. Appropriate HRP-conjugated secondary antibodies were used at 1:5,000. Proteins were visualized using a FujiFilm LAS 4000 imager.

Chemotaxis assay

Migration assays were performed as previously described (Bijlsma et al., 2007). Cells were labeled with 10 µM CellTracker Green (Invitrogen) according to manufacturer's protocol. After labeling, cells were detached with 5 mM EDTA, resuspended in serum free medium, and transferred into FluoroBlok Transwell inserts (BD Falcon) at approximately 5 x 10^4 cells per

insert. Chemoattractant was added to the bottom compartments of the Transwell plates and GFP-spectrum fluorescence in the bottom compartment was measured in a Synergy HT plate reader (BioTek, Winooski, VT) every 2 min for 99 cycles (approximately 3 hours). For analysis of data, see Figure S2 and legend.

TALENs

The pCTIGTALEN expression vector was generated by cloning the *BglII*/*SacI* digested TALEN ORF fragment of pTAL4 into the MCS of pIRES2-eGFP. After sequencing to confirm correct RVD architectures in pCTIG, constructs were further modified by replacing the *SacI*/*BsrG*I IRES:eGFP fragment in the pCTIG backbone with IRES:PuroR or IRES:HygroR fragments from pQCXIP and pIRES-hyg3, respectively, using PCR with primers containing *SacI* and *BsrGI* sites. Each pair of TALEN constructs targeting a locus was modified so that one construct co-expressed HygroR and the other PuroR, conferring transient resistance to both hygromycin and puromycin. TALEN constructs targeting mouse *Shh* and *Ptch2* were designed using Golden Gate cloning (Cermak et al. 2011) into the pCTIG expression vector. The following repeat variable domain architectures were generated: *Shh*: 5' TALEN: NN HD HD HD HD NN NN NN HD NG NN NN HD HD NG NN NG, 3' TALEN: NN HD HD NN HD HD NG HD NG NG NG HD HD NI NI NI HD. *Ptch2*: 5' TALEN: NN NN HD NG NG HD NN NI NN HD NG NG NI HD NG NG HD, 3' TALEN: NG HD NG NN NN NI NG HD HD NG NN HD NI HD HD HD HD. mESCs were transfected with paired TALEN constructs using Lipofectamine 2000. 1 day after transfection, cells were passaged into ES medium containing 100 µg/mL Hygromycin and 0.5 µg/mL Puromycin and cultured for 4 days. Selective medium was then removed and surviving mESC colonies were isolated, expanded and genotyped by sequencing PCR products spanning the TALEN binding sites.

Genotyping

PCR screening was performed on cell lysates using primers flanking the *Shh* and *Ptch2* TALEN binding sites: *Shh:* (5') TGGGGATCGGAGACAAGTC and (3') TCTGCTCCCGTGTTTTCCT, *Ptch2*: (5') AAGGCACAGGGAAAGAGAGTT and (3') ACTTGCCTAGCTTGCACAATG. PCR products were sequenced using Sanger sequencing. Samples with mixed signals indicative of small INDEL mutations were TOPO cloned into PCR2.1 and sequenced to confirm allele sequences. A *Ptch1-/-;Shh+/-* mESC clone harboring a 5bp deletion in *Shh* exon 1 was validated and re-transfected with *Shh* TALENs. A *Ptch1-/-;Shh-/-* clone heteroallelic for 5bp and 4bp deletions with predicted stop codons in exon 1 was characterized for its response to ShhN. A *Ptch1-/-;Ptch2-/-* clone was characterized with a 5bp deletion in exon1 of *Ptch2*.

Acknowledgements
The *Ptch1Δloop2* construct was a gift from Dr. Jessell (Columbia University), *Ptch1* and the *Ptch1*-/- mESCs were a gift of Dr. Scott (Stanford University). *Smo*-/- MEFs were from Dr. Taipale (University of Helsinki). The *Smo*-/- mESCs were a gift from Dr. McMahon (University of Southern California). This work was supported by NIH grant R01GM097035 to HR, and a KWF Dutch Cancer Society Fellowship (UVA 2010-4813) and Project Grant (UVA 2012-5607) for MFB. AA is a trainee on R25GM090110. BR is a predoctoral fellow of CIRM training grant TG2-01164. We would also like to thank S. Mohan, A. Mich, and J. Hardin for lending their technical assistance.

Author contributions
MB, LK, AA and BR performed experiments and interpreted data. AA and BR have contributed equally to this work. All authors have contributed to the written manuscript.

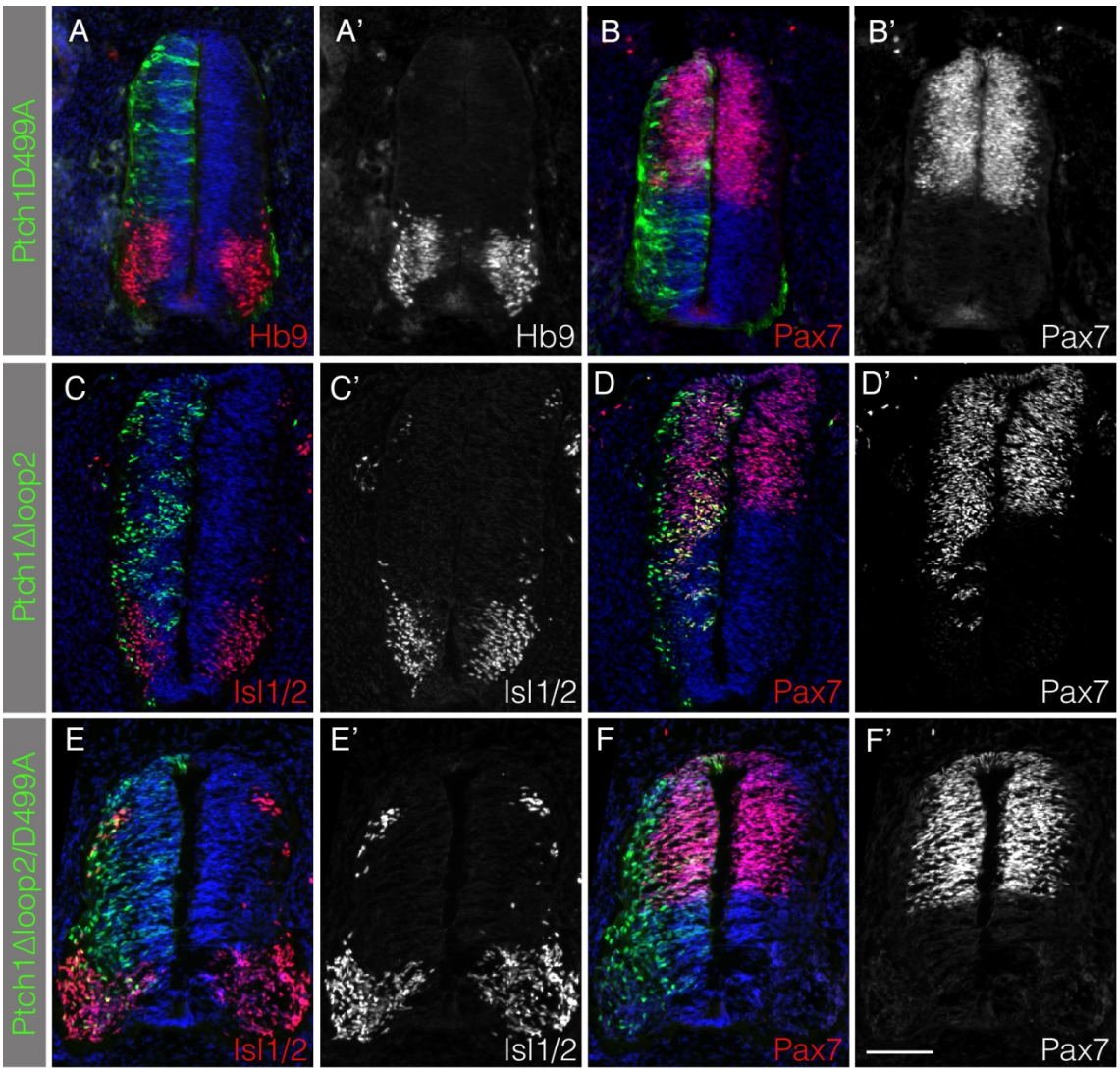

Figure 1. Inhibition of Smo is mediated by the proton-driven antiporter activity of Ptch1

Cross sections of stage 20 HH chicken neural tubes electroporated with *pMES-mPtch1D499A* (A, B), *pCIG-mPtch1Δloop2* (C, D) and *pCIG-mPtch1Δloop2/D499A* (E, F) are labeled in green. Sections are stained with antibodies to Hb9 (A), Islet1/2 (C, E), or Pax7 (B, D, F) as labeled in red or represented in the corresponding gray scale image (′), and DAPI nuclear stain is labeled in blue. Scale bar (F′) is 50µm.

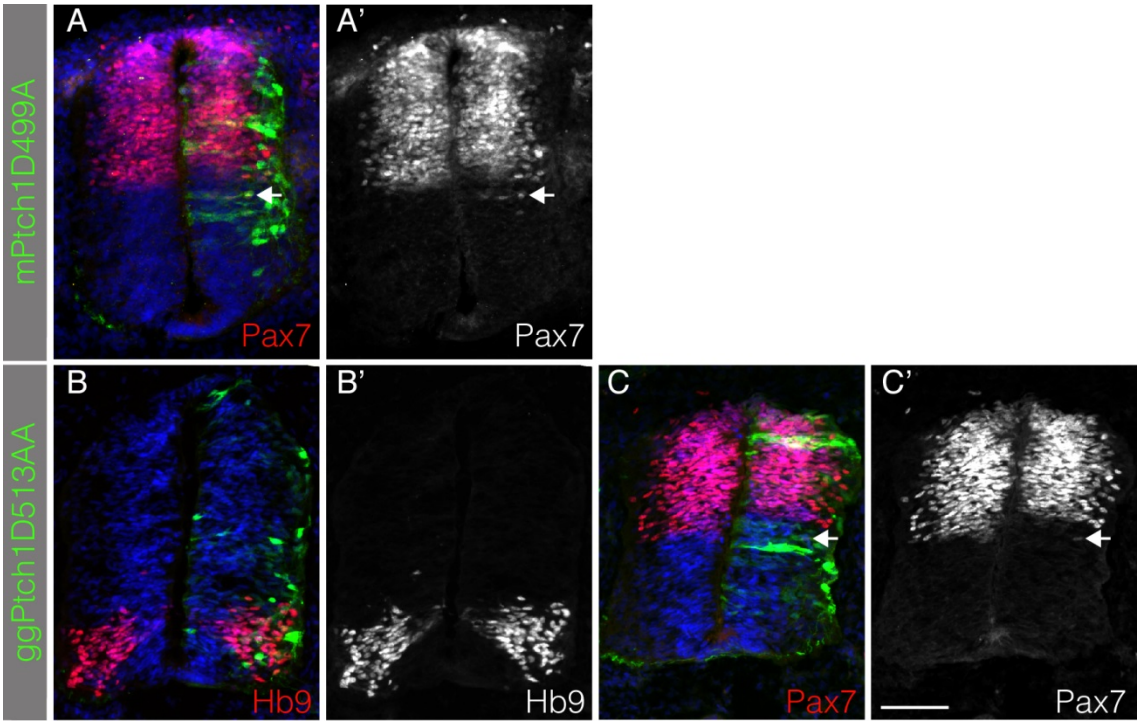

Figure S1. Overexpression of mPtch1D499AA and ggPtch1D513A mutants.
Cross-sections of chicken neural tubes electroporated with *pMES-mPtch1D499A* (A) and a chicken antiporter Ptch1 mutant, *pMES-ggPtch1D513A* (B). Electroporated cells are labeled in green (GFP) and sections are stained with antibodies to Pax7 (A, C), Hb9 (B) as labeled in red or represented in the corresponding gray scale image (‘), and DAPI nuclear in blue. Arrows in A, A’, C, and C’ indicate a cell autonomous induction of Pax7 expression by the Ptch1 antiporter mutants. Scale bar ~50 μm (C′) is 50μm.

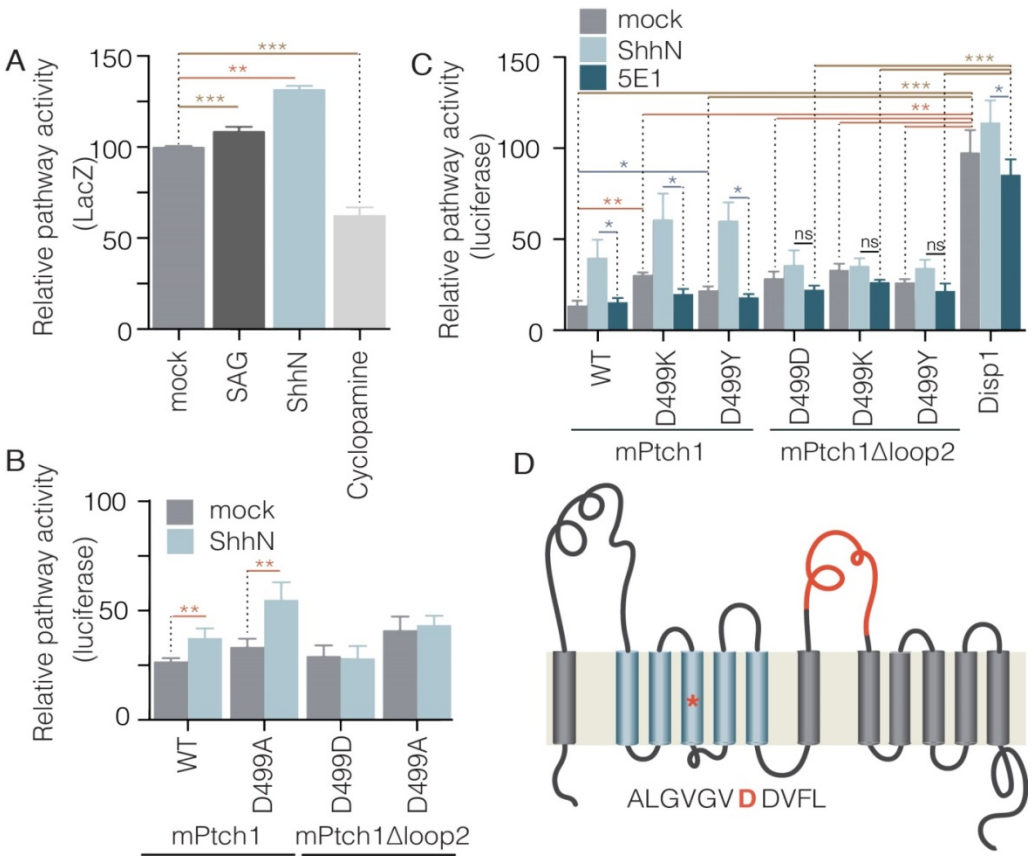

Figure 2. The Shh-binding loop2 of Ptch1 can mediate the Shh response in *Ptch1*-/- fibroblasts independent of the proton-driven antiporter activity.
(A) After *Ptch1*-/- MEFs were grown to confluence, cells were cultured overnight in low serum medium and treated with ShhN conditioned medium, 200 µM SAG, or 1 µM cyclopamine. Cells were lysed and LacZ activity was assessed by determining β-galactosidase levels. Data show mean ± SEM from 3 experiments performed in triplicate. (B, C) *Ptch1*-/- MEFs were co-transfected with Ptch1, Ptch1 mutants, or Disp1 as control vector, and a *Gli-luciferase* reporter and *CMV-Renilla*. When transfected cells reached confluence, cells were cultured overnight in low serum and treated with control conditioned medium (mock), ShhN conditioned medium, or 5E1 conditioned medium. Cells were lysed the next day and luciferase activity was measured. Data are shown relative to control (cells transfected with *Disp1*) and treated with control conditioned medium (mock); mean ± SEM from 3 experiments performed in duplicate. In B and C, levels were normalized to the induction level measured in the *Disp1* transfected cells (100). Statistical significance was tested by ANOVA for all forms of Ptch1 vs Disp1; panel B, one way ANOVA $p=0.0015$; panel C, two way ANOVA $p<0.0001$. Relevant pair-wise Student's t-tests are indicated. For A, B, C *, $p<0.05$; **, $p<0.01$; ***, $p<0.005$. (D) Schematic diagram of Ptch1 mutants. The aspartic acid reside labeled in red denotes the antiporter mutation in Ptch1 which is located in the sterol sensing domain labeled in blue. The Shh binding domain located in loop2 is the second large extracellular loop

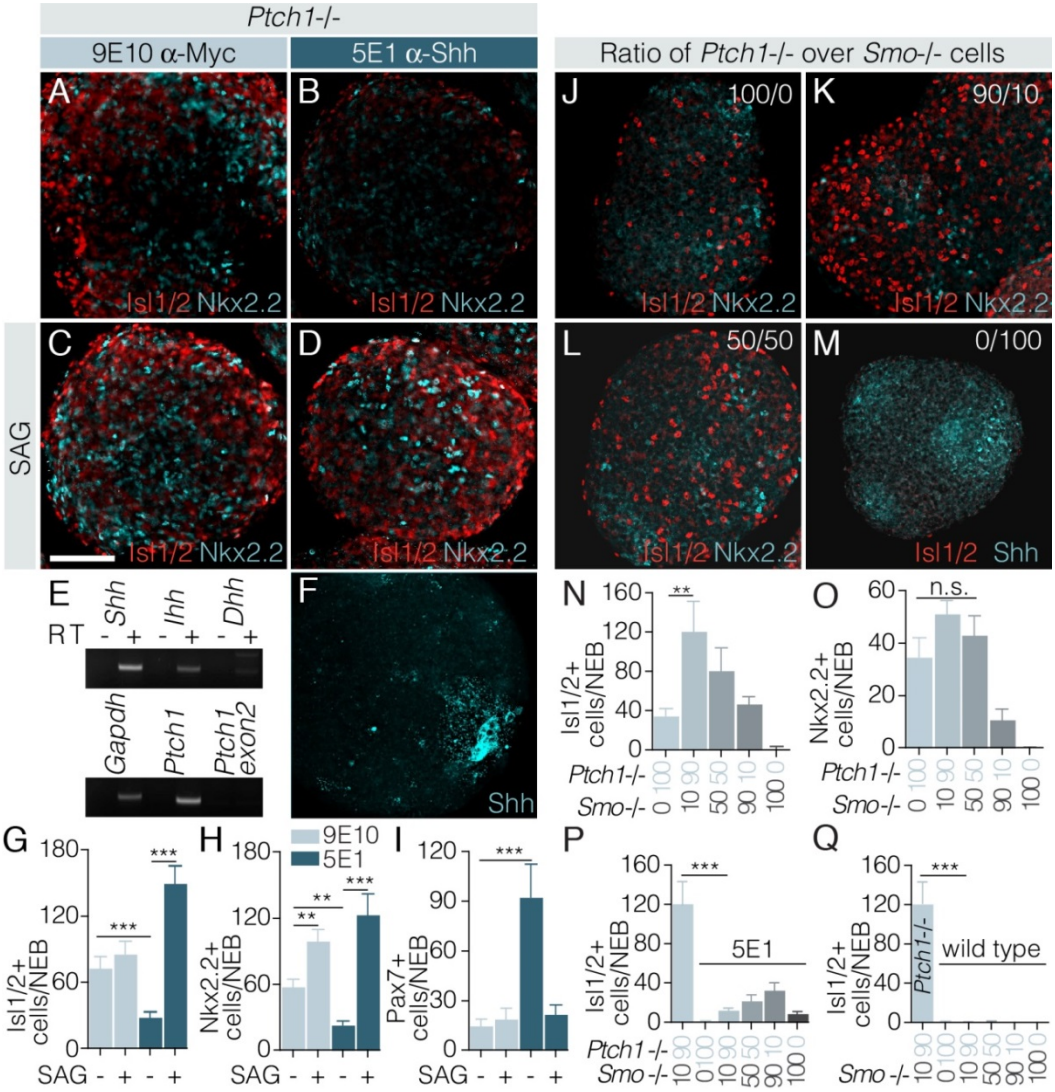

Figure 3. Activation of the Shh response in *Ptch1*-/- mESCs is induced by Shh
(A-D) Embryoid bodies (NEBs) derived from *Ptch1*-/- mESCs were neuralized with 1 µM retinoic acid (RA) in the presence of 1:5 -Shh 5E1 supernatant (B, D), control -Myc 9E10 supernatant (A, C). (C, D) 200 nM SAG was added. Nkx2.2 and Isl1/2 expression was assessed by immunofluorescence after 6 d. (E) RT-PCR analysis for indicated transcripts was performed on RNA isolated from *Ptch1*-/- NEBs. (F) Shh expression was assessed by immunofluorescence using 5E1. (G-I) Numbers of Isl1/2+ (G), Nkx2.2+ (H), or Pax7+ (I) cells per NEB were quantified. Shown is mean ± SEM; n≥20; ***, p<0.005; **, p<0.01. (J-M) *Ptch1*-/- mESCs were mixed with *Smo*-/- mESCs at indicated ratios. Derived NEBs were neuralized with 1 µM retinoic acid and after 7 d, Nkx2.2, Isl1/2, and Shh expression was assessed. (N) Number of Isl1/2$^+$ or (O) Nkx2.2$^+$ cells per NEB was quantified. (P) *Ptch1*-/- mESCs were mixed with *Smo*-/- mESCs, neuralized, and treated with 1:5 -Shh 5E1 supernatant. Isl1/2 expression was assessed. (Q) Wild type (AB1) mESCs were mixed with *Smo*-/- mESCs, neuralized, and Isl1/2 expression was assessed. Shown is mean ± SEM n≥20; **, p<0.01.

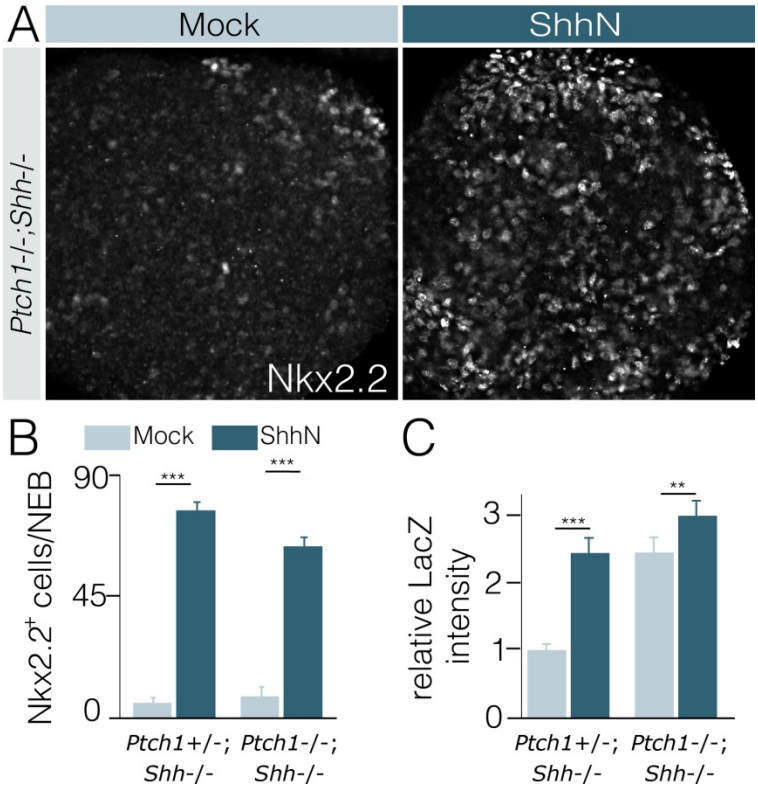

Figure 4. *Ptch1*-/-;*Shh*-/- cells respond to Shh
(A**)** Embryoid bodies (EBs) derived from *Ptch1-/-;Shh-/-* mESCs were neuralized with 1 µM retinoic acid in the absence (mock) or presence of ShhN. At day 5 the EBS were stained for Nkx2.2. (B) the Shh mediated induction of Nkx2.2 was quantified in *Ptch1*+/-;*Shh*-/- and *Ptch1*-/-;*Shh*-/- neuralized EBs. Positive cells per EB were counted. Shown is mean ± SEM; n≥20; ***, p<0.005. (C) The ShhN-mediated induction of LacZ driven by the Ptch1 promoter was measured in *Ptch1*+/-;*Shh*-/- and *Ptch1*-/-;*Shh*-/- EBs. The average of 5 experiments is shown, ± SEM; ***, p<0.005; **, p<0.01.

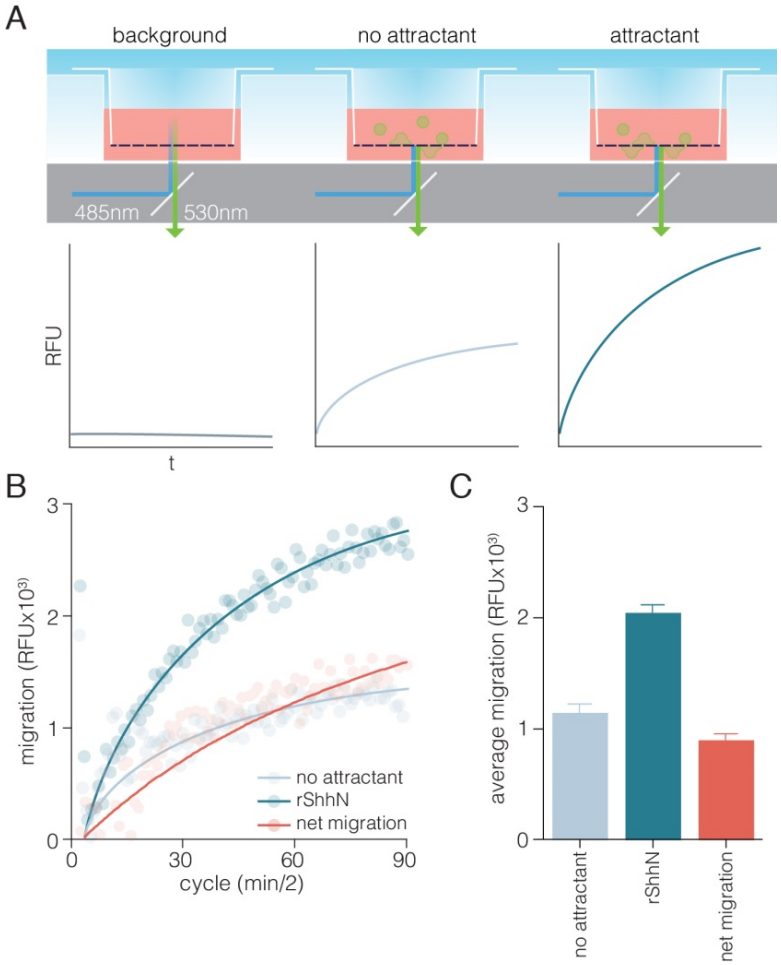

Figure S2. Summary of the modified Boyden chamber migration assay and analysis of results: (A) A Fluoroblok Transwell plate and insert setup is used to measure fluorescence from labeled cells that have migrated through a fluorescence blocking membrane with 8 µm pores. Background fluorescence is measured in time from a well containing medium and these values are subtracted from all other measurements. The 'no attractant' control measures basic cell movement (i.e. movement other than that towards the chemoattractant) for every cell type, transfectant, or other experimental condition. These values are then subtracted from those obtained in the presence of chemoattractant in the bottom compartment of the Transwell setup to yield the specific migration towards a given attractant. Representation as formula; net migration = $(RFU_{attractant}-RFU_{BKG})-(RFU_{no\ att}-RFU_{BKG})$. (B) An example of a chemotaxis experiment using rShhN is shown. Background values are already subtracted, and starting points of migration are set to y=0. To yield specific net migration (indicated in red), values for the no attractant control are subtracted from the chemotaxis towards 5 nM recombinant ShhN. Note that line curves are fitted, rather than plotted means for clarity. (C) The average of migration measured over time as shown in panel B plotted as bar graphs.

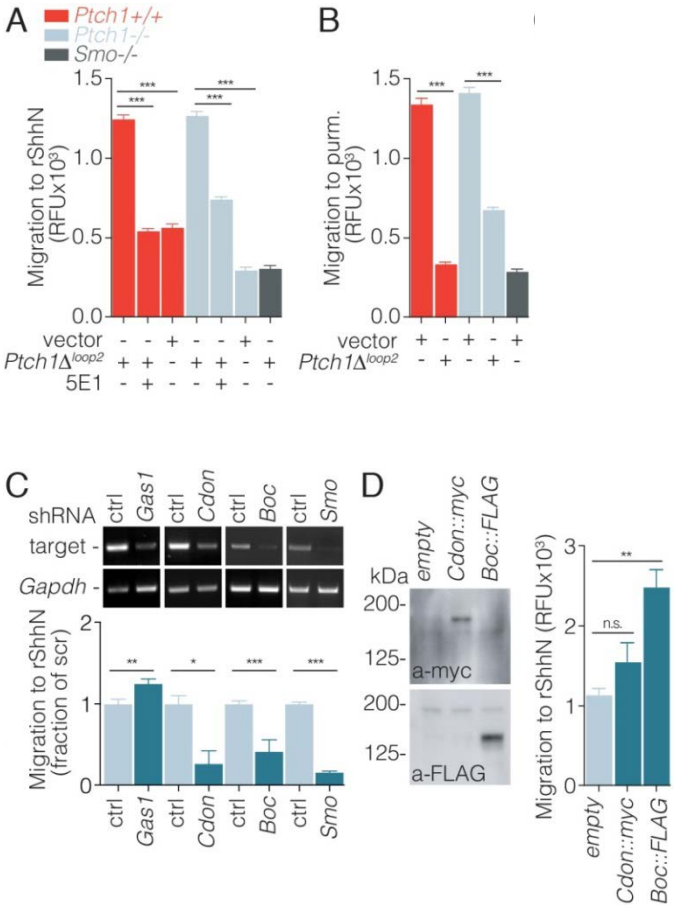

Figure 5. Fibroblast chemotaxis to Shh does not require Ptch1, but is sensitive to Ptch1-mediated inhibition

(A) *Ptch1*+/+ and *Ptch1*-/- MEFs were transfected with vector or *Ptch1Δloop2*, and net migration to 5 nM ShhN was assessed in the absence or presence of 5E1. Vector transfected *Smo*-/- MEFs were included as a control. For technical and quantitative details, see Experimental Procedures. Shown is net migration from 6 experiments, ± SEM; ***, $p<0.005$. (B) As for panel A, using 2μM purmorphamine. Purmorphamine was used rather than SAG, as it is a more consistent Smo agonist in chemotaxis experiments. (C) *Ptch1*-/- MEFs were stably transduced with shRNA constructs against indicated genes or non-silencing controls (ctrl). RT-PCR was performed to assess knockdown efficiency, and net migration to ShhN was assessed. Shown is average net migration from 3 experiments, ± SEM; *, $p<0.05$; ***, $p<0.005$. Statistical significance was assessed by Student's t-test. (D) *Ptch1*-/- MEFs were stably transduced with indicated constructs and Western blot analysis was performed to assess expression levels. Subsequently, net migration of transduced MEFs to ShhN was measured. Shown is net migration from 3 experiments, ± SEM; **, $p<0.01$.

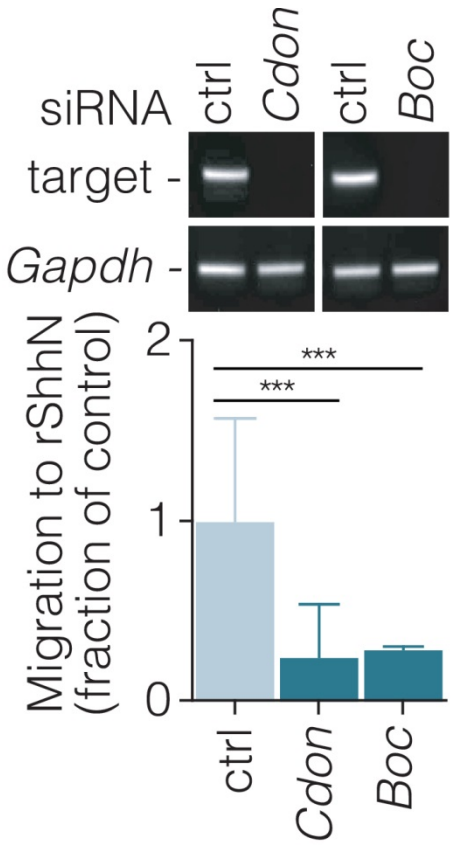

Figure S3. Fibroblast chemotaxis to rShhN requires Cdon and Boc. *Ptch1*-/- MEFs were transiently transfected with siRNA against *Cdon*, *Boc*, or scrambled control and knockdown was assessed by RT-PCR. Net migration to ShhN was assessed as for Figure 3. Shown is average net migration from 3 experiments, ± SEM; *, $p<0.05$; ***, $p<0.005$. Statistical significance was assessed by Student's t-test.

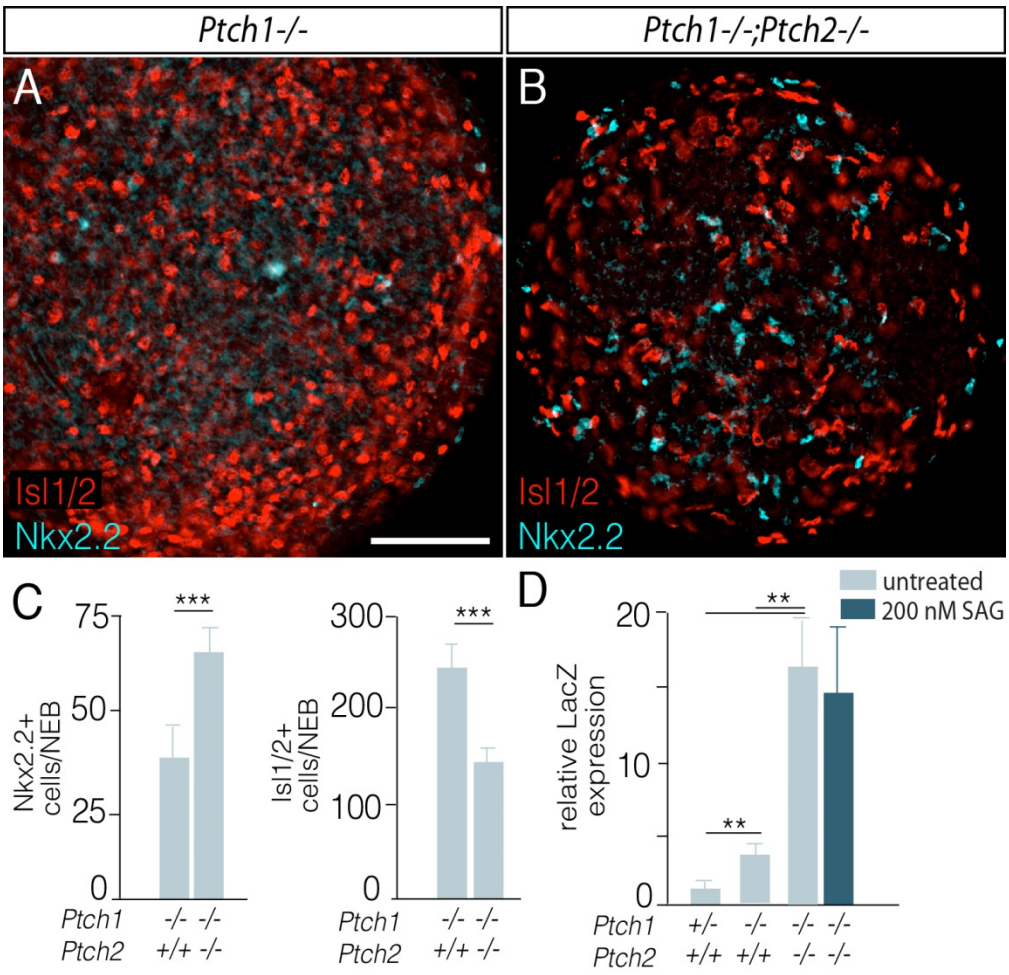

Figure 6. *Ptch1*-/-;*Ptch2*-/- NEBs have a higher level of Shh pathway activation than Ptch1-/- NEBs

(A, B**)** Neuralized Embryoid bodies (NEBs) derived from *Ptch1*-/- (A) and *Ptch1*-/-;*Ptch2*-/-(B) mESCs were stained for Nkx2.2 (cyan) and Isl1/2 (red). (C) Quantification of the expression of Isl1/2 and Nkx2.2. as positive cells per NEB. Shown is mean ± SEM; n≥21; ***, p<0.005. (D) The induction of LacZ driven by the *Ptch1* promoter was measured in *Ptch1*+/-, *Ptch1*-/- and *Ptch1*-/-;*Ptch2*-/- NEBs. The effect of SAG on *Ptch1*-/-;*Ptch2*-/- NEBs was assessed. The average of 4 experiments is shown, ± SEM, **, p<0.01.

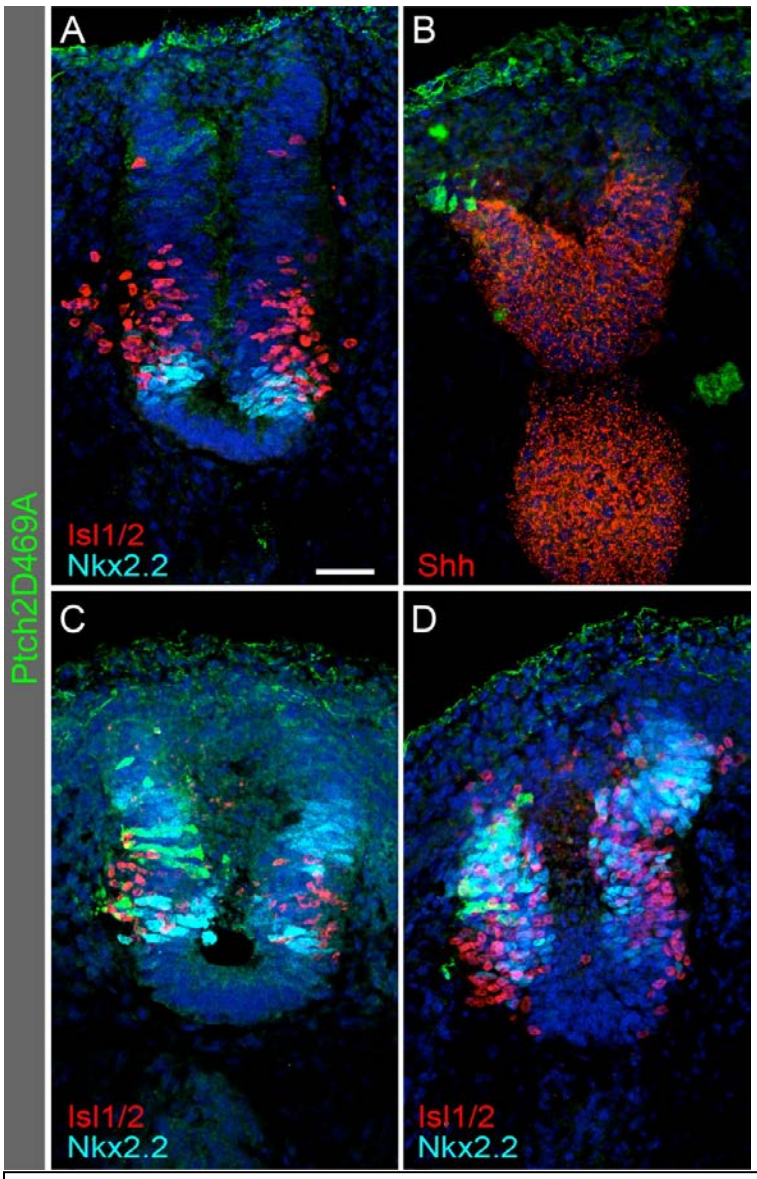

Figure 7. Expression of Ptch2 antiporter mutants causes widespread activation of the Shh response.

(A-D) H&H stage 10 embryos were electroporated with *Ptch2D496A*. Electroporated cells are labeled in green (GFP). (A) At most A/P levels the patterning of the neural tube is normal as assessed by Isl1/2 (red) and Nkx2.2 (cyan) expression. (B) At some caudal levels the domain of Shh expression (red) is increased, although most Shh expressing cells do not express *Ptch2D496A*. (C-D) Similarly at some A/P levels neural tube patterning is severely disrupted as visualized by the expression of Nkx2.2 bilaterally dorsal to the normal domain of Nkx2.2 expression (C) or NkX2.2 positive cells (D) dorsal to the Isl1/2 domain (red). A and C show nearby sections, B and D show nearby sections from a different embryo. Scale bar is 10µm.

References

Allen, B.L. et al., 2011. Overlapping roles and collective requirement for the coreceptors GAS1, CDO, and BOC in SHH pathway function. *Dev Cell*, 20(6), pp.775–787.

Bejsovec, A. & Wieschaus, E., 1993. Segment polarity gene interactions modulate epidermal patterning in Drosophila embryos. *Development*, 119(2), pp.501–517.

Bijlsma, M.F. et al., 2008. Leukotriene synthesis is required for hedgehog-dependent neurite projection in neuralized embryoid bodies but not for motor neuron differentiation. *Stem Cells*, 26(5), pp.1138–1145.

Bijlsma, M.F., Damhofer, H. & roelink, H., 2012. Hedgehog-stimulated chemotaxis is mediated by smoothened located outside the primary cilium. *Science signaling*, 5(238), p.ra60.

Briscoe, J. et al., 2001. A hedgehog-insensitive form of patched provides evidence for direct long-range morphogen activity of sonic hedgehog in the neural tube. *Mol Cell*, 7(6), pp.1279–1291.

Briscoe, J. et al., 1999. Homeobox gene Nkx2.2 and specification of neuronal identity by graded Sonic hedgehog signalling. *NATURE*, 398(6728), pp.622–627.

Cermak, T. et al., 2011. Efficient design and assembly of custom TALEN and other TAL effector-based constructs for DNA targeting. *Nucleic Acids Res*, 39(12), p.e82.

Chan, S. et al., 1987. A novel tumour marker related to the c-myc oncogene product. *Mol Cell Probes*, 1(1), pp.73–82.

Charrier, J.-B. et al., 2002. Dual origin of the floor plate in the avian embryo. *Development*, 129(20), pp.4785–4796.

Charrier, J.B. et al., 1999. Defining subregions of Hensen's node essential for caudalward movement, midline development and cell survival. *Development*, 126(21), pp.4771–4783.

Chen, J.K. et al., 2002. Inhibition of Hedgehog signaling by direct binding of cyclopamine to Smoothened. *Genes and Development*, 16(21), pp.2743–2748.

Corbit, K.C. et al., 2005. Vertebrate Smoothened functions at the primary cilium. *NATURE*, 437(7061), pp.1018–1021.

Crawford, T.Q. & Roelink, H., 2007. The notch response inhibitor DAPT enhances neuronal differentiation in embryonic stem cell-derived embryoid bodies independently of sonic hedgehog signaling. *Dev Dyn*, 236(3), pp.886–892.

Ericson, J. et al., 1996. Two critical periods of Sonic Hedgehog signaling required for the specification of motor neuron identity. *Cell*, 87(4), pp.661–673.

Etheridge, L.A. et al., 2010. Evidence for a role of vertebrate Disp1 in long-range Shh signaling. *Development*, 137(1), pp.133–140.

Goodrich, L.V. et al., 1997. Altered neural cell fates and medulloblastoma in mouse patched mutants. *Science*, 277, pp.1109–1113.

Holtz, A.M. et al., 2013. Essential role for ligand-dependent feedback antagonism of vertebrate hedgehog signaling by PTCH1, PTCH2 and HHIP1 during neural patterning. *Development*, 140(16), pp.3423–3434.

Huangfu, D. & Anderson, K.V., 2005. Cilia and Hedgehog responsiveness in the mouse. *Proc. Natl. Acad. Sci. U. S. A.*, 102(32), pp.11325–11330.

Incardona, J.P., Gruenberg, J. & Roelink, H., 2002. Sonic hedgehog induces the segregation of patched and smoothened in endosomes. *Curr Biol*, 12(12), pp.983–995.

Izzi, L. et al., 2011. Boc and Gas1 each form distinct Shh receptor complexes with Ptch1 and are required for Shh-mediated cell proliferation. *Dev Cell*, 20(6), pp.788–801.

Kawakami, A. et al., 1997. Distributions of PAX6 and PAX7 proteins suggest their involvement in both early and late phases of chick brain development. *Mech Dev*, 66(1-2), pp.119–130.

Kim, H.-S., Nagore, D. & Nikaido, H., 2010. Multidrug efflux pump MdtBC of Escherichia coli is active only as a B2C heterotrimer. *J Bacteriol*, 192(5), pp.1377–1386.

Koudijs, M.J. et al., 2008. Genetic analysis of the two zebrafish patched homologues identifies novel roles for the hedgehog signaling pathway. *BMC Dev Biol*, 8, p.15.

Lee, Y. et al., 2006. Patched2 modulates tumorigenesis in patched1 heterozygous mice. *Cancer Res*, 66(14), pp.6964–6971.

Lu, X., Liu, S. & Kornberg, T.B., 2006. The C-terminal tail of the Hedgehog receptor Patched regulates both localization and turnover. *Genes and Development*, 20(18), pp.2539–2551.

Marigo, V. et al., 1996. Biochemical evidence that patched is the Hedgehog receptor. *NATURE*, 384(6605), pp.176–179.

Meyer, N.P. & Roelink, H., 2003. The amino-terminal region of Gli3 antagonizes the Shh response and acts in dorsoventral fate specification in the developing spinal cord. *Dev. Biol.*, 257(2), pp.343–355.

Milenkovic, L., Scott, M.P. & Rohatgi, R., 2009. Lateral transport of Smoothened from the plasma membrane to the membrane of the cilium. *J Cell Biol*, 187(3), pp.365–374.

Murone, M., Rosenthal, A. & de Sauvage, F.J., 1999. Sonic hedgehog signaling by the patched-smoothened receptor complex. *Curr Biol*, 9(2), pp.76–84.

Nieuwenhuis, E. et al., 2006. Mice with a targeted mutation of patched2 are viable but develop alopecia and epidermal hyperplasia. *Molecular & Cellular Biology*, 26(17), pp.6609–6622.

Nikaido, H. & Takatsuka, Y., 2009. Mechanisms of RND multidrug efflux pumps. *Biochimica et Biophysica Acta*, 1794(5), pp.769–781.

Nikaido, H. & Zgurskaya, H.I., 2001. AcrAB and related multidrug efflux pumps of Escherichia coli. *J Mol Microbiol Biotechnol*, 3(2), pp.215–218.

Placzek, M., Jessell, T.M. & Dodd, J., 1993. Induction of floor plate differentiation by contact-dependent, homeogenetic signals. *Development*, 117(1), pp.205–218.

Rahnama, F., Toftgard, R. & Zaphiropoulos, P.G., 2003. Distinct roles of PTCH2 splice variants in Hedgehog signaling. *Biochem. J.*, Pt.

Resende, T.P. et al., 2010. Sonic hedgehog in temporal control of somite formation. *Proc. Natl. Acad. Sci. U. S. A.*, 107(29), pp.12907–12912.

Rohatgi, R., Milenkovic, L. & Scott, M.P., 2007. Patched1 regulates hedgehog signaling at the primary cilium. *Science*, 317(5836), pp.372–376.

Sasaki, H. et al., 1997. A binding site for Gli proteins is essential for HNF-3beta floor plate enhancer activity in transgenics and can respond to Shh in vitro. *Development*, 124(7), pp.1313–1322.

Smyth, I. et al., 1999. Isolation and characterization of human patched 2 (PTCH2), a putative tumour suppressor gene inbasal cell carcinoma and medulloblastoma on chromosome 1p32. *Hum Mol Genet*, 8(2), pp.291–297.

Stone, D.M. et al., 1996. The tumour-suppressor gene patched encodes a candidate receptor for Sonic hedgehog. *NATURE*, 384(6605), pp.129–134.

Taipale, J. et al., 2000. Effects of oncogenic mutations in Smoothened and Patched can be reversed by cyclopamine. *NATURE*, 406(6799), pp.1005–9.

Taipale, J. et al., 2002. Patched acts catalytically to suppress the activity of Smoothened. *NATURE*, 418(6900), pp.892–897.

Tenzen, T. et al., 2006. The cell surface membrane proteins Cdo and Boc are components and

targets of the Hedgehog signaling pathway and feedback network in mice. *Dev Cell*, 10(5), pp.647–656.

Van Bambeke, F., Balzi, E. & Tulkens, P.M., 2000. Antibiotic efflux pumps. *Biochem. Pharmacol.*, 60(4), pp.457–470.

Wichterle, H. et al., 2002. Directed differentiation of embryonic stem cells into motor neurons. *Cell*, 110(3), pp.385–397.

Chapter 3

Patched1 and Patched2 inhibit Smoothened non-cell autonomously

Brock Roberts and Henk Roelink

Department of Molecular and Cell Biology, 16 Barker Hall, 3204, University of California, Berkeley CA 94720, USA

Submitted to ELife 8/12/15

Summary

Patched-mediated inhibition of Smoothened is central to the hedgehog signaling mechanism. Patched (Ptch) is a putative proton-driven antiporter, and this antiporter activity is required for Smoothened (Smo) inhibition. Here we assessed whether Ptch inhibits Smo activity non-cell autonomously by secreting a Smo inhibitor. Using genome editing we disrupted the core hedgehog pathway genes *Ptch1*, *Ptch2*, *Smo*, *Sonic Hedgehog (Shh) and Dispatched1 (Disp1)* in most combinations in mouse embryonic stem cells (mESCs). Neural differentiation directs each mESC line to a predictable dorso-ventral identity that coincides with the prevailing model of cell autonomous hedgehog pathway regulation in the neural tube. We used these novel cells lines to generate mosaic neural tissues and assessed the non-cell autonomous interactions between cells that differ with regard to their endogenous Ptch1 and Ptch2 status. Genetically encoded reporters of the Hh response were invariably repressed by the presence of Ptch1/2 in nearby cells, regardless of the cell autonomous presence of Ptch1/2 activity. This effect persisted despite genetic disruption of *Shh*, *Disp1*, and *Smo* in several cell lines, demonstrating direct Smo inhibition by Ptch1/2 action, rather than hedgehog ligands or inducers secondary to Smo activation. The presence of Ptch1/2 in nearby cells strongly attenuated Hh response activation by the Smo agonist SAG and by Shh. Relatively few Ptch1/2 expressing cells are sufficient to suppress the activated Hh response in mosaic tissues largely comprised of cells lacking Ptch1/2. We attribute these findings to Ptch1/2-mediated secretion of a Smo inhibitor which consequently affects Smo activity in nearby cells.

Introduction

Hedgehog (Hh) signaling is critically important during embryonic development and its aberrant activation is associated with some of the most common and lethal forms of cancer. Conserved roles as a morphogen and in tissue homeostasis make hedgehog signaling fundamental to most forms of metazoan life (Briscoe & Thérond 2013; Hooper & Scott 2005; Ingham & McMahon 2001).

The putative G-Protein Coupled Receptor (GPCR) Smoothened (Smo) and the proton-driven antiporter-like Hh receptor Patched (Ptch) are conserved multipass transmembrane proteins required for proper hedgehog pathway transduction. The regulatory relationship between Ptch and Smo has been the subject of much study, resulting in the following model: 1) Ptch in its unbound state efficiently inhibits Smo cell autonomously 2) Hh ligand binding to Ptch releases this inhibition and 3) uninhibited Smo redistributes in the cell and activates the transcriptional pathway response.

While this model is widely accepted, the mechanism responsible for Smo repression by Ptch has nevertheless proven elusive. Ptch belongs to the Resistance, Nodulation and Division (RND) family of proton-driven trimeric efflux pumps, which are ubiquitously present in all studied organisms (Nikaido & Takatsuka 2009). RNDs secrete diverse molecular cargos, including small lipophilic and amphiphilic molecules such as antibiotics and lipids. They are well studied in Gram-negative bacteria, where they mediate multidrug resistance by promoting antibiotic efflux from bacterial cells (Tseng et al. 1999).

The finding that Ptch inhibits Smo sub-stoichiometrically has led to a hypothesis whereby Ptch catalytically inhibits Smo activity by regulating the intracellular localization of a Smo regulatory molecule (Taipale et al. 2002). However, despite the discovery of exogenous molecules capable of regulating Smo, no endogenous Smo-regulatory Ptch substrate has been identified (Sharpe et al. 2015). The plant-derived steroidal alkaloid cyclopamine inhibits the Hh response pathway and may mimic the Ptch substrate (J K Chen, Taipale, Cooper, et al. 2002; Incardona et al. 1998). Heterologous Ptch expression in yeast also enhances BODIPY-cholesterol efflux (Bidet et al. 2011). Finally, the closest prokaryotic homolog of Ptch, HpnH, transports bacterial sterols (hopanoids) from the inner to the outer bacterial membrane (Doughty et al. 2011). Steroidal molecules are therefore strong candidates as the Smo-inhibitory Ptch substrate.

As an RND antiporter, Ptch is predicted to secrete its substrate into the extracellular space. This notion is supported by the observation that murine fibroblasts overexpressing Ptch can condition their supernatant such that it inhibits Smo (Bijlsma et al. 2006). However, few reports address non-cell autonomous Smo regulation by Ptch. This may be due to non-cell autonomous Ptch functions unrelated to its transporter activity, such as its ability to sequester hedgehog ligands from the environment and thus suppress the Hh response (Chen & Struhl 1996; Milenkovic et al. 1999; Incardona, Lee, et al. 2000; Strutt et al. 2001). Loss of Ptch can also indirectly activate Smo non-cell autonomously by upregulating Hh ligands, and also reducing their sequestration (Goodrich 1997; Alfaro et al. 2014). These antiporter-independent properties of Ptch may confound efforts to assess non-cell autonomous antiporter-mediated Ptch activity.

To resolve this, we designed a stem cell differentiation based system which allows us to 1) physically combine differentiating cells with different levels of Ptch activity 2) independently

assess the level of hedgehog pathway activation in cells with and without Ptch activity and 3) lacks Hh ligand activity.

Sonic Hedgehog (Shh) patterns the developing vertebrate neural tube through a well-studied transcriptional response (Roelink et al. 1994; Cohen et al. 2013). Shh is expressed in the notochord and floorplate of the neural tube, yielding a ventral to dorsal gradient of Hh pathway activity in which ventral cell types have a high Hh response. This signaling system can be effectively modeled *in vitro* using stem cell differentiation protocols that yield neuralized embryoid bodies (NEBs) (Wichterle et al. 2002; Meinhardt et al. 2014). NEBs are highly responsive to Shh and sensitive to cyclopamine, indicating that Smo activity is subject to regulation in this system (Frank-Kamenetsky et al. 2002). We have previously found that Smo becomes activated in NEBs lacking Ptch1 and Ptch2 (Alfaro et al. 2014).

Using genome editing in conjunction with this stem cell differentiation approach we also confronted the problem of overlapping gene functions by generating complex genotypes in individual cell lines. Hedgehog ligand and receptor paralogs have expanded during evolution. Amniotes have two Ptch paralogs (Ptch1 and Ptch2), three Hh paralogs, Sonic hedgehog (Shh), Indian hedgehog (Ihh), and Desert hedgehog (Dhh), and a single Smo homolog. Dispatched (Disp), an RND antiporter required for hedgehog ligand secretion, appears to have a single functional amniote homolog, Disp1 (Burke et al. 1999). These genes have been comprehensively assessed *in vivo* for their contribution to amniote development (Zhang et al. 2001; Goodrich et al. 1997; Chiang et al. 1996; Ma et al. 2002; Kawakami et al. 2002; Tian et al. 2005). However, compound mutant genotypes necessary to interrogate cell autonomous and non-cell autonomous mechanisms have nevertheless been difficult to generate in vertebrate embryos. For example, despite evidence that *Ptch1*$^{-/-}$ embryos upregulate Shh, which signals through Ptch2, neither *Ptch1*$^{-/-}$*; Ptch2*$^{-/-}$ nor *Ptch1*$^{-/-}$*; Shh*$^{-/-}$ embryos have been reported (Holtz et al. 2013; Alfaro et al. 2014; Zhulyn et al. 2015; Goodrich 1997).

We describe mESCs genetically null for most combinations of *Ptch1*, *Ptch2*, *Smo*, *Shh* and *Disp1*. These cells behave in a manner predicted by the inhibitory cell autonomous activity of Ptch1/2 on Smo when differentiated into mESC-derived neural tissue. We demonstrate that cells with Ptch1/2 activity inhibit the Hh response non-cell autonomously. Furthermore, we find that cells lacking Ptch1/2 can non-cell autonomously enhance responses in neighboring cells to the Smo agonist SAG and also to Shh. We attribute these observations to a fundamental function of Ptch1/2 in secreting a Smo inhibitor via its proton antiporter activity, and propose that mosaic absence of Ptch1/2 activates Smo throughout the tissue environment.

Results

mESC lines with combinatorial genotypes for Ptch1, Ptch2, Smo, Disp1, and Shh

We established a panel of murine embryonic stem cell (mESC) lines using TAL effector endonucleases (TALENs) were designed to target the Hh pathway genes *Shh, Ptch1, Ptch2,* and *Smo* (Cermak et al. 2011). To construct one family of cell lines, TALEN constructs targeting a single gene or multiple genes were transfected into *Ptch1*$^{+/LacZ}$ or *Ptch1*$^{LacZ/LacZ}$ mESC lines (Goodrich et al. 1997). These lines express LacZ under the endogenous *Ptch1* promoter. The resulting null *Ptch1*^{LacZ} allele is a genetically encoded reporter of Hh pathway activity. We also targeted *Shh, Ptch1* and *Ptch2* in *Disp1*$^{-/-}$ mESCs. We reason that within these lines, Dhh and Ihh are unable to mediate paracrine non-cell autonomous effects (Etheridge et al. 2010; Ma et al. 2002). The *Disp1*$^{-/-}$ cell lines are also devoid of *LacZ*, allowing us to measure non-cell autonomous effects on pathway activation when co-cultured with *Ptch1*$^{+/LacZ}$ or *Ptch1*$^{LacZ/LacZ}$ cells.

We previously used this approach to disrupt the *Ptch2* locus within *Ptch1*$^{LacZ/LacZ}$ mESCs (Alfaro et al. 2014). We found that *Ptch1*$^{LacZ/LacZ}$;*Ptch2*$^{-/-}$ NEBs acquired ventral identity and could not be further induced by the Smo agonist SAG, suggesting maximal pathway activation (Chen et al. 2002). We also found that Ptch2 can mediate the response to Shh in the absence of Ptch1. Given the contributions of both Ptch1 and Ptch2 to the interpretation of the Shh signal, we reasoned that a *Ptch1*$^{-/-}$;*Ptch2*$^{-/-}$ genetic background was essential to assess the aggregate contribution of Ptch1/2 to Shh signaling.

In agreement with the roles of Ptch1 and Ptch2 as Smo regulators, *Ptch1*$^{LacZ/LacZ}$;*Ptch2*$^{-/-}$ NEBs differentiated into a highly ventral neural identity, indicated by robust Nkx2.2, Isl1/2 and Olig2 immunostaining (Figure 1G,P). These cells did not respond to the exogenous soluble Shh allele ShhN (data not shown) and *Ptch1*$^{LacZ/LacZ}$;*Ptch2*$^{-/-}$;*Shh*$^{-/-}$ NEBs acquired a similarly ventral identity (Figure 1H,Q). In contrast, relative to *Ptch1*$^{LacZ/LacZ}$ NEBs, *Ptch1*$^{LacZ/LacZ}$;*Shh*$^{-/-}$ NEBs were less ventralized (Figure 1D,E,M,N). Wild type and *Ptch1*$^{+/LacZ}$;*Shh*$^{-/-}$ NEBs, as expected due to their intact cell autonomous Ptch1/2 activity, did not express markers of ventral neural progenitors and instead expressed Pax7, a marker of dorsal neural fate (Figure 1A,B,J,K). These findings suggest that Smo regulation is mediated largely by these two paralogous receptors and that Smo is fully active in their combined absence, independent of Shh.

These cell lines also required functional Smo activity to acquire a ventral fate. *Ptch1*$^{LacZ/LacZ}$;*Smo*$^{-/-}$ and *Ptch1*$^{LacZ/LacZ}$;*Ptch2*$^{-/-}$;*Smo*$^{-/-}$ NEBs were entirely lacking Nkx2.2, Isl1/2 and Olig2 expression and instead expressed Pax7, as did *Smo*$^{-/-}$ NEBs (Figure 1C,F,I,L,O,R). Each clone had abundant Pax6+ nuclei as NEBs, suggesting that neural differentiation was robust (Supplemental).

We separately measured Ptch1:LacZ induction during neural differentiation using *Ptch1*$^{+/LacZ}$ and *Ptch1*$^{LacZ/LacZ}$ mESCs, which was previously assessed *in vivo* (Goodrich 1997). Within 48h of NEB aggregation, Ptch1:LacZ induction was absent in *Ptch1*$^{+/LacZ}$;*Shh*$^{-/-}$ NEBs but was robust in *Ptch1*$^{LacZ/LacZ}$ and *Ptch1*$^{LacZ/LacZ}$;*Ptch2*$^{-/-}$ clones (Figure 2A,B,E). This induction was reduced in *Ptch1*$^{LacZ/LacZ}$;*Shh*$^{-/-}$ in NEBs but remained largely intact in *Ptch1*$^{LacZ/LacZ}$;*Ptch2*$^{-/-}$;*Shh*$^{-/-}$ NEBs. These findings support a role for upregulated Shh in neural progenitors lacking Ptch1, and the loss of Shh dependence in the combined absence of Ptch1/2 (Figure 2C,F). As with the acquisition of ventral neural fate, the Ptch1:LacZ response was absent in *Ptch1*$^{LacZ/LacZ}$;*Smo*$^{-/-}$ and

Ptch1$^{LacZ/LacZ}$;*Ptch2*$^{-/-}$;*Smo*$^{-/-}$ NEBs and thus Smo dependent (Figure 2D,G). Including 10μM retinoic acid 24h after aggregation, as required for neural differentiation, did not alter Smo dependency (Wichterle et al. 2002). Thus in all of the cell lines we generated, regardless of the number of functional *Ptch1/2* alleles, the Hh response is absolutely dependent on Smo function. Our findings in NEBs are consistent with the Drosophila model of Hh signaling, where Smo is epistatic to Ptch, which is in turn epistatic to Hh (Lawrence et al. 1999; Bejsovec & Wieschaus 1993). The Ptch1:LacZ response in *Ptch1*$^{LacZ/LacZ}$;*Ptch2*$^{-/-}$;*Shh*$^{-/-}$ NEBs remained elevated up to 5 days after NEB aggregation, consistent with a lack of Ptch1/2 mediated feedback (Figure 3A) (Holtz et al. 2013).

Cyclopamine is one of a small group of steroidal alkaloids that directly inhibits Hh signaling through binding to Smo with an IC_{50} around 25nM, and it has been suggested that cyclopamine mimics the Ptch1/2 Smo-inhibitory cargo (Incardona, Gaffield, et al. 2000; Cooper et al. 1998). *Ptch1*$^{LacZ/LacZ}$;*Ptch2*$^{-/-}$;*Shh*$^{-/-}$ NEBs cultured in a range of cyclopamine doses and assessed for Ptch1:LacZ induction at its normal peak at 48h after aggregation were inhibited, with an IC_{50} of around 30nM (Figure 3A,B). Nkx2.2+ and Isl1/2+ ventral progenitors were similarly inhibited in NEBs 72h after aggregation (Figure 3C). These results further demonstrate that response pathway activation observed in cells devoid of Ptch1/2 is mediated via Smo activity and that mESCs with complex loss-of-function genotypes for *Ptch1*, *Ptch2*, *Smo*, and *Shh* differentiate as expected, according to the canonical model of Hh signaling.

We employed the same genome editing approach in *Disp1*$^{-/-}$ mESCs to obtain *Disp1*$^{-/-}$;*Shh*$^{-/-}$, *Disp1*$^{-/-}$;*Shh*$^{-/-}$;*Ptch1*$^{-/-}$, and *Disp1*$^{-/-}$;*Shh*$^{-/-}$;*Ptch1*$^{-/-}$;*Ptch2*$^{-/-}$ mESC lines. Whereas in our other family of mESC cell lines, *Ptch1* null alleles were originally generated with *LacZ* targeting, we generated novel *Ptch1* null alleles in *Disp1*$^{-/-}$ mESCs (hereafter we use *Ptch1*$^{LacZ/LacZ}$ and *Ptch1*$^{-/-}$ as notation to distinguish the null *Ptch1* alleles in these two families). Disp1 is required for the secretion and non-cell autonomous paracrine effects of all Hh ligands, but *Disp1*$^{-/-}$ cells respond to Hh ligands normally (Burke et al. 1999; Etheridge et al. 2010; Tsiairis & McMahon 2008). We observed robust ventral neural progenitor identity only in *Disp1*$^{-/-}$;*Ptch1*$^{-/-}$;*Ptch2*$^{-/-}$;*Shh*$^{-/-}$ NEBs (Figure 4C,F). By contrast *Disp1*$^{-/-}$;*Shh*$^{-/-}$ and *Disp1*$^{-/-}$;*Ptch1*$^{-/-}$;*Shh*$^{-/-}$ were largely dorsal (Figure 4A,B,D,E). We thus found Ptch2 to have an important Smo regulatory role within this independently derived family of mESC clones.

Hh pathway activation in Ptch1$^{+/LacZ}$;*Shh*$^{-/-}$ *and Ptch1*$^{LacZ/LacZ}$;*Ptch2*$^{-/-}$;*Shh*$^{-/-}$ *cells is affected by the presence of Ptch1 and Ptch2 in nearby cells*

As RND antiporters, Ptch1 and Ptch2 may promote efflux of their Smo-inhibitory cargo. We tested whether Ptch1/2 expressed from their endogenous loci could inhibit Smo activity in nearby cells by mixing distinct mESC lines in various ratios to generate mosaic NEBs of ~1000 cells. We varied the genotype of one subpopulation of "test repressor" cells with respect to Ptch1/2 and assessed non autonomous Smo repression in "reporter" cells that constituted a second cell subpopulation.

For the population of test repressor cells, in which the Ptch1/2 genotype was varied, we used *Disp1*$^{-/-}$;*Shh*$^{-/-}$ mESCs because cells lacking Ptch1/2 activity might normally upregulate Shh, Ihh and/or Dhh and thus mirror possible non-cell autonomous effects of Ptch1/2 loss on reporter cells. We expect loss of Disp1 to abrogate that possible effect for Ihh and/or Dhh, while these cells are genetically null for Shh, the primary Hh ligand in neural differentiation. We used these

test repressor cells to examine whether in mosaic NEBs, *Disp1*$^{-/-}$;*Shh*$^{-/-}$ or *Disp1*$^{-/-}$;*Shh*$^{-/-}$;*Ptch1*$^{-/-}$ cells differentially repressed Hh pathway activity in reporter cells, relative to mosaics containing *Disp1*$^{-/-}$;*Shh*$^{-/-}$;*Ptch1*$^{-/-}$;*Ptch2*$^{-/-}$ cells.

For the reporter cells we used the genetically encoded Ptch1:LacZ transgene in *Ptch1*$^{LacZ/LacZ}$;*Ptch2*$^{-/-}$;*Shh*$^{-/-}$ mESCs. We reasoned that the absence of Ptch1/2 in reporter cells ensures that Smo cannot be regulated by the cell autonomous activities of these antiporters, maximizing their sensitivity to possible Ptch1/2-mediated non-cell autonomous effects from test repressor cells. We also reasoned that because these reporter cells robustly upregulate Ptch1:LacZ after differentiation in Smo-dependent fashion, non-cell autonomous Smo inhibition would be detectable in reporter cells (Figure 2F, 3A).

We measured Ptch1:LacZ expression in mosaic NEBs 48h after aggregation, when the Ptch1:LacZ response reached its maximum (Fig 3A), and at 120h. When reporter cells were mixed 1:9, 1:1, or 9:1 with *Disp1*$^{-/-}$;*Shh*$^{-/-}$;*Ptch1*$^{-/-}$;*Ptch2*$^{-/-}$ test repressor cells, Ptch1:LacZ signal intensity was consistent with expected values, given the fraction of reporter cells in the NEB (data not shown). We used these Ptch1:LacZ expression levels as baseline measurements. When *Disp1*$^{-/-}$;*Shh*$^{-/-}$;*Ptch1*$^{-/-}$;*Ptch2*$^{-/-}$ cells were replaced with *Disp1*$^{-/-}$;*Shh*$^{-/-}$ or *Disp1*$^{-/-}$;*Shh*$^{-/-}$;*Ptch1*$^{-/-}$ cells at each mixing ratio, Ptch1:LacZ levels significantly declined at both 48h and 120h (Figure 5A,B,C). These results suggest that endogenously expressed Ptch1/2 levels are capable of suppressing Smo activity non-cell autonomously in cells devoid of Ptch1/2 activity, and that Ptch2 alone is sufficient for this effect in a *Ptch1*$^{-/-}$ environment. These observations suggest that Ptch1/2 secrete a Smo inhibitor that can act on neighboring cells.

The decrease in Ptch1:LacZ expression in reporter cells co-cultured with test repressor cells expressing endogenous Ptch1/2 activity was greatest when reporter cells comprised a minority of the mosaic NEB. However, these effects were still observed in NEBs containing as few as 10% Ptch1/2 expressing cells. We wondered whether this reflected heightened Smo sensitivity to the Ptch1/2 substrate in reporter cells, given their lack of Ptch1/2. To address this, we performed the same experiment using the *Ptch1*$^{+/LacZ}$;*Shh*$^{-/-}$ mESCs as reporter cells. NEBs comprised exclusively of these cells did not upregulate Ptch1:LacZ (Figure 2A) during differentiation and did not acquire ventral neural progenitor fates (Figure 1B,K), suggesting that Ptch1/2 mediated cell-autonomous Smo regulation remained intact.

Under the prevailing view, Ptch1/2 constantly regulate Smo cell autonomously and this activity is expected to be more substantial than the non-cell autonomous effects on Smo mediated by Ptch1/2 activity in nearby cells. However if all or most of the cargo of Ptch1/2 is secreted before it becomes inhibitory to Smo in the same cell, we expect Ptch1/2 loss of function in adjacent cells to affect cells proficient for Ptch1/2.

We found robust non-cell autonomous effects of Ptch1/2 activity in NEBs comprised of 10% *Ptch1*$^{+/LacZ}$;*Shh*$^{-/-}$ reporter cells (Figure 5D). We observed only a meager repressive effect in 1:1 mosaics using these cell lines at the earlier time point, and Ptch1 was required (Figure 5E). Mosaic conditions in which Ptch1/2 in the tissue environment influenced Smo activity in cells with normal Ptch1/2 activity indicates Smo activity is similarly regulated in any given cell by Ptch1/2 activity in nearby cells as it is by Ptch1/2 activity in that same cell. This in turn is consistent with the notion that under all conditions, the Smo-inhibitory cargo of Ptch1/2 is secreted before it affects Smo activity. Because Ptch1/2 are feedback antagonists of the pathway and are intact in *Ptch1*$^{+/LacZ}$;*Shh*$^{-/-}$ reporter cells, the pathway activation under conditions where the Smo inhibitor is less abundant tissue-wide may only be transient, explaining the lack of effect

at the later time point. This contrasts with *Ptch1*$^{LacZ/LacZ}$*;Ptch2*$^{-/-}$*;Shh*$^{-/-}$ reporter cells, in which Ptch1/2 cannot become upregulated and dampen pathway activation at later time points.

The Smoothened activation state of Ptch1/2 expressing cells is sensitive to non-cell autonomous Ptch1/2 function in nearby cells

We independently addressed whether cells with normal cell autonomous Ptch1/2 function are subject to Smo inhibition by Ptch1/2 activity in neighboring cells by employing HB9:GFP transgenic mESCs as reporters for motor neuron differentiation. Shh controls ventral neural tube motor neuron development *in vivo* (Jessell 2000; Alaynick et al. 2011; Briscoe & Thérond 2013). Motor neurons also differentiate *in vitro* in NEBs with the differentiation protocol used in this study (Wichterle et al. 2002).

We co-cultured HB9:GFP mESCs with *Ptch1*$^{+/LacZ}$*;Shh*$^{-/-}$, *Ptch1*$^{LacZ/-}$*;Shh*$^{-/-}$ and *Ptch1*$^{LacZ/LacZ}$*;Ptch2*$^{-/-}$*;Shh*$^{-/-}$ test repressor cells, the family of mESCs that we used as the reporter cells in the experiments presented in Figure 5. We observed a small but significant increase in HB9:GFP+ motor neurons when these reporter cells were co-cultured with *Ptch1*$^{LacZ/LacZ}$*;Ptch2*$^{-/-}$*;Shh*$^{-/-}$ test repressor cells as compared to *Ptch1*$^{+/LacZ}$*;Shh*$^{-/-}$ or *Ptch1*$^{LacZ/-}$*;Shh*$^{-/-}$ test repressor cells (Figure 6A,B). This finding thus supported our previous observations of non-cell autonomous Ptch1/2 mediated effects on *Ptch1*$^{+/LacZ}$*;Shh*$^{-/-}$ reporter cell lines because both *Ptch1*$^{+/LacZ}$*;Shh*$^{-/-}$ and HB9:GFP reporter cell lines have normal cell autonomous Smo regulation.

In order to further test if the lack of non-cell autonomous Ptch1/2-mediated inhibition from test repressor cells affects the activity state of Smo in reporter cells, we treated HB9:GFP mosaic NEBs with SAG, a small molecule Smo agonist. SAG is hypothesized to compete with the Smo-inhibitory Ptch1/2 substrate for binding to Smo, and paucity of this inhibitor due to the lack of Ptch1/2 activity in the tissue environment might thus enhance SAG effectiveness (James K Chen, Taipale, Young, et al. 2002; Sharpe et al. 2015).

10nM and 100nM SAG elicited robust motor neuron differentiation when HB9:GFP reporter cells were co-cultured with test repressor cells devoid of Ptch1/2 (Figure 6A,B). However, *Ptch1*$^{+/LacZ}$*;Shh*$^{-/-}$ cells dramatically suppressed this induction at both SAG doses, while *Ptch1*$^{LacZ/-}$*;Shh*$^{-/-}$ cells also suppressed motor neuron induction to an intermediate degree, again supporting a role for Ptch2 in non-cell autonomous Smo inhibition, and consistent with the idea that the Ptch1/2 cargo and SAG are competitors in their ability to alter Smo activation levels.

Three-part mosaic NEBs reveal a non-cell autonomous role for Ptch1/2 in regulating the Shh ligand response

Whereas SAG binds directly to Smo, Shh activates Smo activity indirectly after first binding to Ptch1/2 as an intermediate step, according to the standard Hh signaling model (Chen et al. 2002). To determine whether our previous findings applied to signaling by Shh, we investigated whether disrupting Ptch1/2 activity in test repressor cells within mosaic NEBs enhances Smo activation within a second population of reporter cells, in response to Shh expressed by a third population of cells. To accomplish this we generated three-part mosaic NEBs including a small fraction (1%) of wild type cells expressing Shh under the EF1□under the. These cells functioned as sparse, localized sources of Shh in mosaic NEBs in which

HB9:GFP reporter cells comprised a second minority compartment (5% of cells). We varied the genotype of the third, largest cell compartment (94%) of test repressor cells and measured HB9:GFP+ motor neuron induction.

Three-part mosaic NEBs consisting principally of *Ptch1*$^{LacZ/LacZ}$;*Shh*$^{-/-}$ or *Ptch1*$^{LacZ/LacZ}$;*Ptch2*$^{-/-}$;*Shh*$^{-/-}$ test repressor cells facilitated robust Shh-mediated HB9:GFP+ motor neuron induction in the HB9:GFP reporter cell compartment (Figure 7A,D). In contrast, we observed negligible motor neuron induction in mosaic NEBs principally comprised of *Ptch1*$^{+/LacZ}$;*Shh*$^{-/-}$ test repressor cells (Figure 7A,D). Shh was required for motor neuron induction, as HB9:GFP+ motor neurons were not observed under conditions where Shh overexpressing cells were omitted.

Indirect factors do not mediate non-cell autonomous effects of Ptch1/2 loss on Hh pathway activation

We wondered whether test repressor cells lacking Ptch1/2 sensitized HB9:GFP reporter cells to Shh either by producing other Hh ligands, or unknown factors downstream of Smo activation. To address if Dhh or Ihh derived from *Ptch1*$^{-/-}$;*Ptch2*$^{-/-}$;*Shh*$^{-/-}$ cells explained the enhanced motor neuron induction in HB9:GFP cells, we reconstructed mosaic NEBs using *Disp1*$^{-/-}$;*Shh*$^{-/-}$ test repressor cells. Dhh and Ihh are not expected to signal normally in the absence of Disp1. Shh robustly induced HB9:GFP+ motor neurons in NEBs primarily consisting of *Disp1*$^{-/-}$;*Ptch1*$^{-/-}$;*Ptch2*$^{-/-}$;*Shh*$^{-/-}$ cells, while motor neuron induction was negligible in NEBs primarily consisting of *Disp1*$^{-/-}$;*Ptch1*$^{-/-}$;*Shh*$^{-/-}$ and *Disp1*$^{-/-}$;*Shh*$^{-/-}$ cells (Figure 7B,D). Motor neuron induction again depended on Shh-expressing cells.

The high activity level of Smo in Ptch1/2-deficient cells could result in other downstream factors becoming upregulated and inducing motor neurons. To address this, we generated three-part mosaic NEBs using *Ptch1*$^{-/-}$;*Smo*$^{-/-}$ or *Ptch1*$^{-/-}$;*Ptch2*$^{-/-}$;*Smo*$^{-/-}$ mESCs. HB9:GFP+ motor neurons were induced efficiently only in predominantly *Ptch1*$^{-/-}$;*Ptch2*$^{-/-}$;*Smo*$^{-/-}$ NEBs (Figure 7C,D). This observation again supports overlapping non-cell autonomous roles for Ptch1/2 and argues against Ptch1/2 independent secondary effects in non-reporter cells. It also suggests that weak endogenous Ptch2 expression is sufficient to non-cell autonomously suppress Smo, because Ptch2 expression levels are likely low in *Smo*$^{-/-}$ cells, given its function in WT cells as a Smo dependent feedback antagonist (Holtz et al. 2013).

Four-part mosaic NEBs attribute far-ranging non-cell autonomous effects to Ptch1/2 expressing cells

Guided by our previous observation that mosaic NEBs comprised of as few as 10% Ptch1/2 proficient test repressor cells suppressed Smo in *Ptch1*$^{LacZ/LacZ}$;*Ptch2*$^{-/-}$;*Shh*$^{-/-}$ reporter cells, we titrated this effect in four-part mosaic NEBs. We predicted that Ptch1/2 expressing cells would suppress Shh signaling to HB9:GFP+ reporter cells even when relatively rare within mosaic tissue.

We measured Shh-mediated HB9:GFP+ motor neuron induction in NEBs comprised largely of *Ptch1*$^{LacZ/LacZ}$;*Ptch2*$^{-/-}$;*Shh*$^{-/-}$ cells after introducing a fourth population of *Ptch1*$^{+/LacZ}$;*Shh*$^{-/-}$ cells at various ratios. In NEBs largely comprised of *Ptch1*$^{LacZ/LacZ}$;*Ptch2*$^{-/-}$;*Shh*$^{-/-}$ cells, 10%, 20% and 40% *Ptch1*$^{+/LacZ}$;*Shh*$^{-/-}$ mESCs strongly suppressed motor neuron

induction (Figure 7E). As few as 10% *Ptch1*$^{+/LacZ}$;*Shh*$^{-/-}$ cells were sufficient to suppress motor neurons induction to levels similar to three-part mosaic NEBs comprised principally of *Ptch1*$^{+/LacZ}$;*Shh*$^{-/-}$ cells. This supports the conclusions from our experiments using Ptch1:LacZ in reporter cells and suggests that only a minority of Ptch1/2 expressing cells is required to non-cell autonomously suppress Smo in cellular environments largely devoid of Ptch1/2.

Discussion

Mosaic NEBs composed of mESCs with novel, complex genotypes allow us to study interactions between cell populations with resolution not easily achieved *in vivo*. Within this system, lineage restricted reporters of the Hh response unambiguously indicate non-cell autonomous Smo inhibition by nearby Ptch1/2 expressing cells. One plausible interpretation of these results is that Ptch1/2 activity mediates the secretion of a Smo inhibitor that affects the Hh response both cell autonomously, and also in nearby cells.

The observation that Ptch1/2 expressing cells secrete a Smo inhibitor is explained by the notion that Ptch1/2 are proton-driven efflux pumps in the RND family (Nikaido & Takatsuka 2009). Besides Ptch1/2, Disp1 and NPC1 are also eukaryotic members of this family and all share highly conserved glutamic acid residues required for proton-driven transport. Proton flux is therefore essential for function of Drosophila Ptch, as well as Ptch1/2 and Disp1 in vertebrates (Strutt et al. 2001; Alfaro et al. 2014; Etheridge et al. 2010). NPC1 transports cholesterol across multi-vesicular endosome (MVE) membranes, and likely requires an acidified lumen as well (Karten et al. 2009). These observations suggest that Ptch1/2 and their eukaryotic relatives function in acidified endosomes.

We have previously demonstrated that the late endosome is on the Ptch1 itinerary, and that Shh signaling requires endosomal acidification (Incardona et al. 2002). One possibility is that Ptch1/2 trimers localized to the membranes of late endosomes are active efflux pumps. This activity may enrich the membranes of intraluminal vesicles in multivesicular endosomes (MVEs), or the endosomal lumen, with a Smo inhibitory molecule. Traffic into the exosomal pathway would allow the contents of such vesicles enriched with the Smo inhibitor to enter the extracellular environment and regulate Smo cell autonomously as well as non-cell autonomously.

The nature of the Smo-inhibitory Ptch1/2 cargo remains unknown but several observations suggest that it is a steroidal molecule. Ptch/Disp as well as NPC-1 have sterol sensing domains (SSD) that are conserved with sterol biogenesis regulatory enzymes, and thus likely bind sterols (Incardona 2005). This domain is necessary for Smo inhibition by Ptch in *Drosophila* (Strutt et al. 2001). Ptch1 also mediates cholesterol secretion from fibroblasts (Bidet et al. 2011). The prokaryotic RNDs most highly conserved with Ptch1/2 putatively transport hopanoids, bacterial sterols (Doughty et al. 2011). Further indication that Smo activity can be affected by steroidal molecules comes from the observation that genetic loss of *7-dehydrocholesterol reductase* (*DHCR7*) coincides with reduced Hh signaling (Cooper et al. 2003). This may stem from 7-dehydroxycholesterol (7DHC) accumulation, or that of its derivatives (e.g. vitamin-D), inhibiting Smo (Bae et al. 1999; Bidet et al. 2011; Bijlsma et al. 2006; Incardona et al. 1998; Linder et al. 2015). Finally, the steroidal alkaloid cyclopamine inhibits Smo, causing holoprosencephaly and cyclopia in amniote embryos (Cooper et al. 1998; Incardona et al. 1998; Chen et al. 2002).

Why the Smo-inhibitory Ptch1/2 cargo, despite its likely abundance in cells, fails to inhibit Smo without being acted on (cell autonomously or non-cell autonomously) by Ptch remains unresolved. We show that cyclopamine inhibits Smo in cells devoid of Ptch1/2 (Figure 3B,C), and thus does not require Ptch1/2 activity to inhibit Smo. Similarly, vitamin D3 also inhibits Smo in *Ptch1*$^{LacZ/LacZ}$ cells (Bijlsma et al. 2006). Whereas molecules thought to mimic the action of the Smo-inhibitory cargo of Ptch1/2 are able to inhibit Smo independent of Ptch1/2

activity, the fact that Smo becomes activated in tissues lacking Ptch indicates that the endogenous Smo inhibitor requires Ptch1/2 function to become inhibitory.

This suggests that the Ptch1/2 substrate has restricted intracellular localization in cells without Ptch1/2 function, and that Ptch1/2 enable it to inhibit Smo both cell autonomously and non-cell autonomously. One possibility is that Ptch1/2 transports an amphipathic molecule normally enriched in the cytoplasmic leaflet of the endosomal/MVE membrane to the lumenal leaflet. Inward budding may then generate intraluminal vesicles whose lumenal membranes are enriched with the SMo inhibitor. Subsequent release of these intraluminal vesicles through the exosome pathway would allow the Ptch1/2 cargo to bind Smo in cell membranes of the same cell or in neighboring cells. This model would reconcile the necessary localization of Ptch1/2 to an acidic compartment to be able to perform efflux, with our observation that Ptch1/2 activity can inhibit Smo non-cell autonomously.

Ptch1/2 mutations drive the formation of several tumors, and an important ramification of our finding is that Ptch1/2 disruption enhances not only cell autonomous Hh responses, but also Smo activation in adjacent cells with intact Ptch1/2 activity (Barakat et al. 2010). The finding that genetically normal stromal cells respond to Shh expressing tumors by infiltrating and supporting them heightens the importance of our observations because Ptch1/2 loss in the tumor may affect stromal cell Shh sensitivity non-cell autonomously (Yauch et al. 2008). Our results also predict that even in the absence of Ptch1/2, cells remain sensitive to Hh ligands signaling in nearby cells. Anti-cancer strategies based on ligand sequestration or inactivation should therefore remain viable treatment options.

Hh signaling plays many critical roles during development as a morphogen. Responding cells interpret graded Hh ligand distributions, resulting in stereotyped patterning and Ptch1/2 have complex roles in this process. As Shh receptors, Ptch1/2 bind extracellular Shh and initiate the response. Invariably, Hh signaling induces *Ptch1/2* expression (Holtz et al. 2013) and Ptch1/2 induction then leads to negative feedback, likely by secreting more Smo inhibitor, increasing Shh sequestration, or both. Our finding that Ptch1/2 inhibit the Hh response non-cell autonomously, even in NEBs devoid of all Shh ligand, supports the notion that the non-cell autonomous inhibition mediated by Ptch1/2 primarily is mediated by the antiporter activity of Ptch1/2, rather than by ligand sequestration, and the ability of relatively few Ptch1/2 expressing cells to inhibit the Hh response pathway further supports this idea.

Together these findings indicate that Ptch1/2 activity broadly and communally inhibit Smo in tissues undergoing patterning. According to this model, local sensitivity to Shh is highly buffered and equalized between cells, aiding the formation of a smooth response gradient in the Shh morphogenetic field.

Methods

Cell lines

Ptch1$^{+/LacZ}$ and *Ptch1*$^{LacZ/LacZ}$ mESCs were gifts from Dr. Matthew Scott (Stanford University and HHMI). *Smo*$^{-/-}$ mESCs were a gift from Dr. Andrew McMahon (University of Southern California). HB9:GFP mESCs were a gift from Dr. Thomas Jessell (Columbia University). *Disp1*$^{-/-}$ mESCs and WT mESCs overexpressing Shh were previously described (Etheridge et al. 2010). The AB1 mESC line was used as wild type. mESC lines were maintained using standard conditions in dishes coated with gelatin, without feeder cells.

Materials

Cyclopamine was a gift from Dr. William Gaffield (USDA) (Gaffield et al. 1986). SAG was from EMD Biochemicals (Darmstadt, Germany). Retinoic acid was from Sigma/Aldrich (St. Louis, MO).

Immunostaining

Mouse anti-Pax7, anti-Pax6 and anti-Nkx2.2 were obtained from the Developmental Studies Hybridoma Bank. Goat anti-Olig2 was purchased from R&D Systems (Minneapolis, MN). Guinea pig anti-Isl1/2 was a gift from Dr. Thomas Jessell (Columbia University). In all experiments, donkey and goat Alexa-488 anti-mouse, goat Alexa-568 anti-guinea pig and donkey Alexa-568 anti-goat were used as secondary antibodies. NEBs where mounted in Fluormount-G and positive nuclei quantified. Fixation was performed for 10 min on ice using 4% paraformaldehyde in 1X PBS. Native HB9:GFP fluorescence was imaged directly, after fixation and mounting, without antibody detection.

Imaging and quantification of nuclear progenitor markers

Mounted NEBs were imaged with a Zeiss Observer fluorescence microscope with a 20x objective. Within each experiment, Stacks were deconvolved and resulting images were scrambled before counting. At least 20 NEBs were counted in each experiment. Statistics were performed using the Student's t-test.

Neuralized embryoid body differentiation

mESCs were differentiated into NEBs using established procedures (Wichterle et al. 2002). NEBs were aggregated for 24 h in DFNB medium in Petri dishes rotated at 0.8 Hz. 24h after aggregation, Retinoic acid (RA) was added to 10µM for neural differentiation and for mosaic NEB Ptch1:LacZ measurements. NEBs were fixed 48h after the addition of RA for antibody staining of neural progenitors. NEBs were fixed 96h after the addition of RA for imaging and quantifying HB9:GFP fluorescence.

Reporter gene assay for Ptch1:LacZ activity

NEBs were collected, washed once in PBS and lysed in 100 mM Potassium Phosphate, pH 7.8, 0.2 % Triton X-100. Lysates were analyzed using the Galacto-Light chemiluminescent kit (Applied Biosciences, Foster City, CA) for Ptch1:LacZ expression level. Lysates were normalized for total protein using the Bradford reagent (BioRad, Hercules, CA).

TALENs

TALENs were expressed from polycistronic messages also encoding antibiotic resistance. Transfected mESCs were transiently selected at concentrations titrated to yield ~100 colonies among $>10^6$ transfected mESCs. Transient resistance thus correlated with TALEN expression. We recovered mESC colonies harboring predicted non-functional alleles within each locus at frequencies of 5-90%. Because antibiotic resistance was transient, we repeated the protocol to establish mESC lines with complex mutant genotypes.

TALEN construct cloning, transfection, mESC clone selection and genotyping, as well as repeat variable domain architectures for TALEN constructs targeting *Shh* and *Ptch2,* were previously described (Alfaro et al. 2014).

Repeat variable domain architectures for TALEN constructs targeting *Ptch1* and *Smo* were as follows. *Ptch1* 5': NN NN HD HD NG HD NN NN HD NG NN NN NG NI NI. *Ptch1* 3': HD HD HD NN HD HD NN HD HD NN NN HD HD NG NN HD HD NG NN. *Smo* 5': NN HD NG NN HD NG NN NN NG NI HD NG NN HD NG. *Smo* 3': HD HD HD NN HD NG HD NI NI NN NN HD HD NN HD HD HD.

Genotyping

PCR screening was performed on cell lysates using the following primers flanking the *Ptch1* and *Smo* TALEN binding sites: *Ptch1* Forward: (5') GCAAAGACCTCGGGACTCA (3'). *Ptch1* Reverse: (5') GGAGGGAGGGTTTGAATTTTT (3'). *Smo* Forward: (5') GCACCGGTCGCCTAAGTAGC (3'). *Smo* Reverse (5') GCACACGTTGTAGCGCAAA (3'). PCR products were sequenced and mutant clones selected as previously described (Alfaro et al. 2014).

Mutations

Ptch1$^{LacZ/LacZ}$;*Ptch2*$^{-/-}$ and *Ptch1*$^{LacZ/LacZ}$;*Shh*$^{-/-}$ mESCs were previously described (Alfaro et al. 2014). *Ptch1*$^{+/LacZ}$;*Shh*$^{-/-}$ were heterozygous for 1bp and 10bp deletions in *Shh* exon 1. *Ptch1*$^{LacZ/LacZ}$;*Ptch2*$^{-/-}$;*Shh*$^{-/-}$ mESCs were heterozygous for a 1bp insertion and a 4bp deletion in *Shh* exon 1. *Ptch1*$^{LacZ/LacZ}$;*Smo*$^{-/-}$ were heterozygous for 90bp and 110bp deletions in *Smo* exon 1. *Ptch1*$^{LacZ/LacZ}$;*Ptch2*$^{-/-}$;*Smo*$^{-/-}$ mESCs were homozygous for an 83 bp deletion in *Smo* exon 1. *Disp1*$^{-/-}$;*Shh*$^{-/-}$ were heterozygous for 16bp and 35bp deletions in *Shh* exon 1. *Disp1*$^{-/-}$;*Shh*$^{-/-}$;*Ptch1*$^{-/-}$mESCs were additionally homozygous for a 1bp deletion in *Ptch1* exon 1. *Disp1*$^{-/-}$;*Shh*$^{-/-}$;*Ptch1*$^{-/-}$;*Ptch2*$^{-/-}$ mESCs were additionally heterozygous for 57bp and 10bp deletions in *Ptch2* exon 2.

Acknowledgements
Ptch1$^{LacZ/LacZ}$ and *Ptch1*$^{+/LacZ}$ mESCs were a gift of Dr. Scott (Stanford University). *Smo*$^{-/-}$ mESCs were a gift from Dr. Andrew McMahon (University of Southern California). HB9:GFP mESCs were a gift from Dr. Thomas Jessell (Columbia University).This work was supported by NIH grant R01GM097035 to HR. BR was a predoctoral fellow of CIRM training grant TG2-01164. We would also like to thank C. Jägers, A. Alfaro, A. Luc, B. Cole, J. Hardin and C. Casillas for their technical assistance.

Author contributions
BR performed experiments and interpreted data. Both authors have contributed to the written manuscript.

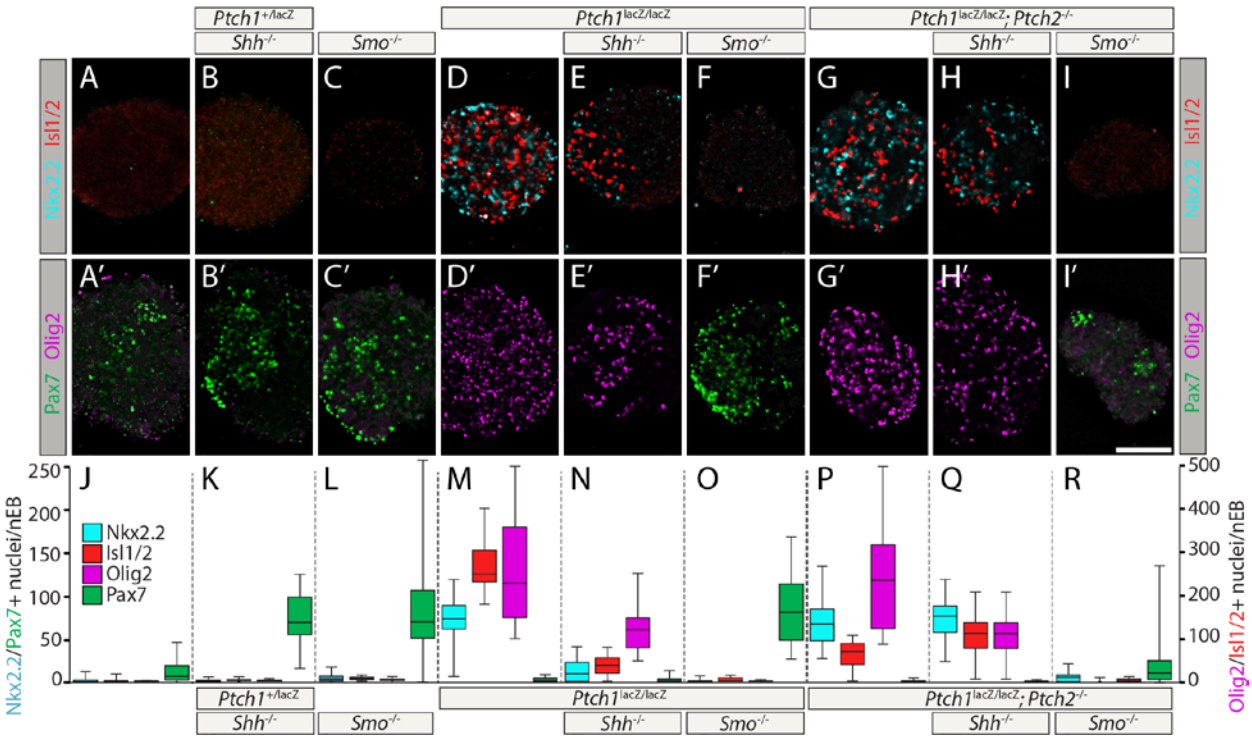

Figure 1. Sequential disruption of Ptch1 and Ptch2 enhances Smo-dependent NEB ventralization.

A-I': mESCs with compound mutant genotypes were differentiated into NEBs, and stained for the ventral markers Nkx2.2 (Cyan), Olig2 (Magenta), Isl1/2 (Red), and the dorsal marker Pax7 (Green). J-R: Nkx2.2, Isl1/2, Olig2, or Pax7 staining quantification (box and whiskers). WT NEBs do not ventralize (A,A',J). Loss of either *Shh* (*Ptch1*$^{+/LacZ}$;*Shh*$^{-/-}$)(B,B',K) or *Smo* (*Smo*$^{-/-}$) (C,C',L) in cells with intact Ptch1/2 function increases Pax7 at the expense of ventral markers. NEBs without Ptch1 (*Ptch1*$^{LacZ/LacZ}$, D,D',M) acquire ventral identity. Subsequent loss of Shh (*Ptch1*$^{LacZ/LacZ}$;*Shh*$^{-/-}$, E,E',N) decreases ventral marker counts. *Ptch1*$^{LacZ/LacZ}$;*Smo*$^{-/-}$ NEBs dorsalize and acquire Pax7 (F,F',O). NEBs devoid of all Ptch1/2 activity (*Ptch1*$^{LacZ/LacZ}$;*Ptch2*$^{-/-}$) acquire ventral identity (G,G',P). *Ptch1*$^{LacZ/LacZ}$;*Ptch2*$^{-/-}$;*Shh*$^{-/-}$ NEBs retain ventral identity (H,H',Q). *Ptch1*$^{LacZ/LacZ}$;*Ptch2*$^{-/-}$;*Smo*$^{-/-}$ NEBs lose their ventral identity and express Pax7 (I,I',R). Scale bar is 100µm.

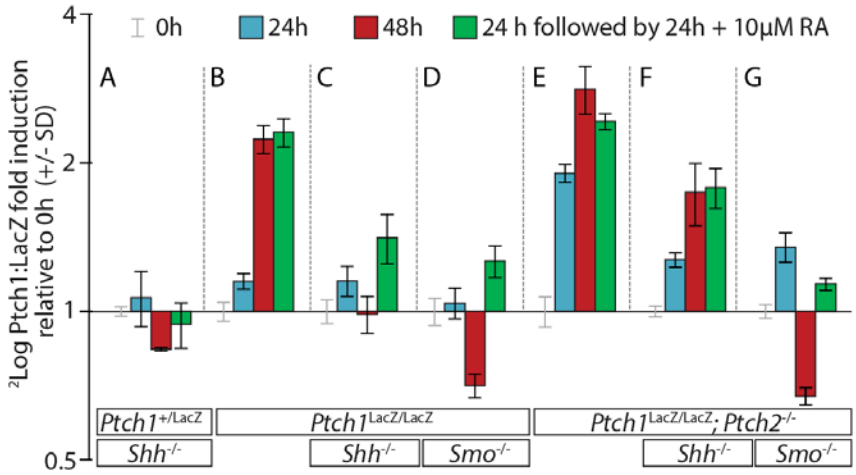

Figure 2. Sequential disruption of Ptch1 and Ptch2 enhances Smo-dependent upregulation of Ptch1:LacZ.

A-G: *Ptch1*$^{+/LacZ}$;*Shh*$^{-/-}$(A), *Ptch1*$^{LacZ/LacZ}$ (B), *Ptch1*$^{LacZ/LacZ}$;*Shh*$^{-/-}$(C), *Ptch1*$^{LacZ/LacZ}$;*Smo*$^{-/-}$ (D), *Ptch1*$^{LacZ/LacZ}$;*Ptch2*$^{-/-}$ (E), *Ptch1*$^{LacZ/LacZ}$;*Ptch2*$^{-/-}$;*Shh*$^{-/-}$ (F), and *Ptch1*$^{LacZ/LacZ}$; *Ptch2*$^{-/-}$;*Smo*$^{-/-}$(G) mESCs were aggregated into NEBs and Ptch1:LacZ levels were measured after aggregation (0h), after 24h (blue) and 48h (red). To induce neuralization NEBs were treated with 10µM retinoic acid (RA) for 24h after 24h in culture (green). Measurements are relative to Ptch1:LacZ levels at (0h), ^{2}Log scale. *Ptch1*$^{LacZ/LacZ}$ NEBs (B) and *Ptch1*$^{LacZ/LacZ}$;*Ptch2*$^{-/-}$ NEBs (E) show high Ptch1:LacZ levels after 48h in culture. *Shh* disruption lowers Ptch1:LacZ expression in cells without Ptch1 (C), but less so in cells devoid of both Ptch1/2 (F). High Ptch1:LacZ expression requires Smo (D,G).

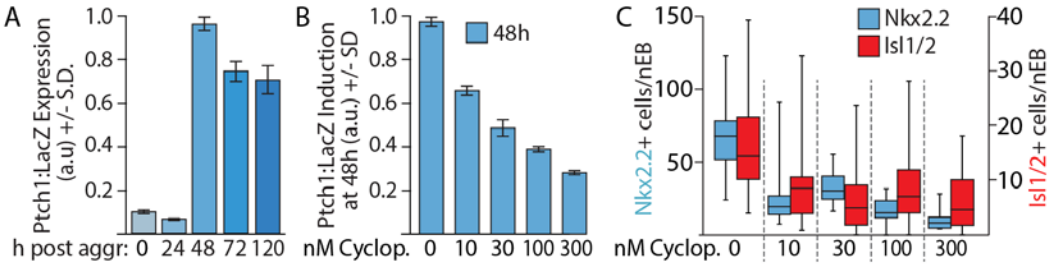

Figure 3. Cyclopamine inhibits the Hh response in *Ptch1*$^{LacZ/LacZ}$;*Ptch2*$^{-/-}$;*Shh*$^{-/-}$ NEBs.

A: Ptch1:LacZ levels were measured up to 120h after NEB formation. 10μM retinoic acid was added 24h after formation. B: NEBs were exposed to 0-300 nM cyclopamine at aggregation (0h) and Ptch1:LacZ was measured at 48h. Ptch1:LacZ levels in 30 nM cyclopamine were approximately half those of untreated NEBs. C: Ventral marker expression (Nkx2.2 and Isl1/2) in NEBs is quantified (box and whisker) in the presence of 0-300 nM cyclopamine.

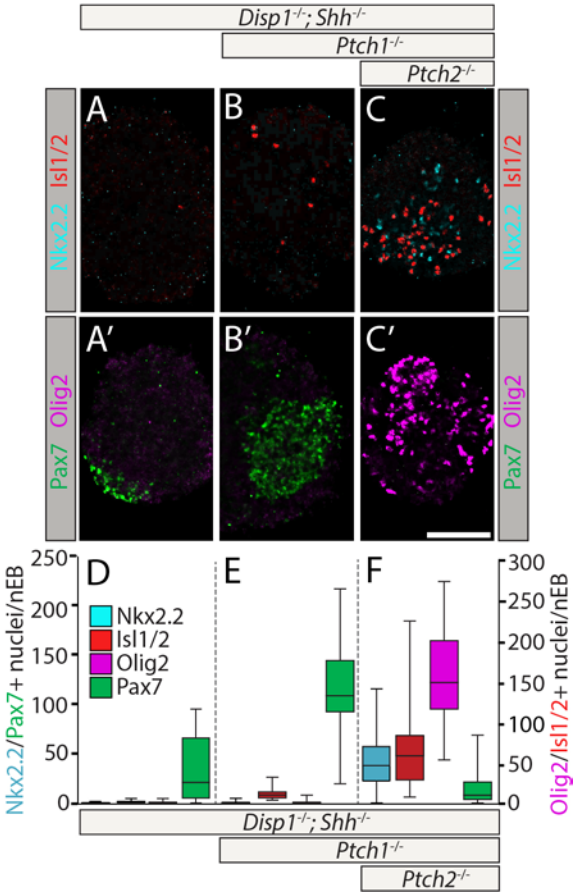

Figure 4. Disp1 absence does not affect cell autonomous Hh pathway upregulation **A-C':** mESCs with compound mutant genotypes were differentiated into NEBs, and stained for the ventral markers Nkx2.2 (Cyan), Olig2 (Magenta), Isl1/2 (Red), and the dorsal marker Pax7 (Green) **D-F:** Quantification (box and whiskers) of cells expressing Nkx2.2, Isl1/2, Olig2, or Pax7. *Disp1*$^{-/-}$;*Shh*$^{-/-}$ NEBs are dorsalized as illustrated by absent ventral markers and Pax7 expression (A,A',D). Subsequent Ptch1 loss (*Disp1*$^{-/-}$;*Shh*$^{-/-}$;*Ptch1*$^{-/-}$) causes minor Isl1/2 expression (B,B',E). Additional Ptch2 loss (*Disp1*$^{-/-}$;*Shh*$^{-/-}$;*Ptch1*$^{-/-}$;*Ptch2*$^{-/-}$) increases Nkx2.2, Isl1/2 and Olig2 expression, indicating ventral identity (C,C',F). Scale bar is 100µm.

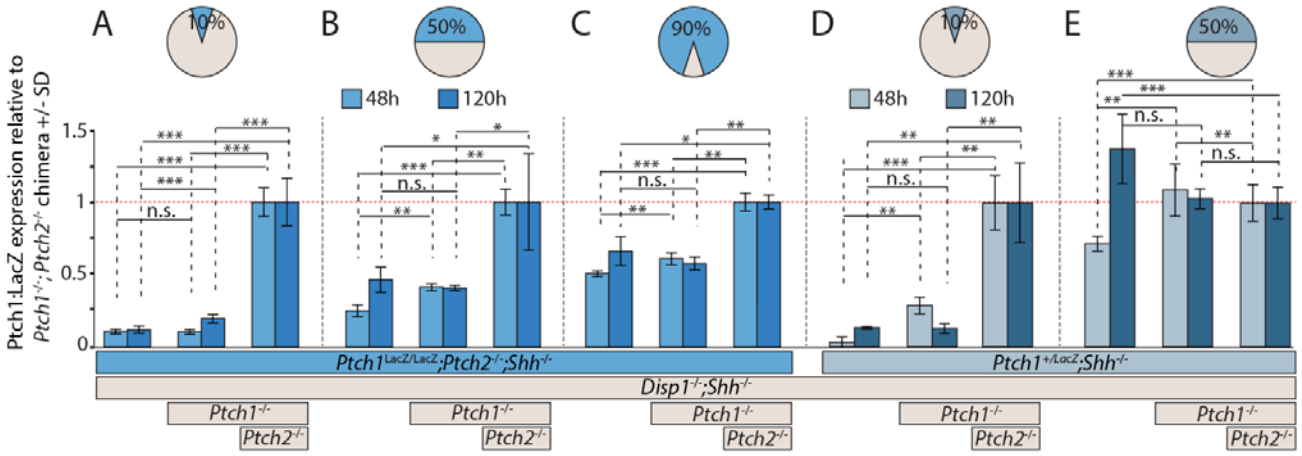

Figure 5. Ptch1 and Ptch2 expressing cells inhibit the Hh response non-cell autonomously.

A-E: Ptch1:LacZ expression in mosaic NEBs consisting of two genetically distinct cell populations. A-C: NEBs consisting of 10% (A), 50% (B), or 90% (C) *Ptch1*$^{LacZ/LacZ}$;*Ptch2*$^{-/-}$;*Shh*$^{-/-}$ cells. Remaining cells consist of *Disp1*$^{-/-}$;*Shh*$^{-/-}$, *Disp1*$^{-/-}$;*Shh*$^{-/-}$;*Ptch1*$^{-/-}$, or *Disp1*$^{-/-}$;*Shh*$^{-/-}$;*Ptch1*$^{-/-}$;*Ptch2*$^{-/-}$ (indicated). Ptch1:LacZ levels in the *Ptch1*$^{LacZ/LacZ}$;*Ptch2*$^{-/-}$;*Shh*$^{-/-}$ cells were assessed after 48 (light blue) or 120 (dark blue) days in culture. D,E: NEBs consisting of 10% (D) or 50% (E) *Ptch1*$^{+/LacZ}$;*Shh*$^{-/-}$ cells. Remaining cells were *Disp1*$^{-/-}$;*Shh*$^{-/-}$, *Disp1*$^{-/-}$;*Shh*$^{-/-}$;*Ptch1*$^{-/-}$, or *Disp1*$^{-/-}$;*Shh*$^{-/-}$;*Ptch1*$^{-/-}$;*Ptch2*$^{-/-}$ (indicated). Ptch1:LacZ levels in *Ptch1*$^{+/LacZ}$;*Shh*$^{-/-}$ cells were assessed after 2 (green) or 5 (dark green) days in culture. When surrounding cells express Ptch1/2, the Hh response is attenuated both in cells devoid of Ptch1 and Ptch2 (A-C) as wells as cell expressing Ptch1 and Ptch2 (D,E). Error bars are s.d., * $p < 0.05$, ** $p < 0.01$, *** $p<0.001$, n.s., not significant (t-test).

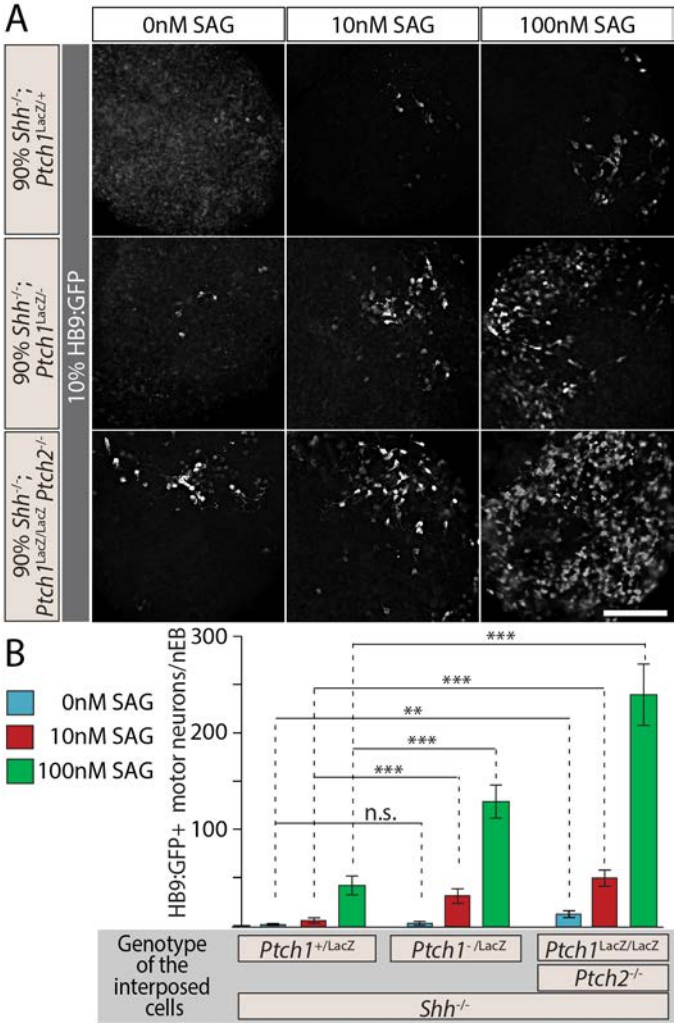

Figure 6. The Hh response to the Smo agonist SAG in HB9:GFP cells is enhanced by the absence of Ptch1 and Ptch2 in neighboring cells.
A: Images of mosaic NEBs consisting of 10% HB9:GFP cells and 90% *Ptch1*$^{+/LacZ}$;*Shh*$^{-/-}$, *Ptch1*$^{LacZ/LacZ}$;*Shh*$^{-/-}$ or *Ptch1*$^{LacZ/LacZ}$;*Ptch2*$^{-/-}$;*Shh*$^{-/-}$ cells (indicated). Mosaic NEBs were cultured in 0nM (blue), 10nM (red) or 100nM (green) SAG. GFP expression in HB9:GFP cells indicates motor neuron differentiation, a measure of Hh pathway upregulation. **B:** HB9:GFP+ cells were quantified. Error bars are s.e.m., n>20, ** $p < 0.01$, *** $p<0.001$, n.s., not significant (t-test). Scale bar is 100µm.

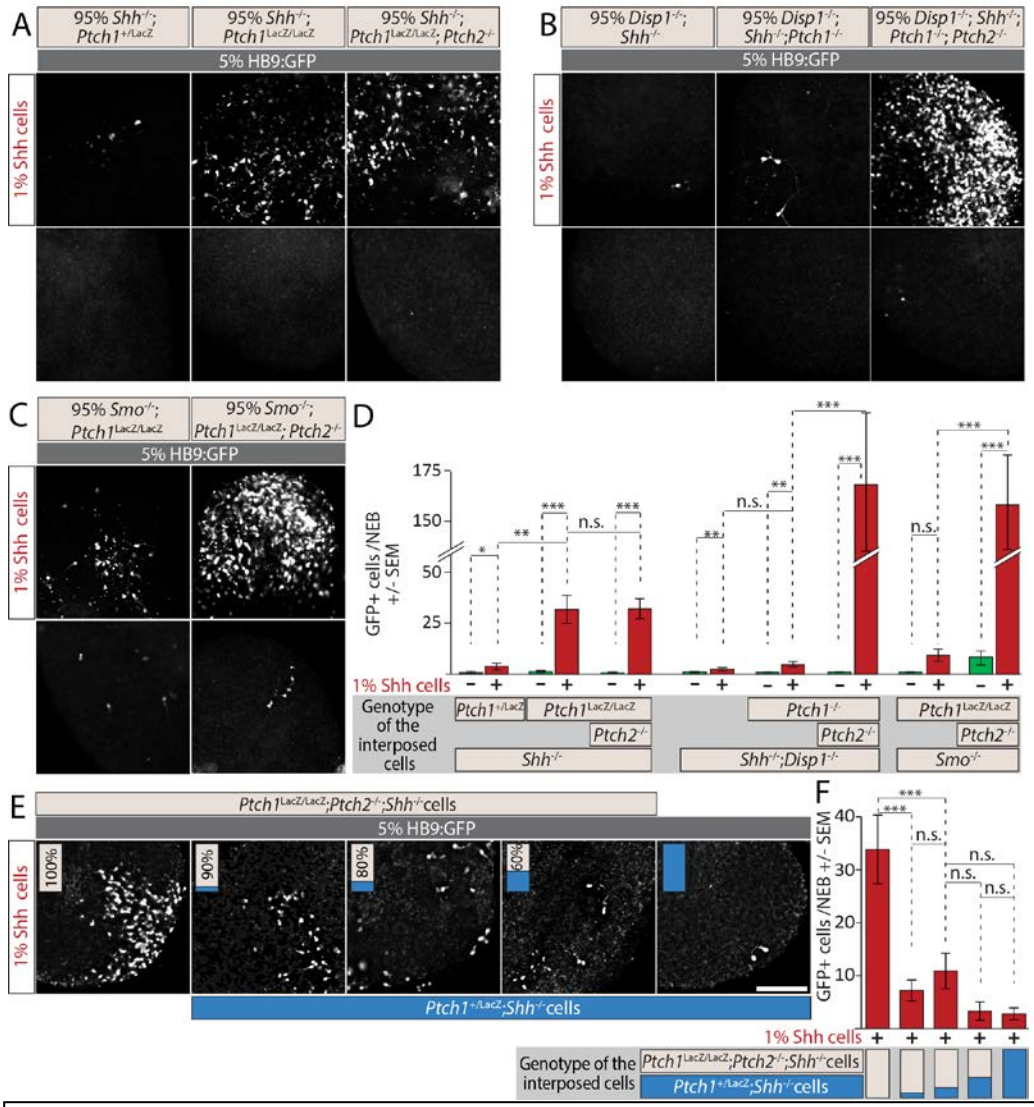

Figure 7. Loss of Ptch1 and Ptch2 in neighboring cells enhances the response to Shh
A-C: Images of two-part and three-part mosaic NEBs showing GFP expression in HB9:GFP cells. All NEBs included 5% HBG:GFP cells, and 1% Shh expressing cells where indicated. A: Remaining 94%/95% of cells were *Ptch1*$^{+/LacZ}$;*Shh*$^{-/-}$, *Ptch1*$^{LacZ/LacZ}$;*Shh*$^{-/-}$ or *Ptch1*$^{LacZ/LacZ}$;*Ptch2*$^{-/-}$;*Shh*$^{-/-}$ (indicated). B: Remaining 94%/95% of cells were *Disp1*$^{-/-}$;*Shh*$^{-/-}$, *Disp1*$^{-/-}$;*Shh*$^{-/-}$;*Ptch1*$^{-/-}$, or *Disp1*$^{-/-}$;*Shh*$^{-/-}$;*Ptch1*$^{-/-}$*Ptch2*$^{-/-}$ (indicated). C: Remaining 94%/95% of cells were *Ptch1*$^{-/-}$;*Smo*$^{-/-}$ or *Ptch1*$^{-/-}$;*Ptch2*$^{-/-}$;*Smo*$^{-/-}$ (indicated). Under all conditions, sequential Ptch1/2 loss greatly enhanced Shh-dependent motor neuron differentiation in HB9:GFP cells. D: HB9:GFP+ cells in (A), (B) and (C) were quantified per mosaic NEB E: Images of three-part and four-part mosaic NEBs showing HBG:GFP+ cells. All NEBs included 5% HBG:GFP cells and 1% Shh expressing cells. Remaining cells were *Ptch1*$^{LacZ/LacZ}$;*Ptch2*$^{-/-}$;*Shh*$^{-/-}$ (gray) and *Ptch1*$^{+/LacZ}$;*Shh*$^{-/-}$ (blue) in indicated ratios. *Ptch1*$^{+/LacZ}$;*Shh*$^{-/-}$ cells suppress Shh-mediated motor induction F: HB9:GFP+ cells in (E) were

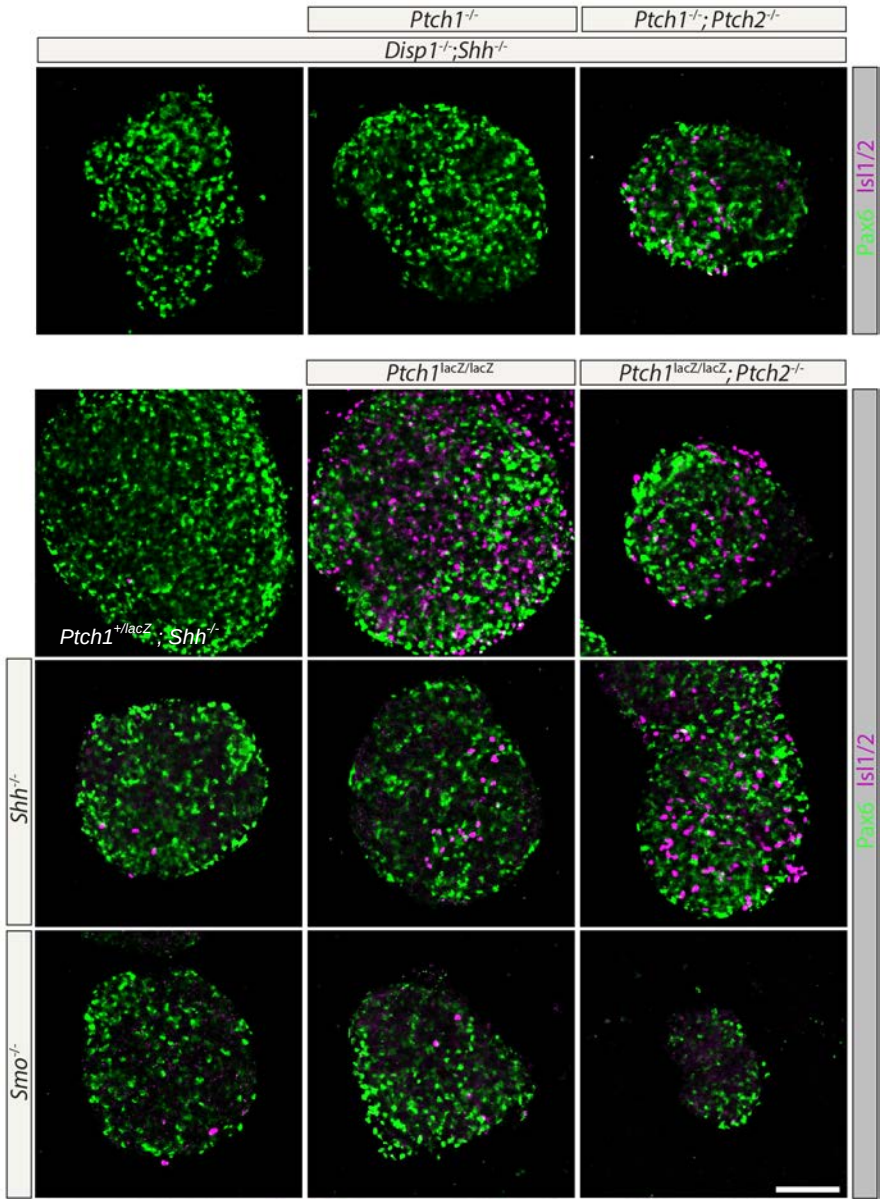

Supplemental Figure 1. Pax6 expression is unimpaired in all modified mESC lines All cell lines used were stained for Pax6 and Isl1/2 after *in vitro* neuralization. Although not all NEBs were equally sized, invariably they express Pax6, indicating the acquisition of neural progenitor fates, regardless of their genotype (indicated). Scale bar is 100µm.

References

Alaynick, W. a., Jessell, T.M. & Pfaff, S.L., 2011. SnapShot: Spinal cord development. *Cell*, 146(1), pp.178–178.e1.

Alfaro, A.C. et al., 2014. Ptch2 mediates the Shh response in Ptch1-/- cells. *Development*, 141(17), pp.3331–3339.

Bae, S.H. et al., 1999. Cholesterol biosynthesis from lanosterol. Molecular cloning, tissue distribution, expression, chromosomal localization, and regulation of rat 7-dehydrocholesterol reductase, a Smith-Lemli-Opitz syndrome- related protein. *J. Biol. Chem.*, 274(21), pp.14624–14631.

Barakat, M.T., Humke, E.W. & Scott, M.P., 2010. Learning from Jekyll to control Hyde: Hedgehog signaling in development and cancer. *Trends in Molecular Medicine*, 16(8), pp.337–348.

Bejsovec, A. & Wieschaus, E., 1993. Segment polarity gene interactions modulate epidermal patterning in Drosophila embryos. *Development*, 119(2), pp.501–517.

Bidet, M. et al., 2011. The hedgehog receptor patched is involved in cholesterol transport. *PLoS ONE*, 6(9), pp.1–11.

Bijlsma, M.F. et al., 2006. Repression of smoothened by patched-dependent (pro-)vitamin D3 secretion. *PLoS biology*, 4(8), p.e232.

Briscoe, J. & Thérond, P.P., 2013. The mechanisms of Hedgehog signalling and its roles in development and disease. *Nature reviews. Molecular cell biology*, 14(7), pp.416–29.

Burke, R. et al., 1999. Dispatched, a novel sterol-sensing domain protein dedicated to the release of cholesterol-modified hedgehog from signaling cells. *Cell*, 99(cc), pp.803–815.

Cermak, T. et al., 2011. Efficient design and assembly of custom TALEN and other TAL effector-based constructs for DNA targeting. *Nucleic Acids Res*, 39(12), p.e82.

Chen, J.K., Taipale, J., Cooper, M.K., et al., 2002. Inhibition of Hedgehog signaling by direct binding of cyclopamine to Smoothened. *Genes and Development*, 16(21), pp.2743–2748.

Chen, J.K., Taipale, J., Young, K.E., et al., 2002. Small molecule modulation of Smoothened activity. *Proceedings of the National Academy of Sciences of the United States of America*, 99(22), pp.14071–14076.

Chen, Y. & Struhl, G., 1996. Dual roles for patched in sequestering and transducing Hedgehog. *Cell*, 87(3), pp.553–63.

Chiang, C. et al., 1996. Cyclopia and defective axial patterning in mice lacking Sonic hedgehog gene function. *NATURE*, 383(6599), pp.407–413.

Cohen, M., Briscoe, J. & Blassberg, R., 2013. Morphogen interpretation: the transcriptional logic of neural tube patterning. *Current opinion in genetics & development*, 23(4), pp.423–8.

Cooper, M.K. et al., 2003. A defective response to Hedgehog signaling in disorders of cholesterol biosynthesis. *Nat Genet*, 33(4), pp.508–513.

Cooper, M.K. et al., 1998. Teratogen-mediated inhibition of target tissue response to Shh signaling. *Science*, 280(5369), pp.1603–1607.

Doughty, D.M. et al., 2011. The RND-family transporter, HpnN, is required for hopanoid localization to the outer membrane of Rhodopseudomonas palustris TIE-1. *Proc. Natl. Acad. Sci. U. S. A.*, 108(45), pp.E1045–51.

Etheridge, L.A. et al., 2010. Evidence for a role of vertebrate Disp1 in long-range Shh signaling. *Development (Cambridge, England)*, 137(1), pp.133–40.

Frank-Kamenetsky, M. et al., 2002. Small-molecule modulators of Hedgehog signaling: identification and characterization of Smoothened agonists and antagonists. *J Biol*, 1(2), p.10.

Gaffield, W. et al., 1986. Carbon-13 and proton nuclear magnetic resonance spectra of Veratrum alkaloids. *J. Nat. Products*, 49, pp.286–292.

Goodrich, L. V., 1997. Altered Neural Cell Fates and Medulloblastoma in Mouse patched Mutants. *Science*, 277(5329), pp.1109–1113.

Holtz, A.M. et al., 2013. Essential role for ligand-dependent feedback antagonism of vertebrate hedgehog signaling by PTCH1, PTCH2 and HHIP1 during neural patterning. *Development*, 140(16), pp.3423–3434.

Hooper, J.E. & Scott, M.P., 2005. Communicating with Hedgehogs. *Nature reviews. Molecular cell biology*, 6(4), pp.306–317.

Incardona, J.P., Gaffield, W., et al., 2000. Cyclopamine inhibition of Sonic hedgehog signal transduction is not mediated through effects on cholesterol transport. *Dev. Biol.*, 224(2), pp.440–452.

Incardona, J.P., 2005. From sensing cellular sterols to assembling sensory structures. *Developmental Cell*, 8(6), pp.798–799.

Incardona, J.P., Lee, J.H., et al., 2000. Receptor-mediated endocytosis of soluble and membrane-tethered Sonic hedgehog by Patched-1. *Proceedings Of The National Academy Of Sciences Of The United States Of America*, 97(22), pp.12044–12049.

Incardona, J.P. et al., 1998. The teratogenic Veratrum alkaloid cyclopamine inhibits sonic hedgehog signal transduction. *Development*, 125(18), pp.3553–3562.

Incardona, J.P., Gruenberg, J. & Roelink, H., 2002. Sonic hedgehog induces the segregation of patched and smoothened in endosomes. *Curr Biol*, 12(12), pp.983–995.

Ingham, P.W. & McMahon, A.P., 2001. Hedgehog signaling in animal development: paradigms and principles. *Genes and Development*, 15(23), pp.3059–3087.

Jessell, T.M., 2000. Neuronal specification in the spinal cord: inductive signals and transcriptional codes. *Nat Rev Genet*, 1(1), pp.20–29.

Karten, B., Peake, K.B. & Vance, J.E., 2009. Mechanisms and consequences of impaired lipid trafficking in Niemann–Pick type C1-deficient mammalian cells. *Biochimica et Biophysica Acta (BBA) - Molecular and Cell Biology of Lipids*, 1791(7), pp.659–670.

Kawakami, T. et al., 2002. Mouse dispatched mutants fail to distribute hedgehog proteins and are defective in hedgehog signaling. *Development*, 129(24), pp.5753–5765.

Lawrence, P.A., Casal, J. & Struhl, G., 1999. The hedgehog morphogen and gradients of cell affinity in the abdomen of Drosophila. *Development*, 126(11), pp.2441–2449.

Linder, B. et al., 2015. A functional and putative physiological role of calcitriol in Patched1/Smoothened interaction. *Journal of Biological Chemistry*, p.jbc.M115.646141.

Ma, Y. et al., 2002. Hedgehog-mediated patterning of the mammalian embryo requires transporter-like function of dispatched. *Cell*, 111(1), pp.63–75.

Meinhardt, A. et al., 2014. 3D Reconstitution of the Patterned Neural Tube from Embryonic Stem Cells. *Stem Cell Reports*, 3, pp.987–999.

Milenkovic, L. et al., 1999. Mouse patched1 controls body size determination and limb patterning. *Development*, 126(20), pp.4431–4440.

Nikaido, H. & Takatsuka, Y., 2009. Mechanisms of RND multidrug efflux pumps. *Biochimica et Biophysica Acta*, 1794(5), pp.769–781.

Roelink, H. et al., 1994. Floor plate and motor neuron induction by vhh-1, a vertebrate homolog of hedgehog expressed by the notochord. *Cell*, 76(4), pp.761–775.

Sharpe, H.J. et al., 2015. Regulation of the oncoprotein Smoothened by small molecules. *Nature Chemical Biology*, 11(4), pp.246–255.

Strutt, H. et al., 2001. Mutations in the sterol-sensing domain of Patched suggest a role for vesicular trafficking in Smoothened regulation. *Curr Biol*, 11(8), pp.608–13.

Taipale, J. et al., 2002. Patched acts catalytically to suppress the activity of Smoothened. *NATURE*, 418(6900), pp.892–897.

Tian, H. et al., 2005. Mouse Disp1 is required in sonic hedgehog-expressing cells for paracrine activity of the cholesterol-modified ligand. *Development*, 132(1), pp.133–142.

Tseng, T.T. et al., 1999. The RND permease superfamily: an ancient, ubiquitous and diverse family that includes human disease and development proteins. *J Mol Microbiol Biotechnol*, 1(1), pp.107–125.

Tsiairis, C.D. & McMahon, A.P., 2008. Disp1 regulates growth of mammalian long bones through the control of Ihh distribution. *Developmental Biology*, 317, pp.480–485.

Wichterle, H. et al., 2002. Directed differentiation of embryonic stem cells into motor neurons. *Cell*, 110(3), pp.385–397.

Yauch, R.L. et al., 2008. A paracrine requirement for hedgehog signalling in cancer. *Nature*, 455(7211), pp.406–10.

Zhang, X.M., Ramalho-Santos, M. & McMahon, A.P., 2001. Smoothened mutants reveal redundant roles for Shh and Ihh signaling including regulation of L/R asymmetry by the mouse node. *Cell*, 105(6), pp.781–792.

Zhulyn, O. et al., 2015. Ptch2 shares overlapping functions with Ptch1 in Smo regulation and limb development. *Dev. Biol.*, 397(2), pp.191–202.

Chapter 4

Conclusions, Reflections and Future Directions

The overlapping functions of Ptch1 and Ptch2

This thesis has attempted to confront an unpleasant reality: that several decades after Ptch emerged as the Hh signaling receptor and negative regulator of Smo, relatively few studies have been performed in vertebrates in which the contributions of Ptch1 and Ptch2 to Smo inhibition can be distinguished. I have attempted to take a harsh approach to this question in using genome editing to entirely rid mESCs of contributions from either paralog. While this approach has been productive in illuminating overlapping roles for these paralogous proteins as Smo regulators, some possibly interesting mechanisms may nevertheless have been missed.

A very large question that emerged from our experiments in which Ptch1 and Ptch2 were overexpressed in the chicken neural tube concerns the heterotrimerization dynamics of these two paralogs. Specifically, why does Ptch1D499A overexpression fail to elicit a neural patterning phenotype, while Ptch2D469A so effectively does (Alfaro et al. 2014)? This fact conflicts with the fact that *Ptch1*$^{-/-}$ embryos exhibit much more devastating neural patterning disruptions than their *Ptch2*$^{-/-}$ counterparts, and the fact that Ptch1Δloop2/D499A fails to disrupt neural patterning, as does Ptch1Δloop2 (Lee et al. 2006; Goodrich et al. 1997). Might Ptch2 antagonize Ptch1/2 heterotrimers to a greater extent than Ptch1, when overexpressed as a dominant negative? The answer to this conundrum is currently unknown and awaits further work.

Another interesting observation concerns the penetrance of Ptch2D469A overexpression. Chick embryos expressing this construct in the neural tube exhibit several neural patterning phenotypes, but at a reduced frequency suggesting precise timing requirements not currently understood (Alfaro et al. 2014). Chick gastrulation proceeds in an anterior to posterior progression, and exogenous DNAs are introduced into cells at various developmental stages. It is possible that Ptch2 is required specifically at a point in development where early fate decisions between germ layers occur, causing local disturbances in floor plate and neural tube patterning. Cells only at specific axial positions during DNA introduction are affected if this view is correct.

Are Ptch1 and Ptch2 biologically unique and if so, in what way? Do they bind Shh equivalently? Is heightened Ptch2 instability biologically meaningful (Kawamura et al. 2008)? Do they transport the same Smo inhibitory substrate(s)? Do Ptch1 and Ptch2 differ with respect to their contributions to cell-autonomous and cell non-autonomous Smo inhibition? These are important questions for future study. Regardless it has been remarkably useful to employ genome editing, coupled with stem cell biology, in order to efficiently generate cells devoid of any Ptch activity that are useful for developmental questions during differentiation. Because Ptch functions catalytically, complete loss of function with genetically null mutations in both genes is a requirement, and this is difficult to fulfill *in vivo* (Taipale et al. 2002). The method presented in this thesis for combining genome editing and stem cell biology may have much to offer future studies in the neural tube.

Ptch1/2 mediated Smo inhibition *in vivo*

Another interesting question involves the lack of non-autonomous Smo inhibition in the vicinity of cells overexpressing Ptch1Δloop2 in the neural tube. This contrasts with the observation that in NEBS, cells expressing Ptch, even at endogenous levels from the *Ptch1* and/or *Ptch2* genomic locus, inhibit Hh pathway activity in adjacent WT cells. There is also no phenotype observed when Ptch1D499A is exogenously expressed in the neural tube, despite the prediction that this allele functions as a dominant negative (Alfaro et al. 2014).

Ptch1Δloop2 clearly functions as an extremely effective Smo inhibitory construct when viewed strictly as a cell autonomous Smo regulator. When expressed in ventral neural progenitors within the neural tube, it is predicteded to dorsalize adjacent cells but does not. Are cell autonomous and non-cell autonomous Smo regulation mechanistically different? Do Ptch1 and Ptch1Δloop2 undergo the same cellular trafficking events? Does this discrepancy lie in the fact that cells in genetically mosaic NEBs co-exist for the entire duration of differentiation, whereas overexpression in the neural tube only captures a fraction of the developmental timing window? Innovative *in vivo* approaches will likely be required to rigorously evaluate the non-autonomous mechanism responsible for Ptch1/2 mediated Smo inhibition.

One possible technical approach to address this question involves genetically mosaic mouse embryos. We show in this thesis that mESCs genetically devoid of many important Hh signaling genes nevertheless undergo robust neural differentiation. It will be necessary to determine whether they are capable of undergoing gastrulation. Generating mosaic clones of *Ptch1*$^{-/-}$*; Ptch2*$^{-/-}$*; Shh*$^{-/-}$ cells within an otherwise wild type neural tube would be very informative because the ventral identity of these cell clones could be assessed at various positions along the dorsoventral axis. It is predicted that clones of this genotype, despite equivalent cell-autonomous Smo regulation, will adopt fates similar to those of cells in their vicinity along the dorsoventral axis, based on different levels of Ptch inhibition by Shh. A variation of this approach might be the generation of *Ptch1*$^{\Delta loop2/\Delta loop2}$*; Ptch2*$^{-/-}$*; Shh*$^{-/-}$ mESCs. We predict that clones of such cells would be unresponsive to Shh ligand and adopt a dorsal identity, even when located ventrally, and would additionally dorsalize surrounding cells. It will be important to determine whether these cells contribute to the neural tube when transplanted to a blastocyst since they will be required to gastrulate rather than simply differentiate. If successful, this approach would mimic NEB experiments *in vivo*.

A twist on this mosaic mouse embryo approach might be to make clones of WT cells, or *Ptch1*$^{\Delta loop2/\Delta loop2}$*; Ptch2*$^{-/-}$*; Shh*$^{-/-}$ cells within *Ptch1*$^{-/-}$ embryos, which have been previously shown to generate highly ventralized neural tubes. It would be interesting to assess whether WT cell clones would be able to dorsalize *Ptch1*$^{-/-}$ cells in their vicinity.

Can Shh signal in cells devoid of Ptch1 and Ptch2?

Another very interesting question for the future is whether Shh can signal in cells entirely devoid of Ptch1/2. It is noteworthy that cells entirely devoid of Ptch1/2 nevertheless do no activate the Hh response for several days after differentiation. This implies the existence of a Smo activator necessary for Hh response activity in the absence of Ptch1/2, a model consistent with findings that Smo can be modulated at its heptahelical domain as well as its N-terminal CRD. One possibility is that Shh binds Smo at the CRD. Recent intriguing work on immortalized fibroblasts derived from *Ptch1-/-; Ptch2-/-* mESCs suggests that Shh can activate the Hh response after transfection but not when added as a soluble ligand, supporting this view (C. Casillas, in preparation). It may not have been previously possible to answer this question, given the need to ensure that Ptch1 and Ptch2 are absent from the signaling environment. It is intriguing to consider whether this possible interaction has never been observed because only Shh expressed within *Ptch1*$^{-/-}$;*Ptch2*$^{-/-}$ cells, as opposed to added in the medium, can bind Smo.

What is the Smo inhibitory Ptch substrate?

Another massive mechanistic question that may be open for assessment by the system described in this thesis, making use of mosaic NEBs, involves the identifying the Smo-inhibitory Ptch substrate molecule. This endeavor will likely require sensitive biochemical techniques. However, because cells truly lacking Ptch1/2 activity are now available in tissue culture for the first time, it may be possible to compare conditioned medium from these cells with those from WT, *Ptch1*$^{-/-}$ and *Ptch2*$^{-/-}$ cells to determine whether any molecule is differentially abundant. This approach has been used with *Ptch1*$^{-/-}$ cells with some success, but the contribution of Ptch2 is in question within this study (Bijlsma et al. 2006). This same approach might be useful for understanding how Disp promotes Hh ligand secretion, which may involve a lipid compartment intermediate that could be detected in culture.

Towards a unified role for RND-SSDs in eukaryotes?

One major impediment to progress in the Hh signaling field has been the incomplete mechanistic understanding of RND transporters, several of which are vital to Hh signaling. It is tempting to speculate about a grand, unified model for their function in eukaryotes, given the finding presented here that Ptch functions in secretion. Because Ptch and Disp require proton antiporter function for their respective roles in Hh signaling, they likely function in the endosomal pathway, where NPC1 is already known to function (Karten et al. 2009; Etheridge et al. 2010; Strutt et al. 2001).

Might each of these molecules act via a surprisingly similar mechanism in endosomes? According to this view, they may differ only with regard to their substrates, and the fate of the endosomes where they sort. For example, NPC1 may act in exchanging protons for cholesterol, enriching the endosomal lumen in cholesterol-rich particles fated for the ER, where they are esterified. Meanwhile, according to this model, Ptch may accomplish something similar with a different lipid or sterol in endosomes fated, at least in part, for the secretory pathway. So too might Disp function in a similar endosome, generating a lumenal particle in which Shh can favorable insert via its dual lipidations. Upon sorting to endosomes bound to exit the cell, these Smo inhibitory complexes (in the case of Ptch) or Shh-loaded liposomes (in the case of Disp) would enter the extracellular space and act non-cell autonomously.

References

Alfaro, A.C. et al., 2014. Ptch2 mediates the Shh response in Ptch1-/- cells. *Development*, 141(17), pp.3331–3339.

Bijlsma, M.F. et al., 2006. Repression of smoothened by patched-dependent (pro-)vitamin D3 secretion. *PLoS biology*, 4(8), p.e232.

Etheridge, L.A. et al., 2010. Evidence for a role of vertebrate Disp1 in long-range Shh signaling. *Development (Cambridge, England)*, 137(1), pp.133–40.

Goodrich, L. V et al., 1997. Altered neural cell fates and medulloblastoma in mouse patched mutants. *Science*, 277, pp.1109–1113.

Karten, B., Peake, K.B. & Vance, J.E., 2009. Mechanisms and consequences of impaired lipid trafficking in Niemann–Pick type C1-deficient mammalian cells. *Biochimica et Biophysica Acta (BBA) - Molecular and Cell Biology of Lipids*, 1791(7), pp.659–670.

Kawamura, S. et al., 2008. Two patched protein subtypes and a conserved domain of group I proteins that regulates turnover. *J. Biol. Chem.*, 283(45), pp.30964–30969.

Lee, Y. et al., 2006. Patched2 modulates tumorigenesis in patched1 heterozygous mice. *Cancer research*, 66(14), pp.6964–71.

Strutt, H. et al., 2001. Mutations in the sterol-sensing domain of Patched suggest a role for vesicular trafficking in Smoothened regulation. *Curr Biol*, 11(8), pp.608–13.

Taipale, J. et al., 2002. Patched acts catalytically to suppress the activity of Smoothened. *NATURE*, 418(6900), pp.892–897.